

The Pennsylvania State University

The Graduate School

Eberly College of Science

**INVESTIGATION OF THE MOLECULAR GENETICS OF
DROSOPHILA SYNAPSE ASSEMBLY**

A Dissertation in
Biochemistry, Microbiology, and Molecular Biology
by
Na Zhao

© 2014 Na Zhao

Submitted in Partial Fulfillment
of the Requirements
for the Degree of

Doctor of Philosophy

August 2014

The dissertation of Na Zhao was reviewed and approved* by the following:

Scott Selleck

Professor and Head of Biochemistry and Molecular Biology

Dissertation advisor

Chair of Committee

Bernhard Lüscher

Professor of Biology, Biochemistry and Molecular Biology, Psychiatry

Richard Ordway

Professor of Biology, Molecular Neuroscience and Genetics

Zhi-Chun Lai

Professor of Biology, Biochemistry and Molecular Biology

* Signatures are on file in the Graduate School

Abstract

The nervous system consists of billions of neurons that interconnect to form functional neural circuits and networks. Synapses, the fundamental units of nervous system, are the highly-specialized cell junctions that mediate intercellular communication. The coordinated synaptic growth and plasticity ensures synaptic transmission upon intrinsic and environmental stimulus. Insight into the mechanism of synapse assembly is critical to our understanding of the nervous system and neurological diseases. In this study, by using the well-established model organism, *Drosophila melanogaster*, I aimed to gain further insight into the important regulatory components involved in synapse development. In particular, serine-threonine kinase Akt, heparan sulfate proteoglycans (HSPGs) and genes affecting cytoskeleton organization were investigated for their functions in the assembly of postsynaptic specializations.

Akt is an integral element of phosphatidylinositide 3-Kinase (PI3K)-Target of Rapamycin (TOR)-Ras homolog enriched in brain (Rheb) signaling, a pathway that known to affect synapse assembly in both vertebrates and *Drosophila*. In this work, the role of Akt in synapse assembly has been examined at the *Drosophila* neuromuscular junction (NMJ), a glutamatergic synapse that displays developmental and activity-dependent plasticity. The single *Drosophila* Akt family member, *Akt1* selectively altered the postsynaptic targeting of one glutamate receptor subunit, GluRIIA, and was required for the expansion of a specialized postsynaptic membrane compartment, the subsynaptic reticulum (SSR).

A novel function of heparan sulfate-modified proteoglycans at the postsynaptic muscle cells has been identified as regulating a cellular membrane trafficking event, autophagy. HSPGs are a ubiquitous class of macromolecules that play important roles in molecular signaling and morphogen distribution in the extracellular spaces. Loss of HS-biosynthesis in the muscle cell disrupted the organization of SSR, and produced changes in mitochondrial morphology and

numbers. Molecular and genetic findings showed these phenotypes were resulted from inappropriate activation of autophagy. Reducing autophagy in animals with globally compromised HS biosynthesis partially rescued the associated lethality, showing that autophagy is critically affected by HS production. Further evidence showed that HSPGs control autophagy via regulation of PI3K, a downstream mediator of a number of growth factors.

A forward genetic screen was performed in our lab, designed to identify potential *Akt1* downstream effectors and other novel genes required for synapse assembly. *DnaJ2* (CG10565) and *Acinus* were identified for their specific requirements in the regulation of glutamate receptor composition and postsynaptic membrane organization respectively. Further experiments revealed that *Acinus* mediates autophagosome maturation. Animals defective for autophagy exhibited disorganization of both SSR membrane structures and α -Spectrin networks, suggesting that autophagy may affect synapse formation via the control of cytoskeletons.

Collectively, my work demonstrated the functional importance of *Akt1*, *Acinus* and HS-biosynthetic genes in synapse development, suggesting that autophagy may act as a determinant for synaptic morphology and function.

Table of Contents

List of Figures.....	X
List of Tables.....	Xiii
Acknowledgements.....	Xiv
Chapter 1: Introduction.....	1
1.1 General overview.....	1
1.2 Structural anatomy of <i>Drosophila</i> NMJ.....	4
1.3 <i>Drosophila</i> NMJ is a glutamatergic synapse.....	6
1.4 Synaptogenesis at the <i>Drosophila</i> NMJ.....	8
1.5 Development and functions of subsynaptic reticulum.....	10
1.6 Research questions.....	13
1.6.1 Neuronal activities regulated by Akt kinase activity.....	10
1.6.2 Neuronal development regulated by heparan sulfate proteoglycans...	16
1.6.3 Cytoskeletal regulation of synapse assembly.....	19
Chapter 2: Materials and Methods.....	21
2.1 Fly genetics.....	21
2.1.1 Fly stocks and husbandry.....	21
2.1.2 Mutagenesis of <i>DnaJ2</i>	22
2.2 Immunohistochemistry and confocal microscopy.....	23
2.2.1 Solutions.....	23
2.2.2 Immunostaining.....	24
2.2.3 LysoTracker staining for live imaging.....	25
2.2.4 Image acquisition and analysis.....	25
2.3 Transmission electron microscopy.....	26
2.4 Molecular biology.....	27
2.4.1 Real-time quantitative polymerase chain reaction.....	27
2.4.2 <i>UAS-DnaJ2</i> transgenes construction.....	28
2.5 Western blotting analysis.....	29
2.6 Statistical Analysis.....	29

Chapter 3: <i>Akt1</i> regulates glutamate receptor trafficking and postsynaptic membrane elaboration at the <i>Drosophila</i> neuromuscular junction.....	30
3.1 <i>Akt1</i> is essential for proper localization of glutamate receptor subunit IIA but not IIB at the postsynaptic specialization.....	30
3.1.1 <i>Akt1</i> mutant shows altered distribution of glutamate receptor IIA.....	30
3.1.2 Cell-type specific inhibition of <i>Akt1</i> affects glutamate receptor IIA localization.....	32
3.1.3 <i>Akt1</i> regulates glutamate receptor composition by selectively influencing GluRIIA targeting to NMJ.....	34
3.2 <i>Akt1</i> is required for subsynaptic reticulum membrane elaboration.....	36
3.2.1 Muscle-specific inhibition of <i>Akt1</i> affects the elaboration of the subsynaptic reticulum.....	36
3.2.2 <i>Akt1</i> is required for maintaining intracellular membrane organization of muscle cells.....	38
3.2.3 Overexpression of constitutive-active <i>Akt1</i> produces ectopic SSR-like membrane structures without affecting SSR organization.....	40
3.3 <i>Akt1</i> does not affect the NMJ targeting of other synaptic proteins.....	41
3.4 Mechanism of <i>Akt1</i> regulated postsynaptic targeting of GluRIIA.....	44
3.4.1 Loss of <i>Akt1</i> function may disrupt the structural integrity of GluRIIA-mRFP fusion protein.....	44
3.4.2 Regulation of GluRIIA localization by <i>Akt1</i> could be partially mediated by dorsal and cactus.....	46
Chapter 4: Heparan sulfate proteoglycans negatively regulate autophagy during development of the <i>Drosophila</i> neuromuscular junction.....	49
4.1 Heparan sulfate biosynthesis is required for the organization of a specialized postsynaptic structure, the subsynaptic reticulum.....	49
4.1.1 Heparan sulfate polymer synthesis and modification.....	49
4.1.2 RNA interference of heparan sulfate biosynthetic genes.....	51
4.1.3 Loss of heparan sulfate disrupts subsynaptic reticulum organization...	52
4.2 Compromising heparan sulfate biosynthesis produces a net increase in autophagy.....	54

4.2.1 Loss of heparan sulfate increases the number of autophagosomes.....	54
4.2.2 Compromising HS biosynthesis produces a net increase in autophagy and not simply an accumulation of autophagosome intermediates.....	57
4.3 Increased autophagy alters mitochondrial number and morphology in HS biosynthesis defective animals.....	59
4.4 Down-regulation of autophagy suppresses phenotypes associated with heparan sulfate biosynthesis deficiency.....	62
4.4.1 Compromising <i>Atg8a</i> or <i>Atg8b</i> function rescues elevated level of autophagy in animals with reduced <i>sfl</i> function.....	62
4.4.2 Reducing the levels of autophagy in HS biosynthesis defective animals rescues lethality.....	64
4.4.3 Reducing autophagy in animals with compromised <i>sfl</i> function rescues mitochondrial and SSR morphological changes.....	66
4.5 Regulation of autophagy in heparan sulfate biosynthesis compromised animals is mediated by PI3K.....	68
4.5.1 Heparan sulfate biosynthetic deficiency does not induce <i>Xbp1</i> mediated ER stress.....	68
4.5.2 <i>PI3k</i> plays a role in heparan sulfate associated autophagy and mitochondrial morphology.....	70
4.5.3 PIP(3,4,5) triphosphate levels are reduced in muscle cells upon inhibition of HS biosynthesis.....	73
Chapter 5: Gene discovery: a forward genetic screen identified two novel regulators of synapse assembly at the <i>Drosophila</i> NMJ.....	76
5.1 An overview of the RNA interference genetic screen to identify genes involved in <i>Drosophila</i> NMJ development.....	76
5.2 <i>Drosophila Acinus</i> governs autophagic degradation of α -spectrin cytoskeleton and affects SSR membrane organization at the NMJ.....	79
5.2.1 <i>Drosophila Acinus</i> affects SSR membrane organization during NMJ development.....	79
5.2.2 <i>Acinus</i> modulates autophagosome maturation in <i>Drosophila</i> muscle cells.....	82

5.2.3 Compromising <i>ATG8a</i> function affects SSR membrane organization..	85
5.2.4 Suppression of autophagy increases α -spectrin level in the postsynaptic density.....	87
5.2.5 Overexpression of α -spectrin in the muscle disrupts SSR membrane organization.....	89
5.3 DnaJ ₂ , a chaperone protein that regulates glutamate receptor composition at the <i>Drosophila</i> neuromuscular junction.....	91
5.3.1 Identification of <i>DnaJ2</i> as a functional requirement for the proper localization of GluRIIA at the NMJ.....	91
5.3.2 <i>In vivo</i> structure-function analysis of DnaJ2 at the <i>Drosophila</i> NMJ....	94
5.3.3 Investigation of functional link between <i>DnaJ2</i> and <i>Akt1</i> in regulating GluRIIA localization at the <i>Drosophila</i> NMJ.....	97
Chapter 6: Discussion.....	99
6.1 <i>Akt1</i> controls two facets of synapse development: glutamate receptor composition and subsynaptic membrane elaboration through distinct mechanisms.....	99
6.1.1 Overview of primary findings.....	99
6.1.2 <i>Akt1</i> regulates subunit-selective targeting of glutamate receptors to the postsynaptic specialization.....	102
6.1.3 The origin of postsynaptic glutamate receptors: local synthesis versus trafficking-based models.....	104
6.1.4 A possible role of <i>Akt1</i> in glutamate receptor protein folding.....	106
6.2 Regulation of autophagy in <i>Drosophila</i> muscle by HSPG and Acinus is critical for SSR membrane organization at the NMJ.....	107
6.2.1 Overview of primary findings.....	107
6.2.2 Detection of a net increase in autophagy level in HS biosynthesis compromised muscle.....	109
6.2.3 SSR and mitochondrial phenotypes were associated with HS-dependent autophagic events.....	110
6.2.4 The mechanism of HS-dependent inhibition of autophagy.....	112
6.2.5 Heparan sulfate, autophagy and intracellular membrane trafficking...	114

6.2.6 Mechanisms for activating autophagy have potential therapeutic utility	115
6.3 An unbiased forward genetic screen to identify regulators of <i>Drosophila</i> NMJ development	115
6.3.1 Overview of primary findings	115
6.3.2 <i>Acinus</i> is required for autophagosome maturation and SSR organization in <i>Drosophila</i>	118
6.3.3 Autophagic degradation of α -spectrin and its implication in postsynaptic membrane organization	119
6.4 Future direction: functional analysis of <i>DnaJ2</i> in regulating glutamate receptor composition	121
6.4.1 Identification and characterization of <i>DnaJ2</i>	121
6.4.2 <i>In vivo</i> structure/function analysis of <i>DnaJ2</i>	122
6.4.3 Isolation of <i>DnaJ2</i> interacting proteins	123
6.4.4 Investigation of the functional link between <i>DnaJ2</i> and <i>Akt1</i>	123
6.5 Summary	124
References	126

List of Figures

Figure 1.1 Schematic of <i>Drosophila</i> larvae abdominal muscles.....	5
Figure 1.2 Diagram of the <i>Drosophila</i> neuromuscular synapse.....	12
Figure 1.3 Akt resides in the center of PI3K-TOR-Akt signaling pathway.....	16
Figure 3.1 GluRIIA localization is modified in <i>Akt1</i> mutants.....	32
Figure 3.2 GluRIIA localization is affected by reduction of <i>Akt1</i> function in muscle cells.....	34
Figure 3.3 Muscle-specific inhibition of <i>Akt1</i> does not disrupt the normal localization of GluRIIB at the postsynaptic density.....	35
Figure 3.4 Normal SSR expansion is dependent on <i>Akt1</i> expression in the muscle.....	37
Figure 3.5 <i>Akt1</i> is required for the integrity of the muscle endomembrane system	39
Figure 3.6 Overexpression of a constitutively-active form of <i>Akt1</i> creates SSR-like membranes distant from the synaptic region.....	41
Figure 3.7 Levels but not localization of synaptic proteins basigin, DLG and syndapin are affected by loss of <i>Akt1</i> function.....	43
Figure 3.8 <i>Akt1</i> may affect GluRIIA targeting to the NMJ by altering its protein configuration.....	45
Figure 3.9 Influence of Akt1 on dorsal and cactus levels and distributions at the NMJ.....	47
Figure 4.1 Heparan sulfate polysaccharide biosynthesis and modification.....	50
Figure 4.2 RNA interference disrupts gene expression required for HS glycosaminoglycan chain biosynthesis and modification.....	52
Figure 4.3 Ultrastructure of the SSR at the NMJ of animals with compromised HS biosynthesis.....	53
Figure 4.4 Accumulation of autophagosomes in animals with compromised HS biosynthesis.....	56

Figure 4.5 Reductions in HS biosynthesis and modification result in a net increase in autophagic flux.....	58
Figure 4.6 Disrupted HS biosynthesis in muscle tissue affects mitochondrial numbers and morphology.....	61
Figure 4.7 <i>ATG8</i> is essential for increased autophagosome formation in HS biosynthesis compromised animals.....	63
Figure 4.8 Mitochondrial and SSR phenotypes associated with loss of HS modification are suppressed by down-regulation of autophagy.....	67
Figure 4.9 ER stress is not induced in animals with inhibited HS biosynthesis....	70
Figure 4.10 PI3K is implicated in the association between HS biosynthesis and autophagy.....	72
Figure 4.11 Reduction of PI3K activity in HS biosynthesis compromised animals	74
Figure 5.1 Flow chart depicting the collection of RNAi lines selected for use and the experimental outputs of this genetic screen.....	78
Figure 5.2 Loss of <i>Acn</i> in the muscle cells results in morphological defects of the SSR.....	81
Figure 5.3 Knockdown of <i>Acn</i> in muscle cells results in accumulation of autophagosome with enlarged size.....	84
Figure 5.4 <i>ATG8a</i> functional reduction results in SSR disorganization and synapse overgrowth.....	86
Figure 5.5 Reduced <i>Acn</i> or <i>ATG8a</i> function leads to over-accumulation of α -spectrin at the NMJ.....	88
Figure 5.6 Overexpression of α -spectrin in the muscle disrupts SSR organization	90
Figure 5.7 Identification of <i>DnaJ2</i> for its requirement for synapse assembly and generation of <i>DnaJ2</i> mutants.....	93
Figure 5.8 DnaJ2 protein structure and subcellular localization in <i>Drosophila</i> muscle cells.....	96
Figure 5.9 In GluRIIA mislocalization, DnaJ2 does not operate upstream of Akt1 in a functionally relevant manner.....	98

Figure 6.1 Model for Akt1's regulatory role at the NMJ.....	102
Figure 6.2 Model of HSPG, Acinus and ATG8a's regulation of autophagy during the development of postsynaptic cell specialization.....	108

List of Tables

Table 1.1 Several genes with conserved functions in <i>Drosophila</i> and vertebrates.....	4
Table 4.1 Reduction of <i>ATG8a</i> or <i>ATG8b</i> function extends the survival stage in HS compromised <i>Drosophila</i>	62

Acknowledgements

First of all, I would like to express my gratitude to my Ph.D. advisor: Dr. Scott Selleck for all the advice and guidance he has given me along the way of my five years study and research. Scott is the funniest advisor and one of the most optimistic people that I have ever known. He has taught me how to enjoy the research, how to build the confidence, and how to achieve the goals. He has been always supportive and he has given me freedom to pursue projects that I am interested in. He has encouraged me to develop independent thinking and problem solving skills, which are super important for anyone who want to be a scientist.

Besides my advisor, I would like to thank the rest of my thesis committee: Dr. Bernhard Lüscher, Dr. Richard Ordway and Dr. Zhi-Chun Lai for their continuous support and encouragement. I offer my sincere appreciation for their valuable suggestions and insightful comments.

My completion of this thesis could not have been accomplished without the supports from my labmates. My sincere thanks go to all the current and previous members in Selleck lab. In particular, I would like to thank our lab manager, Jie Xu, for her collaboration in the HSPG project. She has been a great colleague, a helpful mentor, and a wonderful friend in my life. Claire Reynolds, an intelligent and energetic young graduate student, has given me a lot of helps during my preparation of dissertation and defense. I really do appreciate her supports. Dr. Hyun-Gwan Lee and I collaborate in the *Akt* project and I appreciate his guidance in this research. Dr. Jieli Xu initiated the HSPG project and her findings inspired my research. Joyce Lee, Do Young Kim, Daniel Song and Morgan Brown are undergraduate students who participated in the genetic screen project. *Acinus* won't be discovered without their efforts. Thank you all for being wonderful colleagues and friends.

Last but not least, I would like to thank my parents: Hongquan Zhao and Xiaofei Zhu, for bringing me to the world and for the unconditional love they have given me. I always feel I am so lucky to have them in my life. I thank them from my deepest heart, for everything they have been done for me. I hope, dad and mum, you will be proud of your daughter!

Chapter1: Introduction

1.1 General overview

The synapse is the fundamental unit that conveys cell-cell communications in the nervous system. Synapse formation and refinement are dynamically regulated by numerous inputs from the environment, neuronal activity and gene functions. These processes require changes at both the molecular and the morphological level, allowing previous activity to shape the physiological properties of synaptic communication. Understanding the molecular and genetic mechanisms that shape synapse development and activity-dependent synaptic changes is a central issue in developmental neuroscience.

The *Drosophila* neuromuscular junction (NMJ) is a glutamatergic synapse that serves as an excellent model system to study fundamental questions about synapse development. Unlike the vertebrate NMJ which is a cholinergic synapse, the major excitatory neurotransmitter released at the *Drosophila* NMJ is glutamate, similar to the vertebrate central nervous system (CNS) (Jan and Jan, 1976b). Furthermore, many of the genes regulating synapse development and plasticity, such as Discs-Large (DLG) and Fasciclin-2 (Fas-2), are highly conserved throughout evolution, making it possible to ask fundamental and broadly applicable questions of neurobiology in this relatively simple, easily-accessible model (Table 1.1). The *Drosophila* NMJ is well-known for its regular anatomy and robust plasticity. In each hemi-segment of the larval abdomen, 32 identified motoneurons form morphologically and physiologically stereotypical synapses on 30 identified postsynaptic muscle cells, allowing for robust comparison between individual animals at single-cell resolution (Jan and Jan, 1976a; Johansen et al., 1989; Broadie and Bate, 1993c; Landgraf et al., 1997; Schmid et al., 1999). Gene families comprised of multiple functionally redundant members are less common in *Drosophila* than in higher order model organisms, making the interpretation of genetic experiments less complicated. Regardless of this relative genetic and structural simplicity, the *Drosophila* NMJ is not lacking in

experimental power. For example, the *Drosophila* NMJ is an amenable model system for various experimental techniques including electrophysiology, immunohistochemistry and electron microscopy, as well as live imaging and behavioral studies. The powerful genetic toolbox made available by the *Drosophila* community contributes heavily to the merits of using this model organism. In addition to a variety of mutagenesis approaches, studies of those genes essential for viability are greatly expanded with the usage of the *UAS-Gal4* binary expression system combined with RNA interference, through which loss-of-function effects can be evaluated in a temporally and spatially controlled manner (Brand and Perrimon, 1993; Bosher and Labouesse, 2000; McGuire et al., 2004; Dietzl et al., 2007; Perrimon et al., 2010). Lastly, a short life cycle and easy maintenance make large-scale genetic screens feasible in *Drosophila*, increasing the convenience and efficiency with which the molecular and genetic basis of synapse development and function can be studied.

The *Drosophila* NMJ has been served as a powerful model for studying neuronal diseases caused by defects in synaptogenesis. For example, a dominant genetic disorder, tuberous sclerosis, is caused by mutations in either of two tumor suppressor genes, *tuberous sclerosis complex 1* and *2* (*TSC1/2*) (Pan et al., 2004). Patients often develop benign tumors in brain and other vital organs and are frequently diagnosed with seizures, intellectual disabilities and developmental delay. TSC1 and 2 are components of a highly conserved growth regulatory pathway which includes *Target of Rapamycin* (*TOR*) and *Ras homolog enriched in brain* (*Rheb*). TSC1 and 2 normally suppress the gene function of *Rheb*. Therefore our lab established a tuberous sclerosis disease model by overexpressing *Rheb* at the *Drosophila* NMJ and multiple neuronal disorders in NMJ outgrowth, axon guidance and phototaxis are found to be associated with enhanced *Rheb* activity (Dimitroff et al., 2012). Another well-known neuronal disease model established in *Drosophila* is for fragile X syndrome, an inherited genetic disorder that leads to mental retardation and autism spectrum disorders. Fragile X syndrome is caused by point mutations affecting the *fragile X mental*

retardation 1 (FMR1) gene. In the *Drosophila* model, *FMR1* function negatively regulates the synaptic levels of two heparan sulfate proteoglycans: syndecan and dally-like protein (Friedman et al., 2013). These two proteins act as co-receptors for Wnt and ERK signalings during synaptogenesis. Loss of *FMR1* gene function results in increased levels of syndecan and dally-like protein and consequent defects in synaptic structure and transmission activity.

Investigation of novel regulators controlling synaptic development in *Drosophila* is of great importance and will be instructive to our understanding of human diseases. In this thesis, using *Drosophila* NMJ as the model synapse, I aim to explore the roles of a kinase, an extracellular matrix component and an autophagy-related gene, in the assembly of a functional synapse. Specifically, those regulatory molecules are: (1) Serine-threonine kinase Akt is a component of the highly conserved TSC-PI3K-TOR signaling pathway which is known to be important in human neurological diseases. (2) Heparan sulfate proteoglycan is a class of ubiquitous macromolecules well known for its function in signaling transduction at the cell surface. (3) *Acinus* is a gene responsible for endocytic/autophagic trafficking. Their functions at the *Drosophila* NMJ, especially the postsynaptic field were explored and the results are presented in chapters 3-5 in this thesis.

Table 1.1 Several genes with conserved functions in *Drosophila* and vertebrates

<i>Drosophila</i>	vertebrate	function
Discs-Large (DLG)	postsynaptic density protein 95 (PSD-95)	member of the membrane-associated guanylate kinase (MAGUK) superfamily, plays roles in the clustering of ion channels, receptors and cell adhesion molecules at the synapse
Fasciclin 2 (Fas-2)	neural cell adhesion molecule (NCAM)	member of immunoglobulin (Ig) - related superfamily of cell adhesion molecules, plays roles in axon guidance and neurite outgrowth
shaker	KCNA3 (Kv1.3)	potassium voltage-gated ion channel
cysteine string protein (CSP)	DnaJ homolog subfamily C, member 5 (DNAJC5)	a guanine nucleotide exchange factor (GEF) for Gα proteins, plays a role in neurotransmitter release
Neurexin	Neurexin	presynaptic cell-adhesion molecule, interacts with neuroligin, plays roles in axon guidance and synaptogenesis
bruchpilot	CAZ-associated structure protein (CAST)	active zone protein, involved in neurotransmitter release

1.2 Structural anatomy of *Drosophila* NMJ

The somatic muscles of *Drosophila* larvae are arranged in a stereotyped pattern, repeated in each abdominal segment from A2 to A7 (Figure 1.1). The *Drosophila* muscle is single, multinucleated cell generated by myoblast fusion (Keshishian et al., 1996). During embryogenesis, motoneurons extend axonal projections into the body wall musculature. Each muscle expresses distinct molecular cues that direct the correct targeting of nerve terminals for muscle innervation (Broadie and Bate, 1993c). For each muscle, the synaptic connection has a defined size, shape and site of attachment (Landgraf et al., 1997; Schmid et al., 1999). For each hemi-segment within the region from A2 to A7, there are 30 muscle cells (identified numerically) innervated by 32 motoneurons (Schmid et al., 1999). Each synaptic connection consists of 20-50 boutons, the terminal structures of axonal branches responsible for neurotransmitter release, opposed and surrounded by the subsynaptic membrane compartment of the muscle (Collins and DiAntonio, 2007). Within each bouton, there are approximately 10 active zones, hot-spots for neurotransmitter release that appear in electron microscopic

images as electron-dense “T-bar” structures (Fouquet et al., 2009; Oswald and Sigrist, 2009). Opposite of these active zones are postsynaptic clusters of neurotransmitter receptors, as well as other specialized subsynaptic structures. Based on distinct morphology and neurotransmitter composition, synaptic boutons can be divided into three categories. Type I boutons are the largest neuronal endings found on all muscle fibers, primarily releasing glutamate (Jan and Jan, 1976a; Johansen et al., 1989; Atwood et al., 1993). Type I boutons can be further divided into the subtypes Ib (big) and Is (small) based on size. Type II boutons are much smaller than type I boutons and release octopamine as a co-transmitter (Monastirioti et al., 1995). Type III boutons contain insulin-like peptides and proctolin, and are found exclusively on muscle 12 (Anderson et al., 1988; Gorczyca et al., 1993).

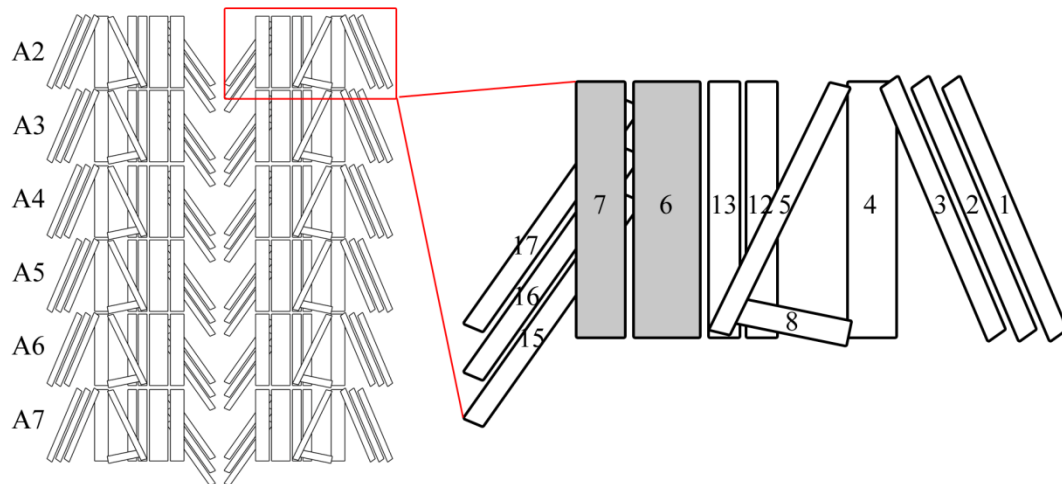


Figure 1.1 Schematic of *Drosophila* larvae abdominal muscles. The body wall muscles of *Drosophila* larvae are arranged as symmetric segmental repeats in the region of A2 to A7. All of the muscle cells have defined size and shape and are named using numerical numbers. The representative hemisegment of A2 is demonstrated in the enlarged view. Several ventral side muscles are demonstrated here. Muscles 6 and 7 (grey) are the most commonly used muscles in morphological and physiological studies. (Updated from Bridget K. Campion, “Hemisegments A2-A7 of the *Drosophila* larval abdomen”)

1.3 *Drosophila* NMJ is a glutamatergic synapse

At the *Drosophila* NMJ, signal transduction through chemical synapses is unidirectional, mediated by voltage- and ligand- gated ion channels. Action potentials produced in the neuron travel along the presynaptic membrane until they reach the axonal terminals. The voltage change on the plasma membrane is sensed by voltage-gated calcium channels, leading to the opening of these channels and influx of Ca^{2+} across the presynaptic cell membrane. Ca^{2+} binds to synaptotagmin, which then interacts with SNARE proteins to trigger fusion of synaptic vesicles with the presynaptic membrane, allowing release of neurotransmitters into the synaptic cleft. Neurotransmitters then bind their corresponding receptors on the postsynaptic membrane, allowing the signal to propagate onward. Postsynaptic receptors are classified as ionotropic or metabotropic depending on their structural and functional characteristics. Ionotropic receptors are ligand-gated ion channels that mediate rapid membrane potential changes (Hollmann and Heinemann, 1994). In contrast, metabotropic receptors, also referred to as G-protein-coupled receptors, do not form ion channels but instead regulate long-term potentiation through second messengers in response to presynaptic signals (Raymond et al., 2000; Pfeiffer and Huber, 2006). Depending on the nature of the presynaptic electric signals, either excitatory or inhibitory receptors are activated, which mediate excitatory postsynaptic potential or inhibitory postsynaptic potential respectively.

L-glutamate is the primary excitatory neurotransmitter used by almost all synapses in the vertebrate central nervous system (Jan and Jan, 1976b; Johansen et al., 1989; Broadie and Bate, 1993c). Ionotropic glutamate receptors can be further classified into NMDA receptors, AMPA receptors and Kainate receptors according to their sensitivity to specific agonists. The *Drosophila* genome encodes 15 putative ionotropic glutamate receptor subunits, including representative of each subtype. Among those, the receptors predominantly responsible for synaptic transmission are A- and B-type glutamate receptors, which are orthologs of vertebrate AMPA and Kainate receptors. Both A- and B-

type receptors are heterotetramers consisting of the essential subunits GluRIIC, IID and IIE, along with one of either IIA or IIB (Marrus et al., 2004; Featherstone et al., 2005; Qin et al., 2005a; DiAntonio, 2006). Neither GluRIIA nor IIB is specifically necessary for viability, however, animals lacking both of them experience embryonic lethality. These two subunits are differentially localized to postsynaptic specializations surrounding distinct subsets of motoneuron endings. While IIB is concentrated at both type Ib and type Is boutons, GluRIIA is only present at high levels around type Ib boutons, indicating that motoneuron innervation may affect postsynaptic glutamate receptor composition through an anterograde signaling mechanism (Marrus et al., 2004). Miniature excitatory junctional potentials (mEJPs) measure the muscle's response to the spontaneous release of a single synaptic vesicle. Since the contents of neurotransmitter vesicles are constant, the amplitude of an mEJP (membrane voltage change, also known as quantal size) is largely determined by postsynaptic properties, namely glutamate receptor composition and density (Jan and Jan, 1976a). Synapses expressing exclusively GluRIIA subunits exhibit significantly larger quantal size than those expressing GluRIIB subunits (DiAntonio et al., 1999; Schmid et al., 2008). This is supported by studies that found a significant reduction in the postsynaptic response to spontaneous neurotransmitter release in GluRIIA mutants (Petersen et al., 1997), along with enhanced long-term depression following high-frequency stimulation (Reiff et al., 2002). The kinetics of synaptic potentials are also different in these two kinds of synapses. The time course of mEJP decay is much shorter in GluRIIA-containing synapses than that of GluRIIB-containing synapses (DiAntonio et al., 1999).

The distinct physiological characteristics of GluRIIA and IIB subunits provide a convenient way to control both developmental and activity-dependent synaptic plasticity, by simply adjusting the ratio of receptor subunits. At the developing NMJ, GluRIIA competes with IIB for the common subunits GluRIIC, IID and IIE. Overexpression of either GluRIIA or IIB substantially decreased the synaptic concentration of the other subunit (Marrus et al., 2004). At immature synapses,

GluRIIA is the predominant glutamate receptor subunit; IIB subunits are increasingly added to the postsynaptic densities as they mature (Schmid et al., 2008). Synapses containing predominantly A-type glutamate receptors, resulting from either transgenic overexpression of GluRIIA, general increase in subsynaptic protein synthesis, or GluRIIB hypomorphic mutants, produces a long-lasting strengthening of synaptic transmission and coordinates morphological changes at the synapse (Sigrist et al., 2002). Enhanced larval locomotor activity strongly increased NMJ outgrowth and postsynaptic accumulation of GluRIIA subunits, resulting in experience-dependent strengthening of signal transmission. However, such adapted synaptic plasticity and functional improvement are completely abolished in GluRIIA mutant animals (Sigrist et al., 2003). Taken together, these findings demonstrate that GluRIIA-containing receptors are the primary glutamate receptors responsible for normal synaptic activity and sensitivity, while GluRIIB containing receptors provide not only functional redundancy but also an important modulatory mechanism during developmental and activity-dependent synapse transmission.

1.4 Synaptogenesis at the *Drosophila* NMJ

During the early stages of embryonic development, positional information directs cell differentiation and myogenesis by controlling the expression of the transcription factor *twist*, which activates mesoderm specific gene expression and promotes somatic muscle formation (Thisse et al., 1987; Yin et al., 1997; Bate et al., 1999). Somatic mesoderm is further differentiated into founder cells and fusion-competent myoblasts which then fuse into multinucleated muscles during stages 11-13 of embryogenesis (Keshishian et al., 1996). The motoneuron growth cones exit the CNS immediately after somatic muscle fiber formation during stage 14 of embryogenesis (Gorczyca et al., 1994). Each motoneuron navigates by following distinct guidance cues to reach their destination on target muscle cells. There is evidence to show that this axonal outgrowth does not completely rely on the presence of target muscles, since ablation of the target muscle does not prevent correct projection into the preferred location (Sink and

Whittington, 1991; Cash et al., 1992). On the postsynaptic side, delineation of NMJ sites is initiated by spontaneous clustering of adhesive molecules such as Fasciclin III and connectin, and is independent of motoneuron innervation (Broadie and Bate, 1993a). Initially, glutamate receptors are distributed homogenously on the membrane surface without obvious clustering (Broadie and Bate, 1993a; Saitoe et al., 1997). Stimulated by motoneuron innervation, glutamate receptors begin to concentrate rapidly to synaptic contact sites and reach a stably high level in 2 hours. Synaptic transmission can be detected within several minutes of the initial motoneuron-muscle contact (Broadie and Bate, 1993a). Neuronal activity is constantly required for glutamate receptor expression and clustering throughout the entire process of embryonic synaptogenesis (Broadie and Bate, 1993b). This was revealed through use of a temperature-sensitive *para* mutant, which exhibits normal synaptic transmission at the permissive temperature (25°C), but experiences increasingly severe reductions in transmission as the temperature raises beyond the restrictive level (30°C) (Suzuki et al., 1971; Broadie and Bate, 1993b). *Para*^{ts} mutant embryos reared continuously at the restrictive temperature, along with embryos that are shifted to restrictive temperatures during the mid-stages of synaptogenesis both show dramatic reductions in glutamate receptor expression. Synaptic transmission and an appropriate concentration of glutamate receptors can be recovered in these animals by shifting embryos back to permissive temperatures at later stages of embryonic development, demonstrating that presynaptic electrical activity is both necessary and sufficient for GluR expression at the NMJ (Broadie and Bate, 1993b). Further studies revealed that junctional clustering of glutamate receptors relies on spontaneous neurotransmitter release, independent of evoked synaptic vesicle exocytosis (Saitoe et al., 2001). Interestingly, non-vesicular release of neurotransmitters negatively regulates glutamate receptor levels at the NMJ (Featherstone et al., 2002; Augustin et al., 2007). Compared with the fast, concentrated release of vesicular glutamate, non-vesicular glutamate is diffusely distributed at the NMJ at relatively low levels (Featherstone et al., 2002). It is possible that these two dynamic and mechanistically distinct processes are

responsible for the delicate regulation of postsynaptic glutamate receptor field formation. While vesicle-mediated glutamate release is required for glutamate localization in a close vicinity to axon terminal boutons, non-vesicular glutamate may play a role in the suppression or elimination of extra-synaptic GluR clustering. This idea is supported by the observation that young GluR clusters are not always associated with active zone markers, whereas almost all GluR specializations older than 10 hours are tightly associated with corresponding presynaptic active zones (Rasse et al., 2005). *In vivo* experiments that monitored dynamic localization of fluorophore-tagged glutamate receptor subunits showed that new synapses are formed *de novo* at sites distant from existing synapses, rather than by division of mature synapses. Glutamate receptors are preferentially incorporated into newly formed synapses until finally the synapses reach a mature size, at which point they become stabilized and experience a fairly low receptor exchange rate (Rasse et al., 2005).

1.5 Development and function of the subsynaptic reticulum

The efficacy of synaptic transmission depends on a number of important pre- and post-synaptic elements, including synaptic release of neurotransmitters and the number and conductance of receptors and channels, as well as the specialized postsynaptic membrane structures. At the *Drosophila* neuromuscular junction, a complex tubulolamellar postsynaptic membrane structure known as the subsynaptic reticulum (SSR) expands parallel to muscle growth during larval development (Jia et al., 1993; Guan et al., 1996). This convoluted and multilayered postsynaptic membrane specialization is formed by both plasma membrane invagination and targeted membrane addition. Extensive membrane infoldings are initiated in the first instar larvae at locations where the surface of the muscle opposes motoneuron terminal boutons. Nascent SSR is generated by plasma membrane invagination. Further extension and tubulation of SSR is facilitated by an F-bar domain containing protein, syndapin (Kumar et al., 2009). The SSR is also greatly expanded by targeted membrane addition throughout larval development. This spatially-restricted exocytosis is tightly controlled by

DLG, a *Drosophila* ortholog of postsynaptic density protein-95 (Lahey et al., 1994; Budnik et al., 1996; Guan et al., 1996). DLG belongs to the membrane associated guanylate kinases superfamily, which is well-known for its role in protein interactions (Kim et al., 1995; Kornau et al., 1995; Tejedor et al., 1997; Thomas et al., 1997; Zito et al., 1997). Membrane addition at the SSR, the small membrane specialization accounting for only 1% of the total muscle surface area, is coordinated by an interaction between DLG and a *Drosophila* t-SNARE protein, Gtaxin (Gorczyca et al., 2007). These two underlying mechanisms of SSR membrane elaboration are mechanistically distinct and occur independently of one another, as evinced by the observation that syndapin activated SSR tubulation in the absence of DLG (Kumar et al., 2009). Moreover, while syndapin overexpression results in local extension and tubulation of existing SSR, overexpression of Gtaxin produces ectopic membrane structures without altering the dimensions of the pre-existing synaptic SSR; again, showing a clear distinction between these two regulatory processes (Gorczyca et al., 2007).

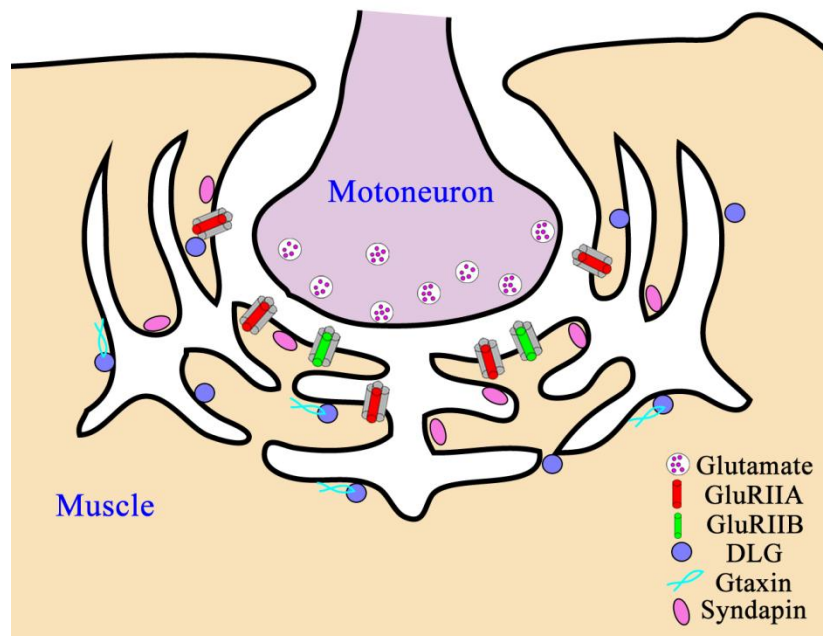


Figure 1.2 Diagram of the *Drosophila* neuromuscular synapse. At the *Drosophila* NMJ, motoneuron terminal is embedded on the muscle surface. SSR, a highly convoluted membrane

elaboration is formed at the neuron-muscle contact site. SSR increases in size and complexity in cohort with muscle growth and synapse maturation. The membrane invagination and expansion are regulated by synaptic proteins DLG, Gtaxin and syndapin.

Although several identified genes are known to regulate SSR development, the function of SSR remains elusive. The convoluted nature of the SSR greatly increases the surface area available for clustering of functionally important postsynaptic proteins such as glutamate receptors, cell adhesion molecules and ion channels. Besides serving as a passive attachment point for these proteins, the SSR may also play an active role in the differential regulation of glutamate receptor localization. The SSR is extensively folded at type Ib boutons, but has a less convoluted structure at type Is boutons (Jia et al., 1993). This is consistent with the observation that GluRIIA subunits are only present at high levels at type Ib boutons, suggesting that the SSR may play a role in the stabilization of A-type glutamate receptors. Most importantly, the SSR has been implicated in local synthesis of synaptic proteins, which constitutes an important mechanism for long-term synaptic plasticity (Sigrist et al., 2000). Large aggregates of translational machinery including translation initiation factors eIF4E and poly A-binding protein (PABP), as well as GluRIIA messenger RNAs, are found within and in the periphery of SSR membrane infoldings, suggesting that the SSR may possess some ER-like properties. Genetically elevated postsynaptic translation leads to increased subsynaptic expression of GluRIIA and a persistent enhancement in synaptic transmission, further supporting the idea that SSR plays an important role in the subsynaptic translation of GluRIIA.

SSR-like structure is not unique to *Drosophila* but was also found at the vertebrate NMJs. For example, an elaborated membrane structure called subsynaptic sarcoplasm was found at the frog neuron-muscle conjunction (Shotton et al., 1979). This structure greatly enlarges the membrane surface available for acetylcholine receptor clustering, showing a similar function as SSR has at the *Drosophila* NMJ. In addition, at the mouse NMJ, membranes beneath the neuronal terminal also folds into a structure that analogous to the SSR at the

Drosophila NMJ (Rafuse et al., 2000). It is possible that genes regulating SSR assembly in *Drosophila* have conserved functions in other species.

1.6 Research questions

1.6.1 Neuronal activities regulated by Akt kinase activity

Synaptic plasticity requires molecular and morphological changes that allow previous activity to shape the physiological properties of synaptic communication. Among those molecules regulating synaptic plasticity, secreted protein growth factors such as brain-derived neurotrophic factor (BDNF) play essential roles in synaptic plasticity, directing developmental and activity-dependent changes at these specialized cell junctions (Lauterborn et al., 2007). One signaling molecule of central importance for the integration of many growth factor inputs is the serine-threonine kinase Akt, also known as protein kinase B. Akt was first identified as an oncogene in a transforming retrovirus isolated from mice, which caused a high frequency of tumorigenesis (Staal et al., 1977). Akt resides in the center of the insulin stimulated PI3K-Akt-TOR signaling pathway (Figure 1.3) (Manning and Cantley, 2007). Insulin binding activates autophosphorylation of its receptor and subsequent activation of PI3K. PI3K activity produces phosphatidylinositol (3,4,5)-triphosphate (PIP3) by phosphorylation of PIP2. Akt possesses an N-terminal pleckstrin homology (PH) domain through which it binds to PIP3. Akt is recruited to the plasma membrane by PIP3 binding, where it receives an activating phosphorylation at threonine 308 from phosphoinositide-dependent kinase 1 (PDK1), another PI3K substrate. A second activation-specific phosphorylation at serine 473 is catalyzed by target of rapamycin complex 2 (TORC2) only after the initial activating phosphorylation has occurred. Akt functions at its highest capacity only after phosphorylation at both sites. Phosphorylation at threonine 308 increases the catalytic activity of Akt approximately 100 fold, while phosphorylation at serine 473 results in another 10 fold increase in activity (Bellacosa et al., 2005).

In mammalian systems, three Akt isoforms govern a broad range of cellular and physiological processes from cell growth to membrane trafficking (Zhang et al., 2002; Manning and Cantley, 2007). Akt1 plays critical roles in cell growth and cell survival (Chen et al., 2001). Akt2 phosphorylation of AS160 influences exocytosis of glucose transporter-containing vesicles, providing an increased capacity for glucose transport across the plasma membrane (Gonzalez and McGraw, 2006; Watson and Pessin, 2006; Grillo et al., 2009). Consistent with a role for Akt2 in glucose uptake and homeostasis, *Akt2* null mice show defects in insulin-stimulated glucose uptake (Nakatani et al., 1999; Cho et al., 2001; Bae et al., 2003; Easton et al., 2005; McCurdy and Cartee, 2005). *Akt3*, the isoform expressed most abundantly in the central nervous system, is essential for normal brain growth, affecting both the number and size of neurons (Tschopp et al., 2005).

Akt signaling is also known to govern neuronal survival and neurite outgrowth directly. Although Akt and S6 Kinase are both PI3K downstream effectors, Akt alone is specifically required for insulin-like growth factor 1 (IGF-1) induced cerebellar neuron survival (Dudek et al., 1997). Expression of wild-type *Akt* promotes neuronal survival, whereas expression of a dominant-negative *Akt* failed to suppress apoptosis caused by deprivation of survival factor IGF-1. Further studies revealed that *Akt* enhances neuronal survival by both increasing the expression of survival genes and by directly inhibiting cytoplasmic apoptotic machinery (Brunet et al., 2001). There is evidence that *Akt* is involved in neuronal outgrowth as well. It has been demonstrated that insulin mediated dendritic spine formation in rat hippocampal neurons is dependent on PI3K and Akt activity (Lee et al., 2011). Expression of a constitutively-active form of Akt strongly potentiated both axonal and dendritic branching and elongation in hippocampal neurons (Jaworski et al., 2005; Kumar et al., 2005; Zheng et al., 2008; Grider et al., 2009). Akt1 also regulates dendrite formation in *Drosophila* peripheral sensory neurons, demonstrating functional conservation of the protein's capacity for neuronal growth regulation (Parrish et al., 2009). In

addition to its roles in neuronal survival and outgrowth, Akt has also been implicated in synapse assembly and synaptic transmission. Phosphorylation of the type A GABA receptor by Akt increases its localization to the postsynaptic specialization, thereby enhancing the receptor-mediated inhibitory transmission in these synapses (Wang et al., 2003; Serantes et al., 2006). Akt1 is also important for synaptic long-term depression at the *Drosophila* NMJ (Guo and Zhong, 2006). Long-term depression is severely disrupted in *Akt1* hypomorphic mutants, a phenotype that was successfully rescued by transgenic expression of wild type *Akt1*, demonstrating a requirement for *Akt1* function in mediating long-term synaptic activity.

Previous studies in our lab showed that target of rapamycin (TOR), a serine-threonine protein kinase, regulates axon guidance, synapse assembly and plasticity (Knox et al., 2007). Further experiments revealed a number of complexities in Tor-directed signaling that affect nervous system development (Figure 1.3) (Dimitroff et al., 2012). Tor complex 1 (TorC1) is critical for normal axonal guidance and organismal behavior, while Tor complex 2 (TorC2) regulates the size and complexity of synapses. Neuronal overexpression of PI3K, a principal mediator of growth factor signaling to Tor, resulted in synaptic overgrowth without disrupting axon guidance or phototaxis. The single *Akt* gene in *Drosophila*, *Akt1*, is a downstream effector of and substrate for phosphorylation by both PI3K and TORC2 (Huang and Manning, 2009). The central role of *Akt1* in signal integration prompted us to explore its function in the development of the *Drosophila* NMJ and our findings are presented in Chapter 3.

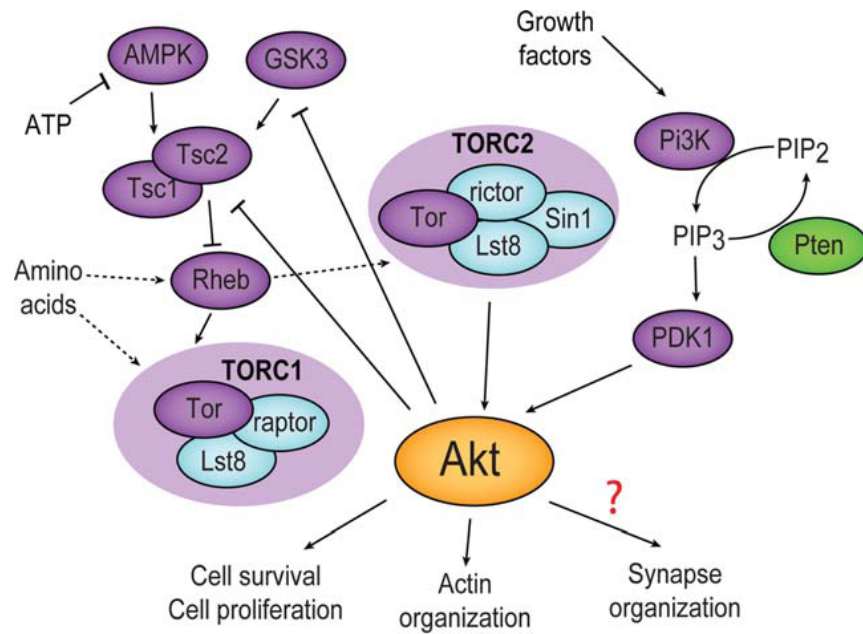


Figure 1.3 Akt resides in the center of PI3K-TOR-Akt signaling pathway. Activation of Akt requires phosphorylation at the threonine and serine residues by PDK1 and TOR complex 2. Akt plays a central role in a number of signaling processes, acting both downstream and upstream of growth factor and nutritional sensor-directed events. The Akt kinase governs a number of cellular activities including cell proliferation, cell survival, and cytoskeleton organization. Its function in synapse development remains unclear and therefore to be the primary goal for this analysis (Adapted from Dimitroff et al., 2012 by Hyun-Gwan Lee in Lee et al. 2013).

1.6.2 Neuronal development regulated by heparan sulfate proteoglycans

Besides of signaling molecules, synaptogenesis and neuronal activities are also controlled by a group of proteins in the extracellular spaces, heparan sulfate proteoglycans. Proteoglycans are a heterogeneous family of extracellular macromolecules composed of core proteins decorated by one or more linear polysaccharide chains. The long unbranched glycosaminoglycan (GAG) chains consist of repeated disaccharides, covalently attached to specific serine residues of the protein backbone via a tetrasaccharide linker (xylose-galactose-galactose-uronic acid) (Izumikawa et al., 2006; Kirkpatrick and Selleck, 2007; Sarrazin et al., 2011). GAG chains can be classified into the following four groups based on their molecular composition: heparan sulfate, chondroitin sulfate, dermatan sulfate and karatan sulfate. Heparan sulfate chains are comprised of alternating

residues of *N*-acetyl glucosamine (*N*-GlcNAc) and either glucuronic acid or iduronic acid, individual units of which may be sulfated. HSPGs can be further divided into three subtypes based on whether and how the core proteins associate with the plasma membrane. Syndecans are a group of single-pass transmembrane proteins, with only one member in *Drosophila* (Spring et al., 1994; Xian et al., 2010). Glypicans are attached to the outer leaflet of the plasma membrane via a glycosylphosphatidylinositol (GPI) anchor (Mertens et al., 1992; Aviezer et al., 1994). The *Drosophila* genome features two identified glypicans, referred to as Dally (division abnormally delayed) and Dally-like (Nakato et al., 1995; Khare and Baumgartner, 2000). The third category of HSPGs contains the secreted proteins agrin, perlecan and proteins of the collagen family. The biosynthesis and modification of heparan sulfate chains occurs in the Golgi apparatus, a process catalyzed in strict progression by members of the exostosin glycosyltransferase (EXT) family and a number of *N*-deacetylase/*N*-sulfotransferases (Izumikawa et al., 2006).

Heparan sulfate-modified proteins are ubiquitous components of the cell surface and extracellular matrix. These highly sulfated macromolecules play crucial roles in regulating developmental signaling pathways, including Wingless/Wnt, hedgehog, the bone morphogenetic protein family, transforming growth factor- β and fibroblast growth factors in a myriad of systems (Lander and Selleck, 2000; Lin, 2004; Hacker et al., 2005; Bishop et al., 2007; Kirkpatrick and Selleck, 2007). In addition to regulating cell specification via these signaling pathways during development, HSPGs participate in cellular processes critical for assembly of the nervous system, including axon path-finding and synaptogenesis. Biochemical and genetic analyses revealed that HSPG functions in axon guidance via interaction with three pairs of ligand/receptors, Slits/Robos, netrins/netrin receptor and Ephrins/Ephrin receptor, by either facilitating the presentation of ligands to their appropriate receptors, or by enhancing ligand binding as co-receptors (Bennett et al., 1997; Ethell and Yamaguchi, 1999; Liang et al., 1999; Ethell et al., 2001; Hu, 2001). Synapse assembly is also influenced by HSPG

function. For example, syndecan, a transmembrane HSPG, is found concentrated at central synapses where it induces the maturation and formation of dendritic spines (Ethell and Yamaguchi, 1999). A GPI-linked HSPG protein, glypican 4, was recently identified as a co-receptor for leucine rich repeat (LRR) protein LRRTM4, an inducer of trans-synaptic communication and synaptogenesis in hippocampal neurons (Siddiqui et al., 2013). During the development of the neuromuscular junction, the HSPG agrin provides critical control over neuronal assembly. Agrin (Z^+ isoform) is secreted from motor neurons to the nerve-muscle basal lamina to induce local aggregation of neurotransmitters and other synaptic proteins essential for postsynaptic assembly (Denzler et al., 1997). Agrin-deficient mice show reduced numbers of pre- and post-synaptic specializations with impaired transmission due to dysregulation of the MAP kinase pathway (Ksiazek et al., 2007). Glycosaminoglycan chain biosynthesis and sulfate-modification are also critical for the morphological development and functional activity of the NMJ. A recent study revealed that two genes affecting heparan sulfation, *sulf1* and *hs6st*, differentially affect synaptic transmission as well as multiple signaling pathways at the *Drosophila* NMJ (Dani et al., 2012).

While a great deal of work in organisms ranging from *C. elegans* to mice has informed the *in vivo* functions of HSPG in synapse development, the cellular processes regulated by this ubiquitous class of extracellular matrix proteins remain incompletely understood. Earlier work from our lab demonstrated that HS biosynthesis is critical for normal assembly of the NMJ in *Drosophila*, affecting both motoneuron and muscle cell development (Ren et al., 2009). For example, the rate of endocytic recycling of synaptic vesicles after neuron firing was dramatically elevated in HS biosynthetic mutants. The levels of ER and Golgi markers in the muscle cell were also altered, suggesting that the organization of these membrane compartments was influenced by loss of HS modification of ECM proteins. However, a molecular mechanism accounting for these diverse phenotypes was not readily apparent. Whether compromising HS biosynthesis

affected other membrane trafficking events in motoneuron or muscle cells? Are those pre- and post-synaptic phenotypes associated or independent? Does loss of HS function influence synaptic organization cell-autonomously? Whether HSPG act as co-receptors for growth factor signaling pathways in their regulation of NMJ assembly, as they do in many other tissues and events? To understand these questions and further explore the mechanistic function of HS, tissue-specific knockdown of genes responsible for HS biosynthesis and modification was conducted in *Drosophila* and the results are presented in Chapter 4.

1.6.3 Cytoskeletal regulation of synapse assembly

Another important element controlling synapse formation and synaptic structure organization is cytoskeleton protein. The cytoskeleton is a fundamental structural component of all cell types and has a myriad of functions in controlling cell formation and stability, such as sculpting and maintaining cell shape, establishing cell polarity and mediating intracellular protein trafficking (Bennett, 1982; Geiger, 1983; Burridge et al., 1988). Cytoskeletal proteins are also highly expressed at the NMJ, where they govern synapse assembly and function directly. Actin is a globular protein that assembles into short filaments. The short F-actin filaments connect with spectrin via protein 4.1 to form a highly cross-linked network at the synapse. This actin-spectrin cytoskeleton structure is important for both pre- and post-synaptic assemblies (Cingolani and Goda, 2008). Synaptic vesicle processes upon neuronal stimulation including loading of neurotransmitters and fusion with the plasma membrane at the presynaptic terminal are dependent upon actin filaments (Dillon and Goda, 2005). Actin filaments have dual functions in regulating the synaptic vesicle pool. On one hand, actin promotes vesicle recycling and prevents vesicles from accessing the plasma membrane by interacting with synapsin (Greengard et al., 1994; Shupliakov et al., 2002; Evergren et al., 2007). On the other hand, actin filament has been shown to help recruit synaptic vesicles to the active zone in an N-ethylmaleimide sensitive factor dependent manner (Nunes et al., 2006). These opposing roles of actin in controlling vesicle mobility may constitute a fine-tuning mechanism for

modulation of neurotransmitter release. At the postsynaptic specialization, actin and the associated protein 4.1 are required for subunit-specific glutamate receptor localization (Chen et al., 2005). The *Drosophila* homolog of protein 4.1, coracle, physically interacts with the C-terminus of glutamate receptor subunit IIA. coracle and actin filaments were shown to be necessary for IIA localization as well as IIA-dependent synaptic transmission. Mutants of coracle or pharmacological disruption of actin significantly reduced the size of A-type receptor clusters without changing the postsynaptic fields of B-type receptors. Interestingly, microtubules, a different cytoskeletal element, seem to affect glutamate receptor localization at the NMJ by a separate mechanism, since overexpression of α -tubulin in the postsynaptic cell results in smaller A-type receptor clusters (Liebl et al., 2005). Spectrin is also abundantly expressed at the NMJ, where it is necessary for stabilization of pre-synaptic structures (Featherstone et al., 2001; Pielage et al., 2005, 2006). Loss of spectrin function in the presynaptic cell leads to severe synapse retraction and depletion of synaptic vesicles (Pielage et al., 2005). Consistent with this finding, neurotransmitter release and subsequent evoked synaptic response were disrupted in spectrin mutants (Featherstone et al., 2001). Moreover, spectrin is required both pre- and post-synaptically for proper organization of the subsynaptic reticulum (Pielage et al., 2005, 2006).

A forward genetic screen designed to explore novel regulators of synapse assembly leads to the finding of Acinus, a known regulator of autophagic and endocytic trafficking. Further analysis connects the function of Acinus in SSR assembly and cytoskeleton organization to its specific regulatory role in controlling autophagy. Considering the critical structural and regulatory roles of spectrin-actin network in synapse development, it is of great interest to know whether Acinus affects subsynapse membrane organization through this intracellular membrane trafficking process, autophagy. This part of work is presented in Chapter 5.

Chapter 2: Materials and methods

2.1 Fly genetics

2.1.1 Fly stocks and husbandry

All fly strains were raised on standard cornmeal/sucrose/agar media at 25°C during embryogenesis and 30°C during larval development under a 12-h/12-h day/night cycle, unless otherwise stated. *Oregon-R* strain obtained from Bloomington *Drosophila* Stock Center (BDSC) served as the wild-type stock for all experiments. *Akt1*¹/*TM3* and *Akt1*⁰⁴²²⁶/*TM3* were two mutant alleles for *Akt1* obtained from the Bloomington *Drosophila* Stock Center. *Akt1*⁰⁴²²⁶ is a hypomorphic allele generated by P-element insertion (Spradling et al., 1999; Gao et al., 2000; Stocker et al., 2002). The null allele *Akt1*¹ is embryonic lethal in homozygotes, but *Akt1*¹/*Akt1*⁰⁴²²⁶ transheterozygotes are semi-viable, and some can survive to the adult stage (Staveley et al., 1998; Stocker et al., 2002). *G14-Gal4*, *24B-Gal4*, *Mef2-Gal4* and *elav-Gal4* transposon-containing stocks (BDSC) were used for muscle and neuronal-specific expression of UAS-regulated transgenes. *UAS-DicerII* was used together with *elav-Gal4* to increase the effectiveness of RNA interference in neurons (Dietzl et al., 2007). *Daughterless (Da)-Gal4* (BDSC) was used for ubiquitous expression of RNAi constructs or transgenes. All of the RNAi strains for experiments and genetic screen were obtained from the Vienna *Drosophila* RNAi Center (VDRC). RNAi lines for experiments are listed here: *UAS-Akt1*^{RNAi} (VDRC#103703), *UAS-sfl*^{RNAi} (VDRC#5070), *UAS-ttv*^{RNAi} (VDRC#4871), *UAS-botv*^{RNAi} (VDRC#37185, VDRC#37186), *UAS-ATG8a*^{RNAi} (VDRC#43097), *UAS-ATG8b*^{RNAi} (VDRC#101922), *UAS-PI3K*^{RNAi} (VDRC#38985), *UAS-Acn*^{RNAi} (VDRC#102407), and *UAS-DnaJ2*^{RNAi} (VDRC#105149). *UAS-mCD8-GFP* (BDSC#5137), *UAS-GFP-mcherry-ATG8a* (BDSC#37749), *UAS-GFP* (BDSC#4775), *UAS-mito-GFP* (BDSC#8442), *UAS-DP110*^{WT} (BDSC#25914) and *EP-DnaJ2* (BDSC#27172) were obtained from the Bloomington *Drosophila* Stock Center. Protein trap line *Bsg-GFP* (Flytrap #G00311) directs the expression of GFP-tagged basigin under

the control of its endogenous promoter. Both *Bsg-GFP* and *UAS-GluRIIA-mRFP* are obtained by Hyun-Gwan Lee from Rolls lab, The Pennsylvania State University, University Park, PA. *UAS-ATG8a-eGFP* is an autophagosomal marker obtained from T. Neufeld, University of Minnesota, Minneapolis, MN and was also used as a dominant-negative *ATG8a* in separate experiments (Kuma et al., 2007). *UAS-Xbp1-EGFP* and *UAS-ninaE^{G69D}* are generous gifts from H. Steller, The Rockefeller University, New York, NY. *UAS- α -Spec-myc* is a gift from G. Thomas, The Pennsylvania State University, University Park, PA. *Cyo; Δ 2-3, TM3 sb/Apxa* is a generous gift from R. Ordway, The Pennsylvania State University, University Park, PA. The constitutively-active forms of *Akt1* (*Akt1^{CA}*) were generated by Hyun-Gwan Lee (Selleck lab) using QuikChange II Site-Directed Mutagenesis Kit (Agilent Technologies, Santa Clara, CA), resulting in the replacement of amino acids threonine 342 (ACC) and serine 505 (AGC) with aspartic acid (GAC). The *Akt1^{CA}* constructs were cloned into *pUAST-attB* vector and then integrated into the third chromosome (99F8) by site-specific P-element mediated germline transformation (Rainbow Transgenic Inc, CA).

2.1.2 Mutagenesis of *DnaJ2*

DnaJ2 (*CG10565*) deletion mutants were generated by imprecise excision of *P{EP}CG10565^{G4964}* from *DnaJ2* genome using a standard method for P-element mobilization (Robertson et al., 1988). The functional transposase resource was provided by a Δ 2-3 construct in which the intron between exon 2 and 3 is removed, allowing for P-element transposition activity in somatic tissues (Laski et al., 1986). *y¹W^{*}; +; P{EP}CG10565^{G4964}/TM3 sb* (male) flies were crossed to *W^{*}; Cyo; Δ 2-3, TM3 sb /Apxa* (female) flies. *P{EP}CG10565^{G4964}* contains a mini-white genetic element, marking the presence of the P-element with partial restoration of eye color. F1 males with mosaic eye coloration were selected, as loss of eye pigment indicates a local transposition event. Those males were crossed to females of the balancer strain *Cyo; TM3 sb /Apxa*, and F2 males with solid white eyes were individually crossed to balancer females to establish independent recovery stocks.

The deletion of flanking sequences was detected by a PCR-based assay with four pairs of primers. Two of the primer sets were designed to amplify a segment from each end of the P-element and the flanking *DnaJ2* genomic sequence. The third set of primers was used to detect large deletions, targeting a 3.9 kb DNA fragment including the full genomic sequence for *DnaJ2*, along with a small portion of *Ac78c*, a gene located immediately 5' to *DnaJ2*. The fourth pair of primers was designed to amplify a 100 bp DNA fragment from sequences immediately flanking the P-element insertion site, for detection of small deletions. 567 independent excision mutation stocks were screened and 15 mutants with deletions ranging from 300 bp to 1.6 kb were isolated. PCR products from those mutants were sequenced to determine the exact size and position of the deletion.

To prepare the DNA sample for PCR, single male flies were mashed and incubated overnight in squishing buffer (10mM Tris-HCl, 1mM EDTA, 25mM NaCl, 200µg/ml Proteinase K, pH 8.2) at 50°C, followed by Proteinase K inactivation at 95°C for 5 minutes.

2.2 Immunohistochemistry and confocal microscopy

2.2.1 Solutions

Ca²⁺ free HL-3 media: 70mM NaCl, 5mM KCl, 20mM MgCl₂, 10mM NaHCO₃, 5mM Trehalose, 100mM Sucrose and 5 mM HEPES, pH7.2

4% paraformaldehyde: diluted from 16% paraformaldehyde (Alfa Aesar, Ward Hill, MA) in PBS

Bouin's fixative solution (Ricca Chemical Company, Arlington, TX) : 0.9% w/v picric acid, 23.8% v/v formaldehyde, 4.8% v/v glacial acetic acid

Phosphate Buffered Saline (PBS): 0.24 g/l KH₂PO₄, 1.44 g/l Na₂HPO₄, 8.0 g/l

NaCl, 0.2g/l KCl, pH 7.4

Phosphate Buffered Saline with Triton (PBST): 0.5% Triton X-100 in PBS

Blocking Buffer: 10% normal goat serum, 5% BSA in PBST

Mounting media: 80% glycerol, 0.12M Tris-HCl, pH8.2

Heparitinase I buffer: 100 mM $\text{NaC}_2\text{H}_3\text{O}_2$, 10 mM $\text{Ca}(\text{C}_2\text{H}_3\text{O}_2)_2$, pH 7.0

2.2.2 Immunostaining

Wandering third instar larvae were dissected in ice-cold Ca^{2+} free HL-3 media and fixed with either Bouin's fixative solution for 5 minutes (for glutamate receptor subunits antibody immunostaining) or 4% paraformaldehyde for 30 minutes, followed by intensive washing with PBS (twice, 20 minutes each) and PBST (three times, 20 minutes each). Muscle preparations with no trace of fixative solution left were blocked in blocking buffer for 1 hour at room temperature and then incubated with primary antibodies for at least 12 hours at 4°C. Samples were intensively washed with PBST (three times, 20 minutes each) and incubated with secondary antibody for 1 hour at room temperature. Muscle preparations were then washed as before and incubated overnight in mounting media before being mounted on glass slides.

Primary antibodies were used at following concentrations: mouse anti-GluRIIA antibody (1:50, 8B4D2, Developmental Studies Hybridoma Bank (DSHB), University of Iowa, Iowa City, IA), rabbit anti-GluRIIB and rabbit anti-GluRIIC antibodies (1:2000, gifts from D. Featherstone, University of Illinois, Chicago, IL), goat anti-horseradish peroxidase (HRP) antibody (1:1000, conjugated with Alexa fluor 488, Jackson ImmunoResearch Laboratories, Inc. West Grove, PA), mouse anti-DLG antibody (1:500, 4F3, DSHB, University of Iowa, Iowa City, IA), rat anti-syndapin antibody (1:100, gift from M. Ramaswami, University of Arizona, Tucson,

AZ), mouse anti-DsRed antibody (1:500, Santa Cruz Biotechnology, Inc.), rabbit anti-dorsal and rabbit anti-cactus antibodies (1:1000, gifts from S. Wasserman, University of California, San Diego, CA), anti-heparan sulfate antibody (1:100, 3G10, Seikagaku, Tokyo, Japan), anti-mitochondria antibody (1:500, 4C7, DSHB, University of Iowa, Iowa City, IA), anti-PIP3 antibody (1:50, MBL international corporation, Woburn, MA), mouse anti-Cysteine string protein (CSP) antibody (1:1000, 6D6, DSHB, University of Iowa, Iowa City, IA), mouse anti- α -spectrin antibody (1:1000, 3A9, DSHB, University of Iowa, Iowa City, IA), Guinea pig anti-Acn antibody (1:1000, gift from H. Krämer, UT Southwestern Medical Center, Dallas, TX). Alexa-fluorescence conjugated secondary antibodies (1:1000) were obtained from Life Technologies (Grand Island, NY).

For heparan sulfate staining, body-wall muscle preparations were fixed in Bouin's fixative for 80 minutes, quenched with 0.5% H₂O₂ for 1 hour, and treated with 20mU heparitinase I (Seikagaku, Tokyo, Japan) in heparitinase I buffer for 2 hours at 37°C. Samples were then incubated overnight with anti-heparan sulfate antibody (1:100, 3G10, Seikagaku, Tokyo, Japan) at 4°C. Signals were amplified using Tyramide Signal Amplification Fluorescence Systems (PerkinElmer, Waltham, MA).

2.2.3 LysoTracker staining for live imaging

Wandering third instar larvae were dissected in Ca²⁺ free HL-3 saline, incubated with LysoTracker Red DND-99 (100nM, diluted from the 1 mM stock solution, Life Technologies, Grand Island, NY) for 5 minutes in the absence of light, rinsed twice with PBS, and imaged immediately. All of the procedures were performed at room temperature.

2.2.4 Image acquisition and analysis

Images were acquired at room temperature using an Olympus Fluoview FV1000 laser-scanning confocal microscope (Olympus America, Lake Success, NY). FV10-ASW 2.1 software (Olympus) was used to capture images. When more

than one fluorophores were detected, sequential line scanning was performed to avoid spectral bleed through artifacts. Images of samples with different genotypes within a single experiment were captured, processed and analyzed using the same settings. Images were presented as Z-stacks of maximum intensity projections using Imaris 7.3 software (Bitplane Inc. Saint Paul, MN). Three-dimensional surface reconstructions were generated from serial images taken by confocal microscopy using Imaris 7.3. Quantification of protein levels were performed using Imaris 7.3 or ImageJ1.42q (NIH) softwares. To measure the level of synaptic proteins (DLG, syndapin, basigin-GFP and mCD8-GFP), immunoreactivity-positive voxels were assayed by counting the total number of voxels (Abundance) and by measuring their average fluorescent intensities. Both values were further normalized by muscle size for each preparation. The number of ATG8a-eGFP, GFP-mcherry-ATG8a, LysoTracker and PIP3 immunoreactivity-positive signals were measured by ImageJ1.42q. The absolute values from each animal were individually normalized by muscle size. Adobe Photoshop CS5 (Adobe Systems Incorporated, San Jose, CA) was then used to crop images and adjust brightness and contrast.

2.3 Transmission electron microscopy

Wandering third instar larvae were dissected in ice-cold Ca^{2+} free HL-3 media and fixed overnight with TEM fixative solution (1.5% Glutaraldehyde, 2.5% Paraformaldehyde, 1.8mM Ca^{2+} in 0.1M Sodium-cacodylate buffer, pH 7.0) at 4°C. Post-fixation (1% Osmium tetroxide in 0.1M Sodium-cacodylate buffer, pH 7.0) and en bloc staining (2% Uranyl acetate) were performed in a dark container for 2 hours each. Samples were washed with 0.1 M sodium cacodylate buffer (pH 7.4) between fixations and before staining. Muscle preparations were then dehydrated (gradient EtOH range from 50% to 100%, 100% Acetone, 70 minutes in total) and infiltrated (1:1 Acetone:Resin, 1:3 Acetone:Resin, 100% Resin, 2 days in total). Samples were embedded in Epon resin at 60°C for ~60 hours, allowing for polymerization. The sample cubes were sectioned to thin (~70nm)

slices and images were obtained with a transmission electron microscope (JEOL1200, Tokyo, Japan) and analyzed by ImageJ1.42q.

The length of active zones was measured as the length of electron dense regions on presynaptic membranes. The SSR thickness was determined by measuring the distance between the presynaptic membrane and the furthest SSR membrane layer. For each bouton, two measurements were recorded for orthogonal or parallel directions and the average values were used for statistical analysis. The density of SSR was measured by counting the numbers of membrane layers in orthogonal or parallel directions and dividing these numbers by SSR thickness (number of layers per μm). The measurement of membrane content provided an alternative way to assess the density of SSR. It was calculated as the area of the electron dense membrane bilayers divided by the total area encompassed by the SSR (with the motoneuron terminal area subtracted out). The number of autophagosomes was counted manually and the values were normalized by muscle area for each graph. Mitochondrial density was determined as the area of electron dense mitochondria divided by the total area of muscle surface.

2.4 Molecular biology

2.4.1 Real-time quantitative polymerase chain reaction

For real-time qPCR, transgenic flies carrying the *UAS-sf1^{RNAi}* construct were crossed with the *Da-Gal4* driver strain for ubiquitous expression. *Da-Gal4* driver flies crossed with the *Oregon-R* strain served as a control. Total RNA was isolated from 30 second-instar larvae for each genotype using RNeasy Mini Kit (QIAGEN). Real-time qPCR analysis was performed by the Genomics Core Facility in The Pennsylvania State University by reverse-transcribing DNase-treated RNA using the High Capacity cDNA Reverse Transcription kit (Life Technologies, Carlsbad, CA) following manufactory protocol. Quantification was performed by adding 5ng of cDNA in a reaction with 2X TaqMan Universal PCR

Master Mix (Life Technologies, Carlsbad, CA) and TaqMan Gene Expression assays in a final volume of 20 μ l. The amplification protocol consisted of 10 minutes at 95°C, followed by 40 cycles of 15 seconds at 95°C and 1 minute at 60°C in the 7300 Real-Time PCR System (Life Technologies, Carlsbad, CA). Ct values of *sfl* and the reference gene *Rp49* were used to determine relative expression levels of *sfl* gene by the delta delta Ct method.

2.4.2 UAS-*DnaJ2* transgenes construction

Total RNA was isolated from *Oregon-R* adult flies using the RNeasy Mini Kit (QIAGEN) and total cDNA was reverse transcribed using SuperScript First-Strand Synthesis System for RT-PCR (Life Technologies, Grand Island, NY). The 1941 bp wild-type *DnaJ2* (*WT-DnaJ2*) cDNA was amplified using primers: 5'-ATGACGAGCGGTACGGTAGCAAC-3' and 5'-ATCCACTTCTAGCTGCTGTG-3'. The PCR product was sequenced and the cDNA sequence was consistent with the predicted gene shown in FlyBase. The mutated *DnaJ2* construct ΔJ -*DnaJ2* was generated by overlap extension PCR, annealing *DnaJ2* fragments upstream and downstream of the J-domain encoding sequence (Primers: 5'-ATGACGAGCGGTACGGTAGCAAC-3' and 5'-CCTAAGGAGTGGGAAGGACCAG-3'; 5'-AGCTTTGACTCAGTGGATC-3' and 5'-ATCCACTTCTAGCTGCTGTG-3'). *H107Q-DnaJ2* was generated using QuikChange II Site-Directed Mutagenesis Kit (Agilent Technologies, Santa Clara, CA), and resulted in the substitution of amino acid Histidine 107 (CAT) with Glutamine (CAA). A *DnaJ2* construct without the DNA-binding domain (ΔDBD -*DnaJ2*) was generated by subcloning of *WT-DnaJ2* using primers: 5'-ATGACGAGCGGTACGGTAGCAAC-3' and 5'-CAGTTCCGGCCACAAATGGGTCT-3', resulting in a truncated form of *DnaJ2* with the entire DBD domain deleted. A GFP encoding sequence was added to the 3'-end of both wild-type and mutated *DnaJ2* constructs. The resultant 8 *DnaJ2* (with or without GFP) constructs were cloned into the *pUAST-attB* vector using NotI and XbaI restriction sites. Plasmids containing each of the constructs were extracted and verified by sequencing. No open reading frame shifting or

second-site mutations were introduced. The *pUAST-DnaJ2* constructs were then integrated into the second chromosome (51D) by PhiC31-mediated site-specific germline transformation (Rainbow Transgenic Inc, Camarillo, CA).

2.5 Western blotting analysis

Wandering third instar larvae were dissected in ice-cold Ca^{2+} free HL-3 media, and the muscle fillet was homogenized in 2% SDS loading buffer immediately after dissection. Total protein extract from muscle preparations was boiled and run on 9% SDS-PAGE, and then transferred onto PVDF membranes. PVDF membranes were incubated overnight with anti-Akt1 (1:100), anti-phosphorylated Akt1 (1:100) or anti- β -Actin (1:100) antibodies (Cell Signaling Technology, Inc., MA) diluted in blocking buffer (5% w/v non-fat dry milk in TBST) at 4°C. Signals were amplified using HRP-conjugated secondary antibody (Cell Signaling Technology, Inc., MA) and detected using Pierce ECL Western Blotting Substrate (Thermo Scientific, IL).

2.6 Statistical Analysis

Statistical analyses for quantitative data were performed with Minitab Release 16 (Minitab, State College, PA). All data points were presented as mean \pm SEM. Distribution of data was determined using individual distribution identification. Comparisons between two groups were performed using Student's t-tests for normally distributed data or Mann-Whitney test for non-parametric data. Comparisons between more than two groups were performed using ANOVA for normally distributed data or Kruskal-Wallis for non-parametric data. If significant difference was found, Tukey's test or Mann-Whitney test was performed for comparisons between individual groups.

Chapter 3: *Akt1* regulates glutamate receptor trafficking and postsynaptic membrane elaboration at the *Drosophila* neuromuscular junction*

*Work described in this chapter is part of the published research article with the same title (Lee et al., 2013). Experiments described in 3.1-3.2.2 and 3.3 were performed by both Hyun-Gwan Lee and Na Zhao. Figures 3.1-3.5 and 3.7 were generated by Hyun-Gwan Lee based on those experiment results.

3.1 *Akt1* is essential for proper localization of glutamate receptor subunit IIA but not IIB at the postsynaptic specialization

3.1.1 *Akt1* mutant shows altered distribution of glutamate receptor IIA

Akt is at a nexus of many signaling processes, regulating diverse physiological functions such as cell growth and proliferation, glucose metabolism, cytoskeleton organization, apoptosis and cell survival (Altomare and Testa, 2005; Bellacosa et al., 2005; Manning and Cantley, 2007). In keeping with its high levels of expression in the central nervous system, *Akt* has been implicated in insulin-dependent neuronal survival (Dudek et al., 1997; Brunet et al., 2001) and long-term synaptic depression (Guo and Zhong, 2006). However, the possible involvement of *Akt* in developmental regulation of synaptic plasticity has not been well addressed. There is a single *Akt* homolog in *Drosophila*, *Akt1*, facilitating genetic and cellular studies of *Akt* function in synapse assembly. The *Drosophila* NMJ has long served as a powerful model for exploring the genetic and molecular mechanisms of developmental and activity-dependent plasticity. We therefore explored *Akt1* function in synapse development using this well-characterized model system.

The role of *Akt1* in regulating synaptic localization of glutamate receptors was determined by examining the distribution and level of GluRIIA, one of the subunits that constitutes the A-type glutamate receptor at the *Drosophila* NMJ (DiAntonio, 2006). We performed immunocytochemical experiments on muscles 6 and 7 in wild-type and the *Akt1* transheterozygous mutant *Akt1*¹/*Akt1*⁰⁴²²⁶. *Akt1*¹ is a null allele harboring a point mutation (F327I) which, when homozygous,

causes embryonic lethality (Staveley et al., 1998; Stocker et al., 2002). *Akt1*⁰⁴²²⁶ is a hypomorphic allele bearing a P-element insertion that reduces the expression of *Akt1* (Spradling et al., 1999; Gao et al., 2000; Stocker et al., 2002). *Akt1*¹/*Akt1*⁰⁴²²⁶ transheterozygous animals exhibit partial functional reduction of this essential gene, which allowed us to conduct experiments in third instar larvae. The distribution of GluRIIA was examined in these animals using a well-characterized monoclonal antibody, anti-GluRIIA (Featherstone et al., 2002; Marrus et al., 2004; Qin et al., 2005a; Karr et al., 2009). GluRIIA (red) immunoreactivity was detectable at the postsynaptic specialization and showed co-localization with the neuronal marker anti-HRP (green) in wild-type animals (Figure 3.1 A and B). Partial loss of *Akt1* function, achieved by *Akt1*¹/*Akt1*⁰⁴²²⁶, altered the distribution and level of GluRIIA at the NMJ. While synaptic GluRIIA immunoreactive puncta showed dramatic reductions in both number and intensity (arrows), extrasynaptic GluRIIA immunoreactivity was found within repeated bands throughout the muscle cells (Figure 3.1 C and D). This latter phenotype was more prominent in muscles 15 and 16 and was observed to a lesser extent in muscles 6 and 7, the postsynaptic cells typically used for electrophysiological analysis (arrowheads in Figure 3.1 C and D).

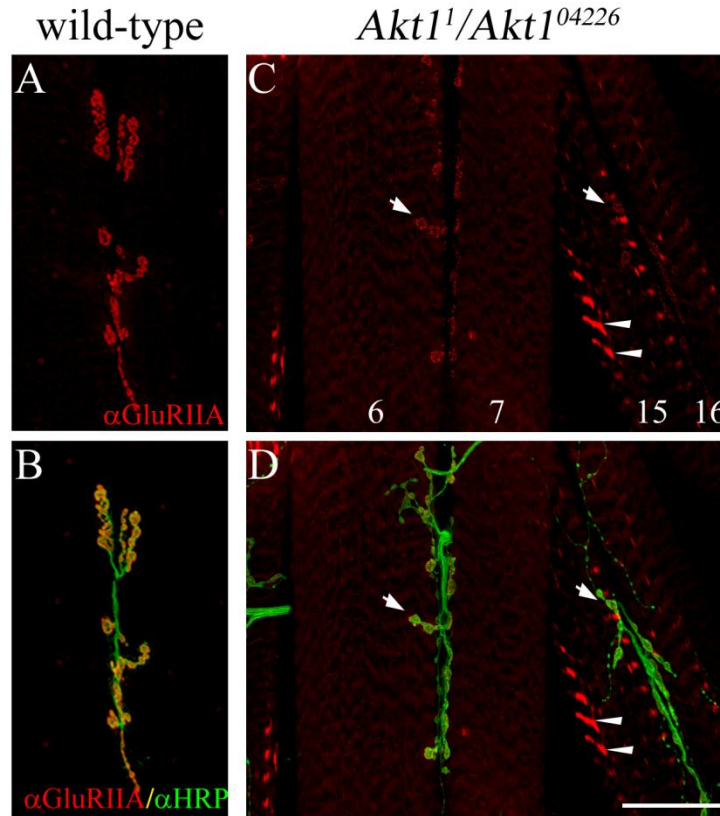


Figure 3.1 GluRIIA localization is modified in *Akt1* mutants. GluRIIA localization at the NMJ was examined using monoclonal anti-GluRIIA antibody (red). Anti-HRP antibody detected neuronal projections (green). **A-B** In wild-type animals, GluRIIA was located in the postsynaptic specialization that surrounds the motoneuron boutons. **C-D** *Akt1*¹/*Akt1*⁰⁴²²⁶ mutants showed reduction of GluRIIA at synaptic boutons (indicated by arrows) and redistribution to intracellular bands (faint staining in muscles 6 and 7, and more prominent staining in muscles 15 and 16; indicated by arrowheads). Scale bar in A-D, 50 μ m.

3.1.2 Cell-type specific inhibition of *Akt1* affects glutamate receptor IIA localization

To confirm the loss of postsynaptic GluRIIA phenotype seen in *Akt1*¹/*Akt1*⁰⁴²²⁶ mutants, cell-type specific expression of an *Akt1* RNAi construct was conducted using the *Gal4-UAS* binary expression system (Brand and Perrimon, 1993). Knockdown of *Akt1* in the motoneuron with *elav-Gal4* had no effect on GluRIIA distribution (data not shown). Multiple muscle-specific *Gal4* driver lines *G14*, *24B* and *Mef2* were tested and showed to have different expression levels

(*G14<24B<Mef2*). However, all of those *Gal4* lines, when combined with the *Akt1^{RNAi}* transgenic construct, resembled the phenotype seen in *Akt1¹/Akt1⁰⁴²²⁶* mutants. For example, *24B-Gal4* directed muscle-specific expression of *Akt1^{RNAi}* produced a dramatic loss of GluRIIA at the synapse and a redistribution of GluRIIA into intracellular bands throughout the muscle cell, which has the similar phenotype as observed in *Akt1¹/Akt1⁰⁴²²⁶* mutants (Figure 3.2). The temperature-dependent nature of Gal4 proteins in *Drosophila* further enable the determination of whether GluRIIA localization was influenced by *Akt1* gene dosage (Duffy, 2002). Yeast transcription activator Gal4 protein has minimal activity at 18°C and exhibits maximal activity at 30°C without affecting fertility or viability. Therefore, *Gal4*-directed transcriptional activation allows for different levels of *Akt1^{RNAi}* expression and consequently loss of *Akt1* function, simply by altering the animal rearing temperatures. As expected, at 18°C, GluRIIA has normal distribution in animals expressing the *Akt1^{RNAi}* transgene as in control flies (Figure 3.2 A and E). However, at 25°C, animals expressing the *Akt1^{RNAi}* construct showed clear accumulation of extrasynaptic GluRIIA (Figure 3.2 F). The most severe reduction of *Akt1* function was achieved at 30°C, and GluRIIA was completely lost from the postsynaptic site and increasingly localized within intracellular bands (Figure 3.2 G and H, arrows indicate synaptic boutons lacking GluRIIA immunoreactivity; arrowheads indicate extrasynaptic GluRIIA shown in bands). Collectively, these findings demonstrate that localization of GluRIIA at the NMJ is affected by *Akt1* function in a dosage-dependent manner.

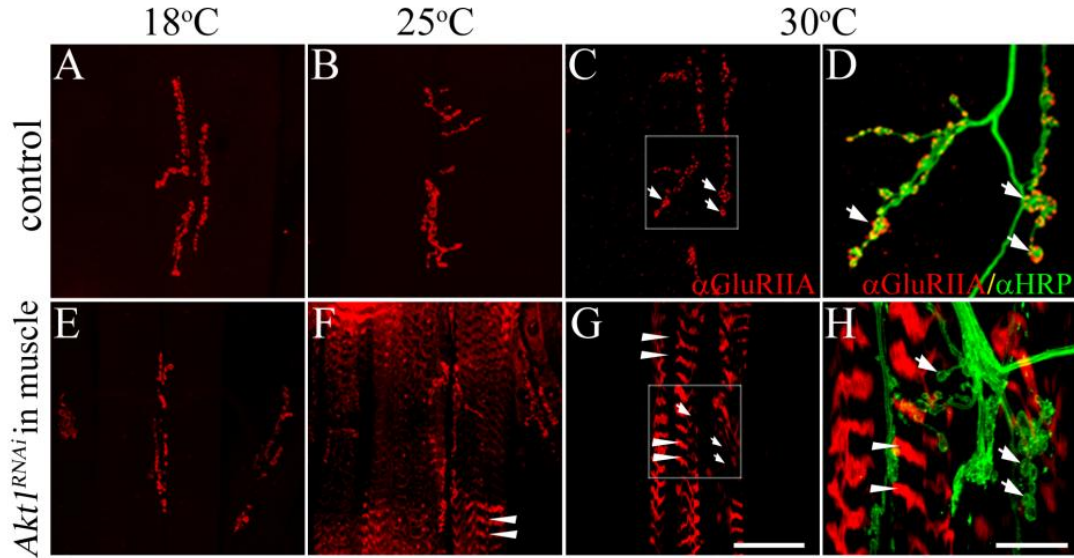


Figure 3.2 GluRIIA localization is affected by reduction of *Akt1* function in muscle cells. *Akt1* function was compromised by *24B-Gal4* directed muscle-specific expression of an *Akt1*^{RNAi} construct. *UAS-Akt1*^{RNAi}/+ animals bearing a copy of the *UAS-Akt1*^{RNAi} transgene but no *Gal4* transcription activator were used as controls. *Gal4* transcriptional activation is temperature-dependent, permitting a graded level of *Akt1* inhibition from 18°C (minimal level of inhibition) to 30°C (maximal level of inhibition). **A-D** In control larvae, GluRIIA immunoreactivity was normally concentrated in the postsynaptic boutons at all temperatures (boutons are indicated by arrows). **D** High magnification view of the inset in **C**, GluRIIA immunoreactivity was merged with anti-HRP immunoreactivity to show the motoneuron boutons surrounded by GluRIIA clusters (arrows). **E-H** In *Akt1*^{RNAi} expressing larvae (*24B-Gal4>UAS-Akt1*^{RNAi}), GluRIIA mislocalization (arrowheads) was detected with greater inhibition of *Akt1* function at higher temperatures (25°C (**F**) or 30°C (**G** and **H**)) but not at 18°C (**E**). **H** Enlarged view of inset in **G**, neuronal projections were visualized with anti-HRP antibody. Bare synaptic boutons lacking GluRIIA immunoreactivity are indicated with arrows while ectopic GluRIIA distributions within intracellular bands are indicated by arrowheads. Scale bars in A-C and E-G, 50µm, in D and H, 5µm.

3.1.3 *Akt1* regulates glutamate receptor composition by selectively influencing GluRIIA targeting to NMJ

While GluRIIC, IID and IIE are shared by both types of glutamate receptors, the IIA subunit is specifically required for the tetramer of A-type receptors, while IIB constitutes the fourth subunit of B-type receptors (DiAntonio, 2006). GluRIIA and

IIB are distinct in their synaptic localizations, developmental expression patterns and physiological properties, and compete for access to GluRIIC when forming functional receptors (Currie et al., 1995; Petersen et al., 1997; DiAntonio et al., 1999; Marrus et al., 2004). Therefore, differential regulation of these two subunits could be an important mechanism for synaptic plasticity. To evaluate the role of *Akt1* in glutamate receptor composition, the distribution of glutamate receptor subunit IIB was examined in animals with knockdown of *Akt1* in the muscle. In the animals with reduced *Akt1* function, GluRIIB was properly localized to the postsynaptic density, whereas GluRIIA was completely lost from synaptic boutons and redistributed exclusively into intracellular bands (Figure 3.3). Further study showed that the indispensable subunit GluRIIC was also appropriately localized to the postsynaptic specialization in the animals with reduced *Akt1* function (data not shown), indicating that extrasynaptic GluRIIA was unlikely to be assembled into functional receptors with the other three subunits. The fact that these larvae with compromised *Akt1* function were still viable and motile must be due to the correct delivery of GluRIIB to the postsynaptic specialization. These findings demonstrate that *Akt1* selectively regulates the delivery of GluRIIA to the synapse without affecting the normal localization of IIB, suggesting the possibility that this mechanism could regulate glutamate receptor composition, thereby influencing the physiological properties of this synapse.

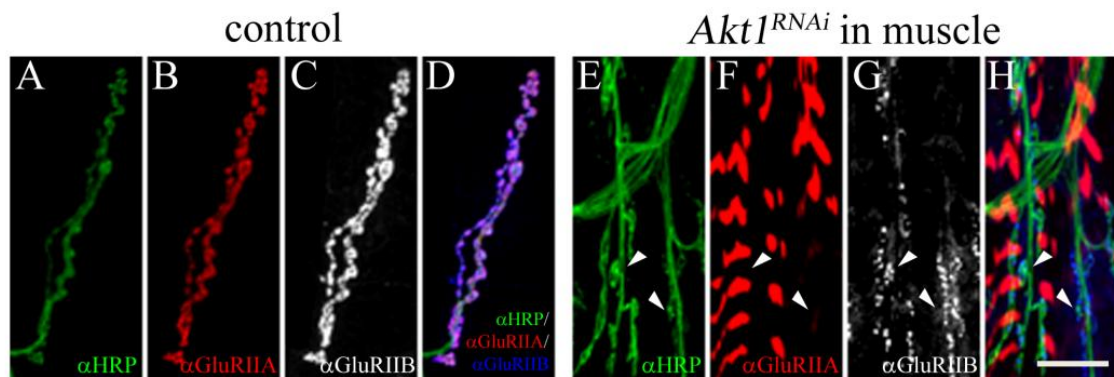


Figure 3.3 Muscle-specific inhibition of *Akt1* does not disrupt the normal localization of GluRIIB at the postsynaptic density. To compromise *Akt1* function in the muscle, an *Akt1*^{RNAi}

construct was expressed under the control of *24B-Gal4* (*24B-Gal4>UAS-Akt1^{RNAi}*). *UAS-Akt1^{RNAi}/+* animals served as the control. GluRIIA was detected with monoclonal anti-GluRIIA antibody (red) and GluRIIB was detected with polyclonal anti-GluRIIB antibody (grayscale). Anti-HRP (green) staining was used to visualize neuronal projections. **A-D** In control animals, GluRIIA, GluRIIB, and anti-HRP immunoreactivities co-localized in synaptic boutons. **E-H** In animals with inhibited *Akt1* expression, GluRIIB localized properly at the postsynaptic sites while GluRIIA was entirely mislocalized into stripes in the muscle. Synaptic boutons docked with GluRIIB but not GluRIIA are indicated with arrows. Scale bar in A-H, 50µm.

3.2 *Akt1* is required for subsynaptic reticulum membrane elaboration

3.2.1 Muscle-specific inhibition of *Akt1* affects the elaboration of the subsynaptic reticulum

Subsynaptic reticulum is a postsynaptic membrane complex that consists of multi-layered membrane infoldings at the neuron-muscle contact site (Jia et al., 1993; Lahey et al., 1994; Budnik et al., 1996; Guan et al., 1996). During larval development, the SSR expands exponentially in both size and complexity, acquiring an elaborate appearance by the third larvae instar stage (Guan et al., 1996). In order to determine if *Akt1* also plays a role in SSR elaboration, transmission electron microscopy (TEM) was used to examine the ultrastructure of the SSR in animals with reduced *Akt1* function. At the *Drosophila* NMJ, motoneuron boutons are embedded in the invaginated surface of the muscle membrane (Jia et al., 1993). In a TEM cross section of a single bouton, the SSR was a complex set of infolded membranes within the muscle cell that surrounded the nerve terminal (Figure 3.4 A, MN: motoneuron). The dimensions and complexity of the SSR were dramatically reduced in larvae expressing *Akt1^{RNAi}* in the muscle cell, as evidenced by reduced cross-sectional lengths and an apparent decrease in the complexity of membrane infoldings (Figure 3.4, compare SSR thickness in A to B). To quantify the decreases in SSR membrane elaboration, the single bouton cross-sectional images were examined in control and *Akt1^{RNAi}* animals, and the SSR membrane thicknesses at directions either parallel or orthogonal to the plasma membrane were measured. We found that

measuring in either direction, SSR thicknesses were significantly decreased when *Akt1* expression was inhibited by RNA interference (Figure 3.4 C). The average length of the presynaptic active zones was unchanged, indicating that the influence of reduced *Akt1* function was restricted to the postsynaptic side without affecting motorneuron features (Figure 3.4 A-C, active zone was shown as electron dense region between two arrowheads). This experiment demonstrates that *Akt1* is required for the proper expansion of the SSR.

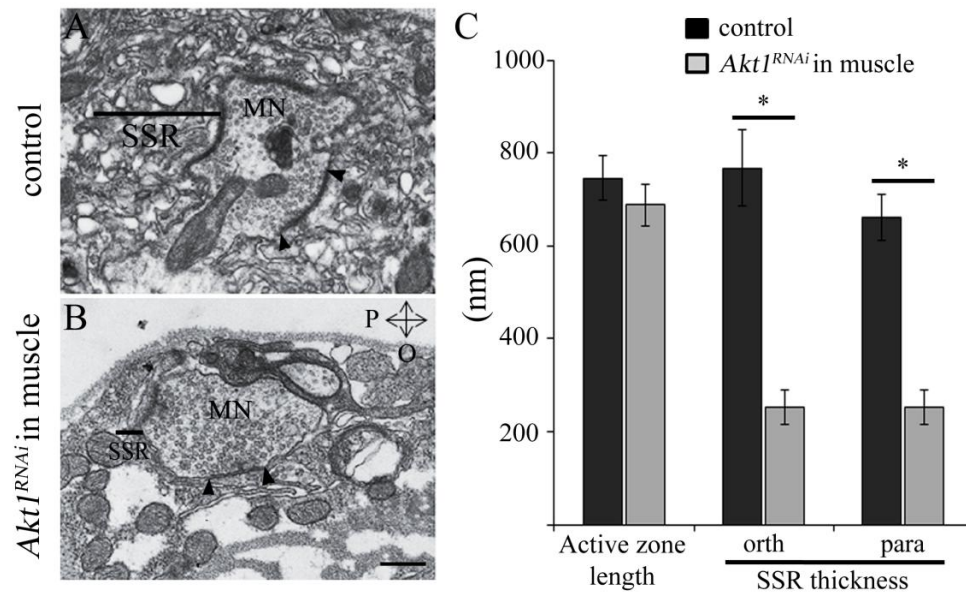


Figure 3.4 Normal SSR expansion is dependent on *Akt1* expression in the muscle. **A** Transmission electron microscopy showed the multi-layered membrane structure of the SSR surrounding the motoneuron terminal in a control animal (*UAS-Akt1*^{RNAi}/+). The approximate parallel thickness of the SSR is indicated by the black bar. **B** SSR thickness was dramatically reduced in *Akt1* compromised larvae (*24B-Gal4>UAS-Akt1*^{RNAi}). Each motoneuron terminal was surrounded by one or two layers of membrane parallel to the presynaptic membrane, which was distinct from the folded arrangement in control larvae. **C** The size of the SSR was determined by measuring its thickness in two dimensions: parallel or orthogonal to the muscle surface. Compared to control animals, SSR thicknesses were significantly decreased in both dimensions by reduced *Akt1* function in the muscle (*24B-Gal4>UAS-Akt1*^{RNAi}). The average length of active zones (neurotransmitter vesicle releasing sites, electron dense region between two arrowheads) was not affected by the loss of *Akt1* function. * denotes p < 0.05, n=15 each. Student's t-test was

used for statistical analysis. MN, motorneuron. P, parallel; O, orthogonal to the axis of muscle surface. Scale bar in A and B, 0.5 μ m.

3.2.2 *Akt1* is required for maintaining intracellular membrane organization of muscle cells

To confirm our TEM result, the SSR membrane development in *Akt1* loss-of-function animals was further examined with confocal fluorescent microscopy. The SSR and the entire muscle endomembrane system were visualized using a GFP tagged mouse transmembrane receptor protein mCD8-GFP, a commonly used membrane marker (Lee and Luo, 1999). The intracellular membrane system of muscle cells consists of two morphologically distinct architectures: a cortical membrane compartment located above the muscle nucleus, and a subcortical membrane network located below the nucleus that connects to the contractile apparatus (Gorczyca et al., 2007). The cortical membrane compartment is at the same depth as the SSR, and there is evidence to show that the postsynaptic scaffold protein DLG, which is the homolog of mammalian PSD-95, traffics through the cortical membrane compartment to the SSR (Thomas et al., 2000; Gorczyca et al., 2007). As previously reported, mCD8-GFP expression in the muscle cell revealed a complex set of membranous structures including a cortical domain (c), the nuclear envelope (n), and a subcortical network (sc) in control animals (Figure 3.5 A). The SSR was also prominently labeled by mCD8-GFP expression in the muscle, as evidenced by co-localization with DLG (Figure 3.5 B-D). Reduction of *Akt1* function by muscle-directed RNAi expression affected several aspects of endomembrane organization. First, the cortical membrane domain was almost entirely missing in animals expressing *Akt1*^{RNAi}. Second, the subcortical membrane domain was compressed, resulting in a dramatic reduction in muscle thickness in animals with inhibited *Akt1* expression (Figure 3.5 E). Last but not least, the mCD8-GFP labeling of the SSR was also dramatically decreased upon muscle-directed *Akt1*^{RNAi} expression, consistent with the TEM finding that loss-of-*Akt1* reduced SSR elaboration (Figure 3.5 F-H). This experiment demonstrates that *Akt1* function is critical for SSR membrane

elaboration as well as the organization of intracellular membrane compartments during muscle cell development.

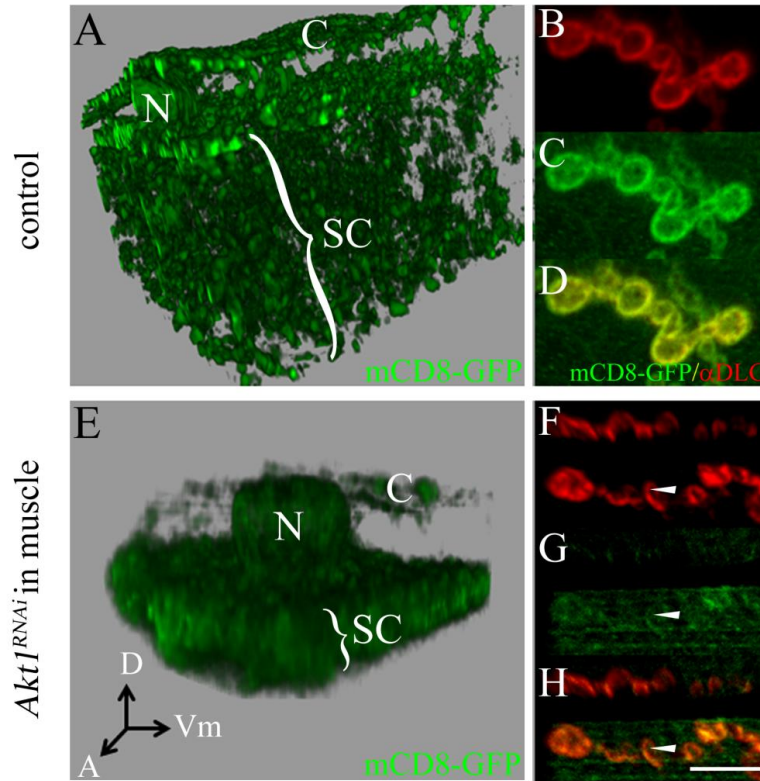


Figure 3.5 *Akt1* is required for the integrity of the muscle endomembrane system. To visualize the intracellular membrane networks, mCD8-GFP was expressed in muscle cells using the muscle-specific driver line *G14-Gal4*. Three dimensional re-construction using serial confocal images revealed muscle membrane structures across the depth of an extra-synaptic region. Cortical and subcortical membrane domains are separated by the nuclear layer. **A** In control larvae (*G14-Gal4*, *UAS-mCD8-GFP*/+), cortical and subcortical membrane networks were normally developed and organized. **B-D** In control animals, the SSR was labeled by mCD8-GFP (green) and the postsynaptic density was stained with anti-DLG antibody (red). mCD8-GFP labeling and anti-DLG immunoreactivity overlapped, indicating proper SSR elaboration in control animals. **E** Animals with muscle-specific *Akt1* knockdown (*G14-Gal4*, *UAS-mCD8-GFP*>*UAS-Akt1*^{RNAi}) showed collapse of the cortical domain and a thinned subcortical domain. **F-H** mCD8-GFP labeled SSR was dramatically reduced by loss of *Akt1* function (arrowheads). DLG localized correctly to the synapse with a modest reduction in its level. C, cortical membrane domain; SC, subcortical membrane domain; N, nucleus; A, anterior; D, dorsal; and Vm, ventral midline. Scale bars in B-D and F-H, 5µm.

3.2.3 Overexpression of constitutive-active *Akt1* produces ectopic SSR-like membrane structures without affecting SSR organization

We next investigated whether overexpression of *Akt1* had an impact on the formation and maintenance of SSR. A constitutively-active form of Akt1 (*Akt1*^{CA}) was employed in which the amino acids threonine (342) and serine (505) were replaced with Aspartic acid, a phosphomimetic of activated Akt1 (Kaplan et al., 2008; Wang et al., 2012). NMJs of control or animals overexpressing the *Akt1*^{CA} transgene were evaluated at the electron microscopic level, and no differences were found in the dimensions or complexity of the SSR or the length of active zones (Figure 3.6 compare A to B). However, muscle-directed expression of *Akt1*^{CA} did produce a number of highly folded membraneous structures in the cytoplasm or underneath the plasma membrane, resembling the folded structure of SSR (Figure 3.6 C-E). These membrane structures formed in the absence of nerve terminals and were distant from existing synaptic regions; however, synaptic proteins DLG and Gtaxin were found within these membrane infoldings, indicating these ectopic membrane elaborations had some SSR-like functional properties (data not shown).

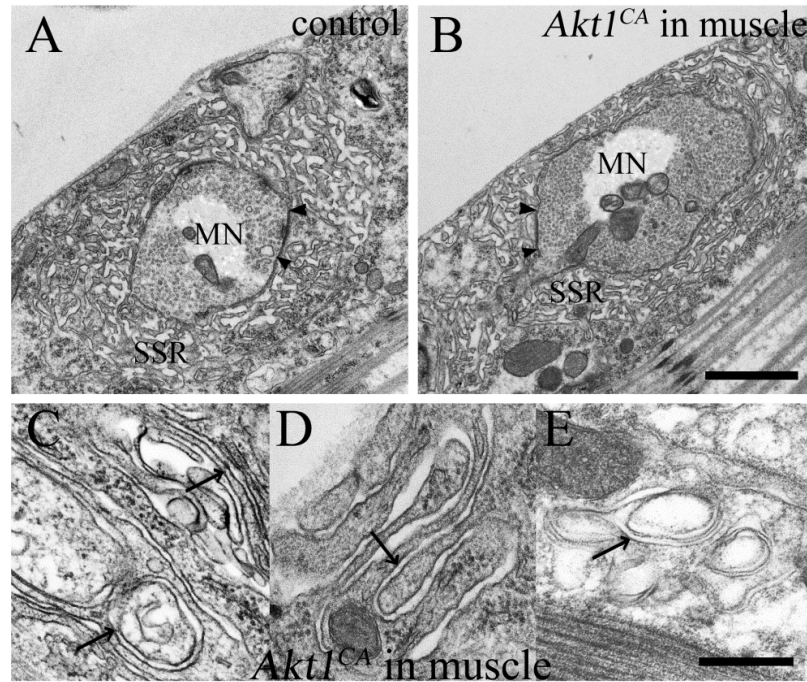


Figure 3.6 Overexpression of a constitutively-active form of *Akt1* creates SSR-like membranes distant from the synaptic region. To further investigate the function of *Akt1* in SSR development, transmission electron microscopic photographs were taken in control (*UAS-Akt1^{CA}/+*) and animals overexpressing the constitutively-active form of *Akt1* in the muscle (*Mef2-Gal4>UAS-Akt1^{CA}*). **A** SSR membrane elaboration surrounding motorneuron terminal was demonstrated in control animals. **B** Overexpression of *Akt1^{CA}* in muscle cells did not affect SSR development. **C-E** Ectopic membranous structures were observed in the cytosol (C and E) or underneath the plasma membrane (D) in animals overexpressing *Akt1^{CA}*. Arrows point to multi-layered membrane infoldings. Scale bars in A-B, 0.5 μ m; in C-E, 0.1 μ m.

3.3 *Akt1* does not affect the NMJ targeting of other synaptic proteins

Given that loss of *Akt1* function resulted in abnormalities in SSR elaboration and intracellular membrane organization, we asked if GluRIIA mislocalization was a specific consequence of mis-regulation by *Akt1*. The fact that GluRIIB and IIC correctly localized to the NMJ in the absence of *Akt1* demonstrated the specific need of *Akt1* for GluRIIA localization. To further investigate whether other cytoplasmic or secretory proteins require *Akt1* for correct targeting to the postsynaptic specialization, we examined three other synaptic proteins, basigin,

DLG and syndapin, for their localization in animals with reduced *Akt1* function. basigin is a transmembrane protein located principally at the synapse and is required for synaptic function (Besse et al., 2006; Besse et al., 2007). DLG and syndapin are cytoplasmic proteins targeted to postsynaptic specializations, where they promote SSR expansion (Lahey et al., 1994; Budnik et al., 1996; Guan et al., 1996; Thomas et al., 2000; Kumar et al., 2009). Basigin was visualized using a protein trap strategy by which GFP tagged basigin was expressed under its endogenous promoter, allowing for observation of the protein's subcellular distribution (Morin et al., 2001). As expected, basigin-GFP was highly concentrated at the NMJ and co-localized with anti-GluRIIA immunoreactivity in control animals bearing no *Gal4* driver (Figure 3.7 A). Reduction of *Akt1* function in the muscle to a degree that completely disrupted GluRIIA localization did not alter the targeting of basigin to the synapse (Figure 3.7 B). DLG (green) detected with mouse monoclonal anti-DLG antibody and syndapin (red) detected with rat polyclonal anti-syndapin antibody both exhibited normal localization to the postsynaptic specialization at the NMJ (Figure 3.7 C-H). The fluorescence of DLG, syndapin, basigin and mCD8-GFP (use the data shown in figure 3.5) in animals with compromised *Akt1* function were measured and quantified for their intensity and abundance and then compared with wild-type levels (Figure 3.7 I). In those animals with *Akt1*^{RNAi} expression in the muscle, the immunofluorescent intensities of DLG and syndapin did not change, while basigin-GFP showed a modest but significant decrease in its intensity. Analysis of protein abundance (total number of immunoreactive-positive voxels) showed significantly reduced levels of basigin and syndapin while DLG level was lower but did not achieve statistical significance. The most striking decrease was observed for mCD8-GFP signal levels, in both intensity and abundance. The fact that these synaptic proteins (DLG, syndapin and basigin) showed much more reduction in abundance but less reduction in intensity was probably due to a decreased synaptic size and relatively unaffected targeting ability. Although SSR size was dramatically reduced as evidenced by decrease in mCD8-GFP labeling, DLG, syndapin and basigin were still concentrated and correctly localized to the

SSR. Taken together these findings demonstrate that reduction of *Akt1* affects the localization of GluRIIA specifically, without affecting the synaptic targeting of other transmembrane (basigin, GluRIIB) or cytoplasmic (Dlg, syndapin) proteins.

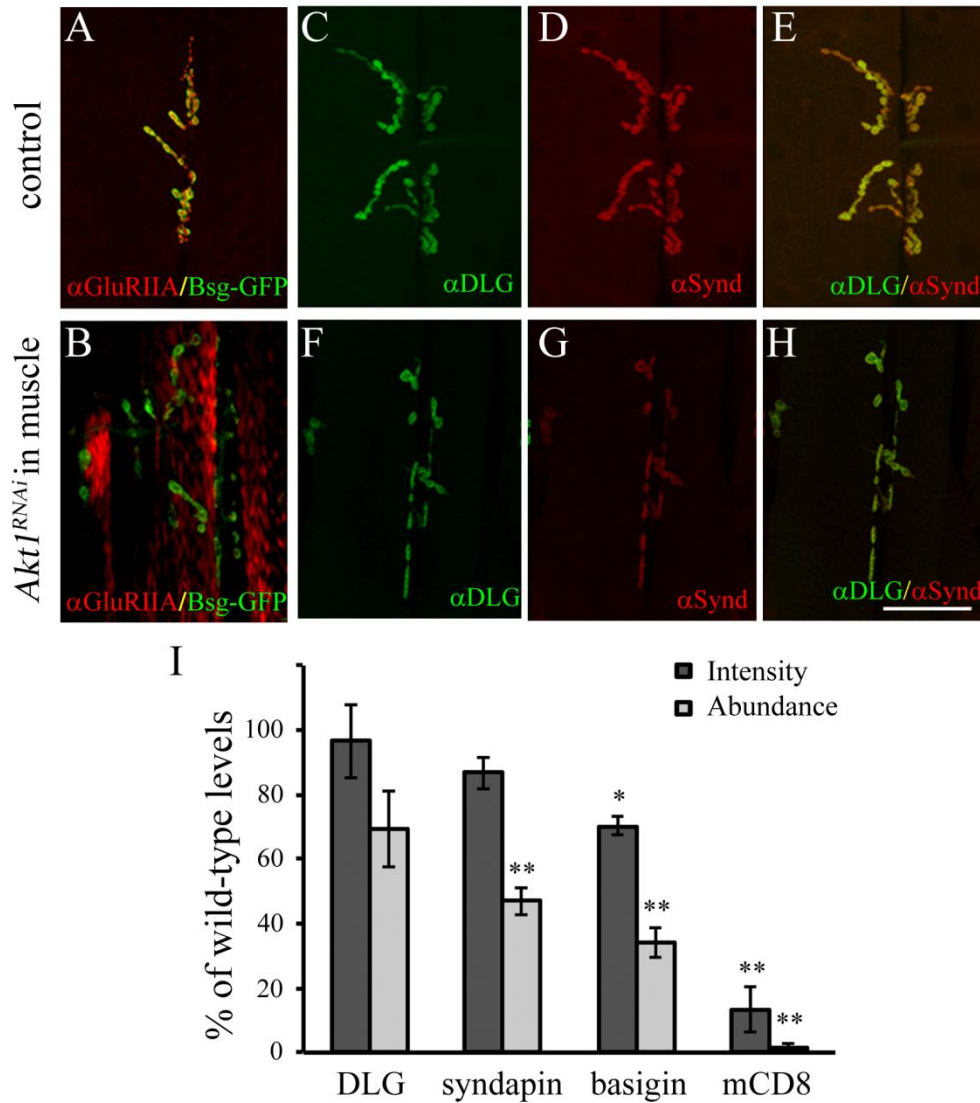


Figure 3.7 Levels but not localization of synaptic proteins basigin, DLG and syndapin are affected by loss of *Akt1* function. **A** In control larvae (*UAS-Akt1^{RNAi}/+*), basigin (green) colocalized with GluRIIA (red) at the postsynaptic density. **B** In *Akt1*-compromised larvae (*G14-Gal4>UAS-Akt1^{RNAi}*), basigin localized correctly to postsynaptic specialization while GluRIIA was completely mislocalized. **C-E** In control larvae (*UAS-Akt1^{RNAi}/+*), DLG (green) and syndapin (red) showed normal postsynaptic localization. **F-H** Although decreased in levels, DLG and syndapin localized correctly to the postsynaptic region in animals expressing *Akt1^{RNAi}* in the muscle (*G14-*

Gal4>UAS-Akt1^{RNAi}). I Quantitative analysis of the protein levels for DLG, syndapin, basigin-GFP and mCD8-GFP at the NMJ. The values of signal intensities and protein abundance in *Akt1^{RNAi}* animals were compared with control (*UAS-Akt1^{RNAi}/+*) and presented as percentage of wild-type levels. * denotes $p < 0.05$, ** denotes $p < 0.01$, DLG: n=10, syndapin: n=12, basigin: n=6, mCD8: n=11. Student's t-test was used for statistical analysis. Scale bar in A-H, 30 μ m.

3.4 Mechanism of *Akt1* regulated postsynaptic targeting of GluRIIA

3.4.1 Loss of *Akt1* function may disrupt the structural integrity of GluRIIA-mRFP fusion protein

To further explore the mechanism of the GluRIIA mislocalization phenotype produced by knockdown of *Akt1*, we examined the distribution pattern of an exogenously expressed GluRIIA-mRFP recombinant protein (Rasse et al., 2005; Schmid et al., 2008). This allowed us to visualize the transgenic GluRIIA-mRFP by detecting either the fluorescence of the mRFP protein or the immunoreactivity of a mouse monoclonal antibody anti-DsRed which recognizes mRFP epitope. The postsynaptic specialization was visualized by mCD8-GFP labeling in the muscle (Figure 3.8 A and E). GluRIIA-mRFP was concentrated at the NMJ of control flies, showing precisely overlapped mRFP fluorescence and anti-RFP immunoreactivity (Figure 3.8 B-D). Consistent with our earlier results looking at the endogenous GluRIIA, compromising *Akt1* function in the muscle resulted in dramatic loss of GluRIIA-mRFP at the synapse, detected by either mRFP fluorescence or anti-RFP antibody (Figure 3.8 F-H). Surprisingly, the redistribution of GluRIIA-mRFP into intracellular bands was only detected with the anti-RFP antibody, but not by mRFP fluorescence (Figure 3.8 F-H, arrowheads). This result suggests that muscle-specific reduction of *Akt1* function might disrupt the structural integrity of the GluRIIA-mRFP fusion protein, resulting in loss of fluorescence, while the RFP-epitope was intact and found redistributed into intracellular membrane structures, as detected by anti-RFP antibody. It is possible that GluRIIA-mRFP could not fold properly without *Akt1* function, and that this disruption in folding altered the protein configuration necessary for mRFP fluorescence emission.

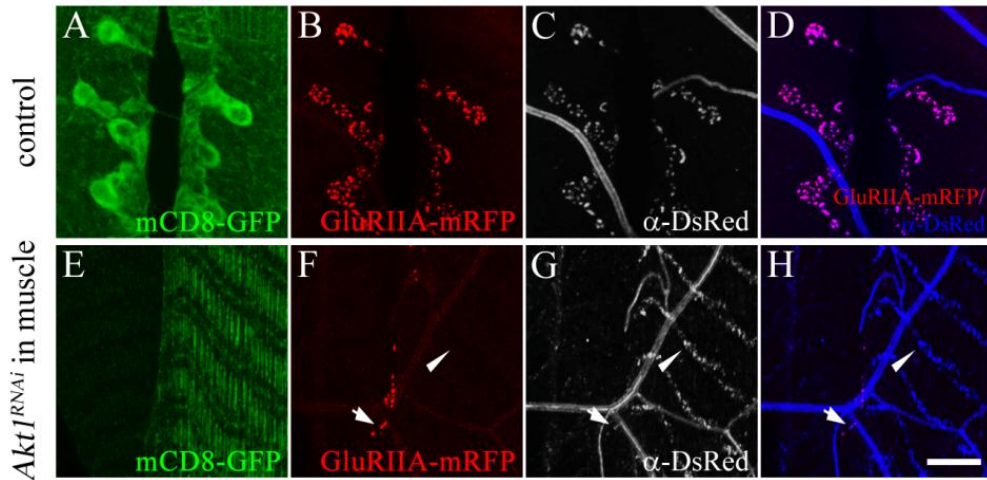


Figure 3.8 *Akt1* may affect GluRIIA targeting to the NMJ by altering its protein configuration. GluRIIA-mRFP was expressed under the control of UAS enhancer and detected with either mRFP fluorescence or an anti-RFP antibody (anti-DsRed). mCD8-GFP was expressed in the muscle, labeling SSR and plasma membranes. **A-D** GluRIIA-mRFP fluorescence (red) co-localized with anti-DsRed signals (Grey) at the NMJ in control animals (*G14-Gal4, UAS-mCD8-GFP; UAS-GluRIIA-mRFP/+*). mCD8-GFP labeled SSR showed normal elaboration. **E-H** Both GluRIIA-mRFP fluorescence and immunostaining were reduced significantly at the postsynaptic specialization (arrows) upon inhibition of *Akt1* function (*G14-Gal4, UAS-mCD8-GFP; UAS-GluRIIA-mRFP>UAS-Akt1^{RNAi}*). However, the redistribution of GluRIIA-mRFP protein into an intracellular membrane compartment was detected only with anti-RFP antibody, but not RFP fluorescence in *Akt1* compromised animals (arrowheads). mCD8-GFP was eliminated from the NMJ in animals expressing *Akt1^{RNAi}*. Scale bar in A-H, 5 μ m.

3.4.2 Regulation of GluRIIA localization by Akt1 could be partially mediated by dorsal and cactus

The mechanism of Akt in promoting insulin-induced translocation of type A GABA receptors to the cell surface involves phosphorylation of GABA_AR β subunits at several conserved sites (Wang et al., 2003; Serantes et al., 2006). However, unlike GABA_AR β subunits, sequence analysis revealed that GluRIIA bears no consensus sequence (RXRXXS/T) for Akt1 mediated phosphorylation (Manning and Cantley, 2007), and therefore its localization at the NMJ is unlikely to be regulated by direct phosphorylation. Dorsal and cactus are the *Drosophila*

homologs of NF- κ B and I κ -B, two signaling molecules downstream of Akt pathway (Ozes et al., 1999; Heckscher et al., 2007; Dan et al., 2008). These two proteins have been shown to localize to postsynaptic specializations and regulate GluRIIA concentration at the NMJ in a manner independent of their transcriptional activator activity (Heckscher et al., 2007). To determine whether *Akt1*'s effects on GluRIIA localization could be mediated at least in part by an influence on dorsal or cactus, the levels and distributions of these two proteins at the NMJ were evaluated. As previously described, dorsal and cactus were concentrated at the postsynaptic specializations of type Ib boutons in control animals (Figure 3.9 A, B and E, F). With RNAi mediated knockdown of *Akt1* in the muscle cells, both dorsal and cactus levels dramatically decreased at the NMJ (Figure 3.9 C, D and G, H). In addition to the reduction of dorsal levels at the NMJ, in some animals, dorsal was redistributed into an intracellular compartment in the muscle cell, coincident with mislocalized GluRIIA (Figure 3.9 L-N; arrowheads indicate mislocalized GluRIIA and dorsal in stripes, arrows indicate dorsal signal remaining at the synaptic boutons). Although the penetrance of this phenotype was modest (24%), it was reproducible across three different sets of experiments. These findings show that reduction of *Akt1* function affects the postsynaptic concentration of dorsal and cactus, two potential *Akt1* downstream targets known to regulate GluRIIA levels, suggesting that loss of GluRIIA at the postsynaptic specialization in *Akt1* compromised animals could be due to a mis-regulation of dorsal and cactus.

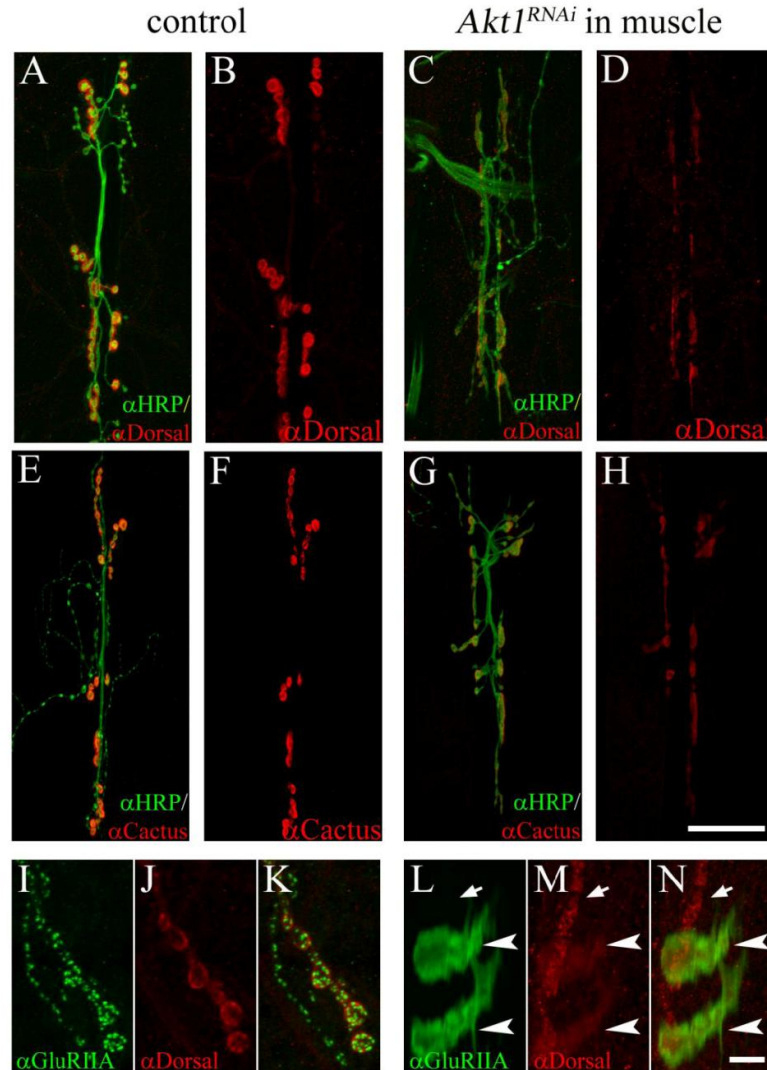


Figure 3.9 Influence of Akt1 on dorsal and cactus levels and distributions at the NMJ. **A-B** In control animals (*UAS-Akt1^{RNAi}/+*), dorsal (detected by anti-dorsal antibody, red) was localized to the postsynaptic specialization. Neuronal projections were visualized by anti-HRP staining (green). **C-D** *Akt1* function was compromised by expressing *UAS-Akt1^{RNAi}* under the control of muscle-specific driver *24B-Gal4*. Dorsal levels at the NMJ were dramatically reduced. **E-F** Cactus (detected by anti-cactus antibody, red) was concentrated at the NMJ in control animals. **G-H** Inhibition of *Akt1* function in the muscle (*24B-Gal4>UAS-Akt1^{RNAi}*) resulted in reduced level of cactus at the NMJ. **I-K** In control animals, dorsal immunoreactivity (red) co-localized with GluRIIA immunoreactivity (green) at the postsynaptic specialization. **L-N** In muscles where *Akt1* expression was inhibited, both dorsal and GluRIIA were redistributed into intracellular bands (arrowheads). The effect on dorsal was modest, with a substantial portion of the protein correctly localized to the NMJ (arrows). Scale bars in A-H, 50 μ m; in I-N, 5 μ m.

In summary, it is demonstrated that *Akt1* is specifically required for the assembly of A-type glutamate receptors. Using a transgenic RNA interference approach executed by the *UAS-Gal4* binary expression system (Duffy, 2002; McGuire et al., 2004), *Akt1* function was inhibited exclusively in postsynaptic muscle cells. As a result, GluRIIA was lost from the postsynaptic site and redistributed within intracellular bands in the muscle, while distributions of IIB at the postsynaptic density were not affected. In addition to regulating glutamate receptor composition, further studies revealed that *Akt1* is required for membrane elaboration of the postsynaptic specialization, the SSR. These findings demonstrated that *Akt1* serves a critical role in two fundamental elements of synapse development. We provide novel evidence here suggesting that Akt1 may regulate glutamate receptor localization via dorsal and cactus, two signaling molecules known to affect GluR post-translational trafficking (Heckscher et al., 2007).

Chapter 4: Heparan sulfate proteoglycans negatively regulate autophagy during development of the *Drosophila* neuromuscular junction

4.1 Heparan sulfate biosynthesis is required for the organization of a specialized postsynaptic structure, the subsynaptic reticulum

4.1.1 Heparan sulfate polymer synthesis and modification

Heparan sulfate proteoglycans are a heterogeneous family of complex biological macromolecules composed of one or more linear sulphated polysaccharides covalently attached to a core protein (Kirkpatrick and Selleck, 2007; Sarrazin et al., 2011). As important constituents of the cell surface and extracellular matrix, HSPGs play pivotal roles in growth factor signaling, morphogen gradient formation, basement membrane integrity, and neuronal development (Bernfield et al., 1999; Perrimon and Bernfield, 2000; Tumova et al., 2000; Yamaguchi, 2001; Bulow and Hobert, 2004; Lin, 2004; Yan and Lin, 2009). The structural and functional heterogeneity of HSPGs is due to the enormous diversity in composition and modification of HS chains in combination with the variety of core proteins (Lindahl et al., 1998). While a great deal of work in *Drosophila* has informed the *in vivo* functions of proteoglycans core proteins such as syndecan, Dally and Dally-like in synapse development, the cellular processes specifically affected by heparan sulfate chain polymerization and modification remain underappreciated. Our experiments, presented in chapter 4, were aimed at investigating the cellular phenotypes resulting from compromised HS biosynthesis and sulfation at the NMJ.

Earlier analysis of heparan sulfate function in NMJ assembly using mutants that compromise HS biosynthesis and modification produced notable phenotypic effects in both pre- and post-synaptic cells (Ren et al., 2009). To extend these studies with more dramatic reductions of HS biosynthetic function throughout embryonic and larval development in a cell type-specific manner, RNAi constructs derived against either *tout velu* (*ttv*), *brother of tout velu* (*botv*) or

sulfateless (sfl) mRNA were expressed using cell-type specific *Gal4* lines (Perrimon et al., 1996; Bellaiche et al., 1998; Lin and Perrimon, 1999; Duffy, 2002; Han et al., 2004; Takei et al., 2004). A summary of the HS-biosynthetic pathway is provided in Figure 4.1, including the enzymatic steps performed by the proteins encoded by the target genes used in the studies reported here. *botv* encodes an *N*-acetyl glucosamine transferase I that adds the first *N*-acetyl glucosamine (*N*-GlcNAc) residue of the HS chain to the tetrasaccharide linker that attaches to a serine residue of the core protein (Izumikawa et al., 2006). *ttv* and *sister of tout velu (sotv)* harbor both *N*-GlcNAc transferase II and glucuronic acid (GlcA) transferase II activities, adding the GlcNAc-GlcA disaccharide units to the elongating HS polymer. Compromising the function of *botv*, *ttv*, or *sotv* therefore affects synthesis of the HS chain. *sfl* encodes an *N*-deacetylase/*N*-sulfotransferase required for *N*-sulfation of *N*-GlcNAc (depicted by yellow diamonds in Figure 4.1). This is an early step in HS modification that affects subsequent sulfations at multiple *O*-linked positions (shown as green, purple and blue diamonds in Figure 4.1). Structural analysis of glycosaminoglycans (GAGs) produced in *sfl* mutants has shown that in the absence of *sfl*, very little sulfated polymer is produced, leaving *N*-Acetyl heparosan in its place (Toyoda et al., 2000).

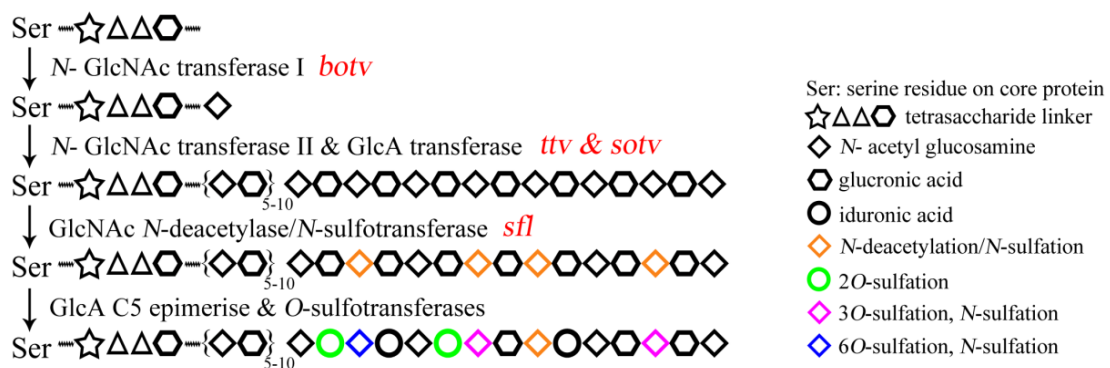


Figure 4.1 Heparan sulfate polysaccharide biosynthesis and modification. Biosynthesis of heparan sulfate glycosaminoglycan chain is a sequential reaction involving chain initiation, elongation and modification. HS chains are attached to serine residues on the core protein via a tetrasaccharide linker (xylose-galactose-galactose-uronic acid). The first monomer *N*-GlcNAc is

added by *N*-GlcNAc transferase I, encoded in *Drosophila* by *botv*. Polymerization of subsequent monomers is catalyzed by *N*-GlcNAc transferase II and GlcA transferase II (*Drosophila* genes *ttv* and *sotv*). The initial polymer comprising alternating *N*-GlcNAc and GlcA is further decorated with sulfate groups at multiple locations. *sfl* encodes an *N*-deacetylase/*N*-sulfotransferase that converts acetyl groups on *N*-GlcNAc to sulfate groups. Additional modifications catalyzed by GlcA C5 epimerase and specific *O*-sulfotransferases may then take place.

4.1.2 RNA interference of heparan sulfate biosynthetic genes

To evaluate the effects of RNAi-mediated knockdown of *sfl*, *ttv* or *botv* *in vivo*, a ubiquitously expressed *Gal4* (*Da-Gal4*) construct was used to drive the *UAS-RNAi* constructs throughout development. Levels of heparan sulfate polymer were assessed with a monoclonal antibody 3G10 which recognizes a desaturated uronate epitope produced by heparitinase digestion of HS (David et al., 1992). Consistent with previous reports, in wild-type flies, HS (red) was concentrated at the NMJ, where it strongly co-localized to axon terminals (detected with anti-HRP antibody, green) (Figure 4.2 A-C). RNAi directed against either *ttv* or *botv* (two different RNAi strains VDRC#37185, VDRC#37186 were used for *botv* inhibition) drastically reduced HS levels at the NMJ in third instar larvae (Figure 4.2 D-L). Since *sfl* function would not affect production of the undecorated uronate epitope, and hence 3G10 immunoreactivity, the impact of *sfl* reduction on HSPG biosynthesis cannot be assessed by 3G10 immunostaining. Instead, efficiency of *sfl* RNA silencing was determined by measuring *sfl* mRNA levels in second instar larvae (the latest developmental stage to which *Da-Gal4>UAS-sfl^{RNAi}* larvae survive) using real-time qPCR. RNAi of *sfl* reduced the mRNA level over 50 fold (Figure 4.2 M).

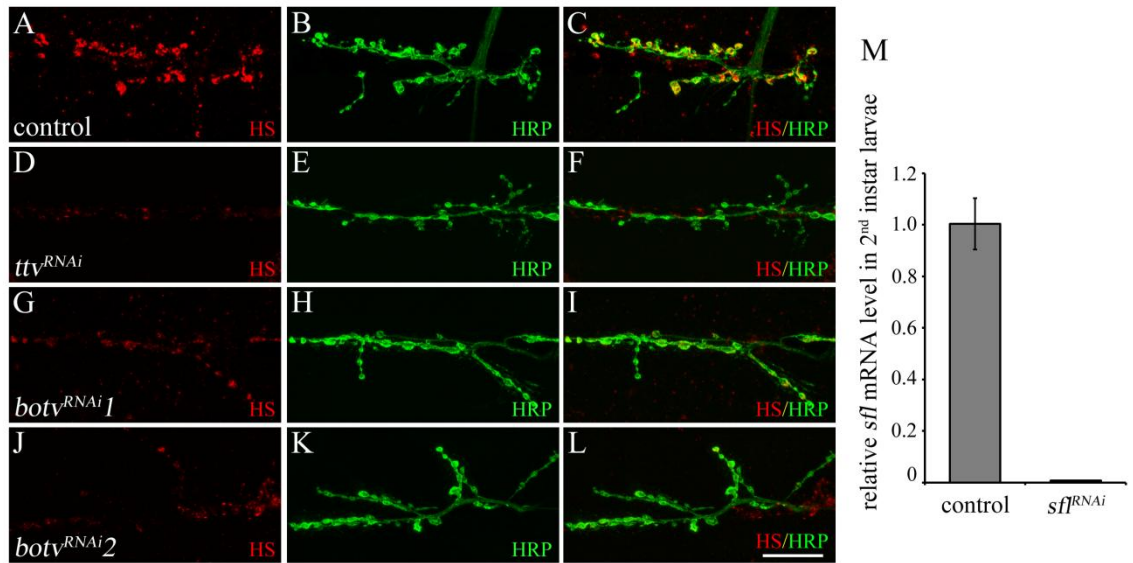


Figure 4.2 RNA interference disrupts gene expression required for HS glycosaminoglycan chain biosynthesis and modification. A-L The *Drosophila* NMJ at muscles 6 and 7 is shown stained with 3G10 (red) antibody to label HS polysaccharides and anti-HRP (green) antibody to visualize the motoneuron projections. A-C In control (*Da-Gal4/+*) animals lacking an RNAi construct, HS was enriched around synaptic boutons. This was evinced by co-localization with anti-HRP immunoreactivity. D-L In animals expressing *ttv* or *botv* transgenic RNAi constructs ubiquitously, 3G10 immunoreactivity decreased dramatically, whereas anti-HRP immunoreactivity was unaffected. M Relative mRNA levels of *sfl* gene were measured with real-time qPCR in controls and animals ubiquitously expressing *sfl*^{RNAi}. Scale bar in A-L, 30μm. Error bars denote STDEV.

4.1.3 Loss of heparan sulfate disrupts subsynaptic reticulum organization

Transmission electron microscopy was used to assess NMJ ultrastructure in animals with reduced *sfl* or *ttv* function by examining cross sections of motoneuron terminals and the underlying postsynaptic specialization of the muscle cell. Reduction of either *sfl* or *ttv* function with muscle-directed RNAi changed the morphology of the SSR, producing enlarged spaces between membrane layers (Figure 4.3; compare B, C to A). The change in SSR structure was quantified by determining the SSR membrane content, calculated as the area of the electron dense membrane bilayers divided by the total area encompassed by the SSR (with the motoneuron terminal area subtracted out).

This provided a measure of the relative extent of membrane elaboration for a given postsynaptic field. This ratio of areas was significantly reduced in animals with either *sfl* or *ttv* RNA interference in the muscle cell, confirming the morphological change observed in the electron micrographs (Figure 4.3 D). These findings indicate that for unit area of the postsynaptic specialization, less membrane complexity is found within the SSR of animals with compromised HS biosynthesis.

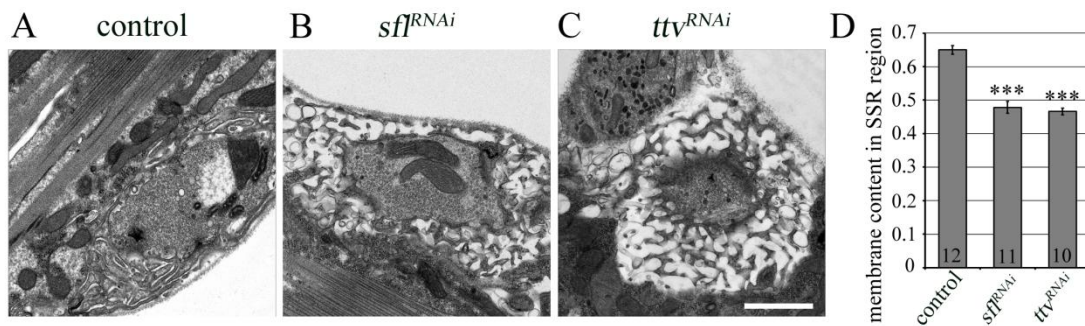


Figure 4.3 Ultrastructure of the SSR at the NMJ of animals with compromised HS biosynthesis. **A** Electron micrographs of control (*Mef2-Gal4/+*) animals showed that SSR comprised multiple compactly assembled membrane stacks surrounding the presynaptic nerve terminal. **B** and **C** In animals where *sfl* and *ttv* genes were suppressed by muscle cell directed RNA interference (*Mef2-Gal4>UAS-sfl*^{RNAi} and *Mef2-Gal4>UAS-ttv*^{RNAi}), SSR organization was severely disrupted. The empty spaces between membrane layers were extended dramatically. **D** Quantitative analysis of membrane content in the SSR region showed significant decreases in *sfl*^{RNAi} or *ttv*^{RNAi} expressing muscles comparing with control. Scale bar in A-C, 1μm. Error bars denote SEM. ***, p < 0.001. Numbers at the bottom of the bars indicate sample sizes. ANOVA was used for statistical analysis, followed by Tukey's test. (TEM analysis was performed by Jieli Xu and Na Zhao. Statistical analysis and figure composition were performed by Na Zhao)

4.2 Compromising heparan sulfate biosynthesis produces a net increase in autophagy

4.2.1 Loss of heparan sulfate increases the number of autophagosomes

Transmission electron microscopy of the NMJ revealed other changes associated with RNA interference of *sfl* in the muscle cell. The cytoplasm of the

muscle cell was filled with numerous double-membrane enclosed structures, an architecture suggestive of macroautophagosomes (Figure 4.4 B, indicated by yellow arrows). This phenomenon was not found in control flies where no RNAi construct was expressed (Figure 4.4 A). Quantitative analysis showed that RNAi of *sfl* in the muscle produced significantly more of these double-membrane vesicular structures compared to control animals (Figure 4.4 C).

Macroautophagosomes form during autophagy, a conserved process in which cytoplasmic components are enveloped and delivered to lysosomes for degradation (Klionsky and Emr, 2000; Klionsky, 2007; Mizushima et al., 2008). Autophagy is commonly viewed as a stress response mechanism, allowing cells to endure detrimental conditions such as starvation or other cellular stressors. To understand the nature of the intracellular membrane structures we observed in the muscle cells of animals with compromised HS biosynthesis, we examined the levels of lysosomal vesicles and autophagosomes, using LysoTracker dye and eGFP-tagged ATG8a respectively. LysoTracker is a red fluorophore linked to a weak base that selectively binds to and accumulates within acidic intracellular compartments, mainly lysosomes and autolysosomes (autophagosome-lysosome fusion vesicles) (Via et al., 1998). ATG8a is a ubiquitin-like protein that becomes covalently conjugated to lipids on the autophagosome vesicle membrane and mediates vesicle expansion during autophagosome formation (Nakatogawa et al., 2007). In *Drosophila*, LysoTracker and ATG8a-eGFP have been widely used for studying autophagy in fat body cells, gut and salivary gland tissues (Rusten et al., 2004; Scott et al., 2004; Scott et al., 2007; Wang et al., 2010). Our analysis showed that LysoTracker and ATG8a-eGFP can be employed as autophagic markers in muscle cells. A few scattered ATG8a-eGFP-positive patches were detected in control animals (*Mef2-Gal4/+*), representing the basal level of autophagy under normal circumstances (Figure 4.4 D). RNAi directed against *sfl*, *ttv* or *botv* all significantly increased the levels of ATG8a-eGFP-labeled vesicles in the muscle cell (Figure 4.4 E-G). Quantitative analysis showed that the average number of ATG8a-eGFP-positive structures was

significantly higher in animals expressing RNAi against *sfl*, *ttv*, or *botv* compared to control flies (Figure 4.4 H). RNAi of *sfl* resulted in the greatest accumulation of ATG8a-eGFP-labeled structures, consistent with the result of TEM analysis showing that compromising *sfl* had the greatest effect on these autophagic structures (Figure 4.4 B and H).

While ATG8a-eGFP detects autophagosome formation, LysoTracker staining provides a way to assess the later stages of the autophagy progressing. In control flies, LysoTracker-positive structures are concentrated at the perinuclear region (Figure 4.4 I). Reduction of *sfl* function by RNA interference significantly increased the number of lysosomal vesicles labeled with LysoTracker and slightly altered the perinuclear distribution pattern seen in control muscles (Figure 4.4 J and K). However, inhibition of *ttv* or *botv* function did not affect the level of lysosomal vesicles labeled with lysoTracker (Figure 4.4 K). Taken together, these findings suggest that HS is critical for the suppression of autophagosome production, but RNAi mediated knockdown of different enzymes produces different levels of effect. Earlier studies of mutants in these three HS-biosynthetic enzyme encoding genes indicated that *sfl* null alleles caused the most severe phenotypes in larval stages (Ren et al., 2009). Loss of *sfl* function produces HSPGs with unsulfated GAG chains, a form of the molecule that may well interfere with a number of signaling systems and produce a dominant-negative effect. Loss of the other enzymes that are required for polymer formation (*ttv*, *botv*) would produce only truncation of the GAG attachments, and might even result in the synthesis of other GAG chains in place of HS, such as chondroitin sulfate, which might provide some functional capability. Both *ttv* and *sotv* are bifunctional enzymes, having both *N*-GlcNAc transferase II and GlcA transferase II activities (Han et al., 2004; Takei et al., 2004; Izumikawa et al., 2006). There is evidence to show that *ttv* and *sotv* function redundantly in regulating morphogen signaling, suggesting that *sotv* may functionally compensate for the loss of *ttv* function in autophagosome formation (Bellaiche et al., 1998; The et al., 1999; Han et al., 2004).

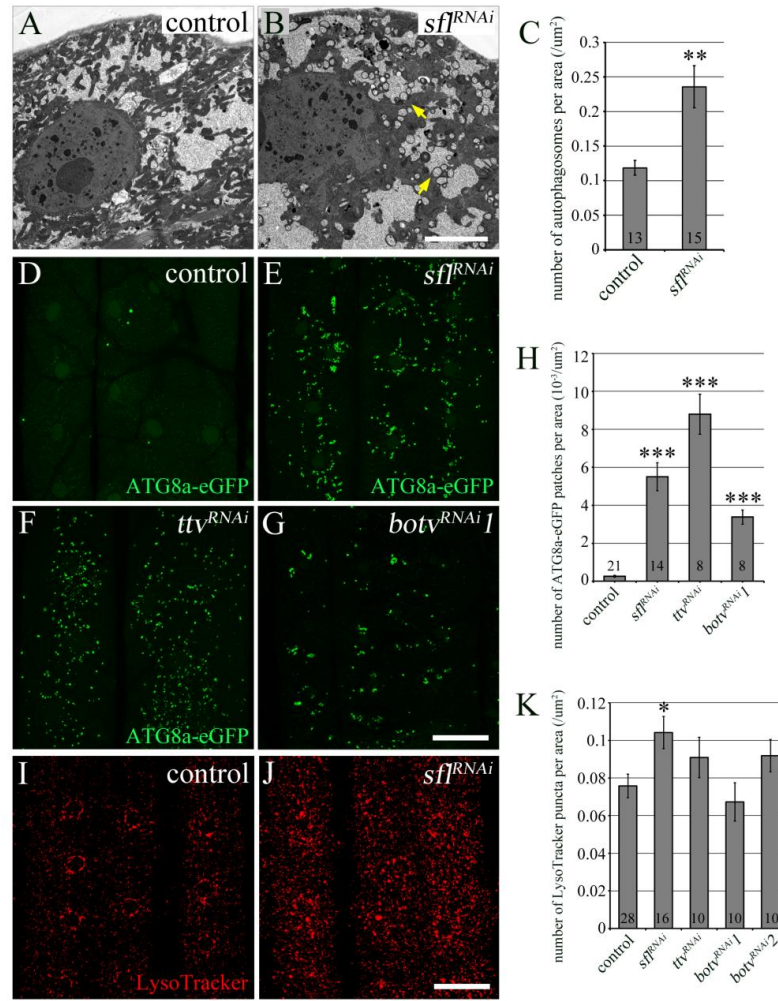


Figure 4.4 Accumulation of autophagosomes in animals with compromised HS biosynthesis. **A** and **B** Electron micrographs of the perinuclear region in controls and animals with reduced *sfl* function in the muscle. Compared with control (*Mef2-Gal4/+*), larvae expressing *sfl* RNAi in the muscle (*Mef2-Gal4>UAS-sfl^{RNAi}*) exhibited marked accumulation of double-membrane autophagic structures. **C** Reduced HS modification mediated by *sfl^{RNAi}* in the muscle resulted in an approximately two fold increase in the number of autophagosomes. **D-G** To detect the level of autophagy, autophagosomes were visualized with autophagic marker ATG8a-eGFP. In the muscle cells where HS biosynthesis was interrupted by RNA silencing of *sfl*, *ttv* or *botv*, ATG8a-eGFP-positive patches were notably more numerous than that in controls (*UAS-ATG8a-eGFP; Mef2-Gal4/+*). **H** Average number of ATG8a-eGFP-positive patches in the muscles 6 and 7. Animals with RNAi mediated inhibition of HS biosynthetic genes *sfl*, *ttv* or *botv* all showed significantly higher level of autophagosome accumulation. **I** and **J** Detection of autophagy levels by live imaging of LysoTracker, a red fluorophore dye that binds specifically to acidic organelles

such as lysosomes and autolysosomes. **I** In control muscles (*Mef-Gal4/+*), LysoTracker-positive structures evenly distributed in the cytosol as puncta with a mild concentration in the areas surrounding the nucleus. **J** Animals with muscle-specific expression of *sfl^{RNAi}* (*Mef-Gal4/UAS-sfl^{RNAi}*) showed increases in both the number of LysoTracker-positive puncta and the fluorescent intensity of these structures. **K** Compared to controls, the average number of LysoTracker-positive structures was significantly increased in *sfl^{RNAi}* expressing animals, but not in *ttv^{RNAi}* or *botv^{RNAi}* expressing animals. Scale bars in A-B, 5µm; D-G and I-J, 50 µm. Error bars denote SEM. *, $p < 0.05$; **, $p < 0.01$; ***, $p < 0.001$. Numbers at the bottom of the bars indicate sample sizes. Student's t-test was used for penal C; ANOVA was used for penal H and Kruskal-Wallis for penal K, followed by Tukey's test or Mann-Whitney test. (Data collection of the level of ATG8a-eGFP positive vesicles was performed by Jie Xu. Data analysis and figure composition was performed by Na Zhao.)

4.2.2 Compromising HS biosynthesis produces a net increase in autophagy and not simply an accumulation of autophagosome intermediates

An increased number of autophagosomes does not necessarily indicate a net increase in autophagy, since accumulation of autophagosomes could result from a blockade in their delivery to, and fusion with, their ultimate cellular destination, the lysosome. To determine if the increases in autophagosomes found in animals with compromised HS biosynthesis in the muscle were accompanied by a net increase in autophagy, we employed an ATG8a marker that is tagged with both GFP and mCherry fluorescent epitopes (Nezis et al., 2010). This construct produces both GFP and mCherry fluorescence in non-acidic compartments. However, GFP emission is lost immediately after the molecule arrives in the lysosome. Protonation in the acidic environment of the lysosome disrupts the protein structure necessary for GFP fluorescence, while mCherry fluorescence is highly stable and resistant to acidic environments (Kneen et al., 1998; Kimura et al., 2007). Thus, the number of GFP and mCherry double-fluorescing structures (yellow) provides a measure of early autophagosomes, whereas structures having solely mCherry signal (red) indicate the relative number of autolysosomes (Figure 4.5 A). In control animals, a portion of the mCherry fluorescent puncta overlapped with GFP fluorescent puncta, consistent with the shared labeling of early autophagosomes (Figure 4.5 B-D). In animals bearing either *sfl* or *ttv* RNAi

constructs, the levels of GFP and mCherry double-positive vesicles were elevated compared to control animals, paralleling the results obtained from analysis of ATG8a-eGFP constructs (Figure 4.5 E-J). In addition, the number of mCherry-exclusive fluorescing structures was significantly increased in both *sfl*^{RNAi} and *ttv*^{RNAi} expressing animals compared with controls (Figure 4.5 B-K). This finding shows that a net increase in autophagic flux to the lysosome occurred when HS biosynthesis was compromised.

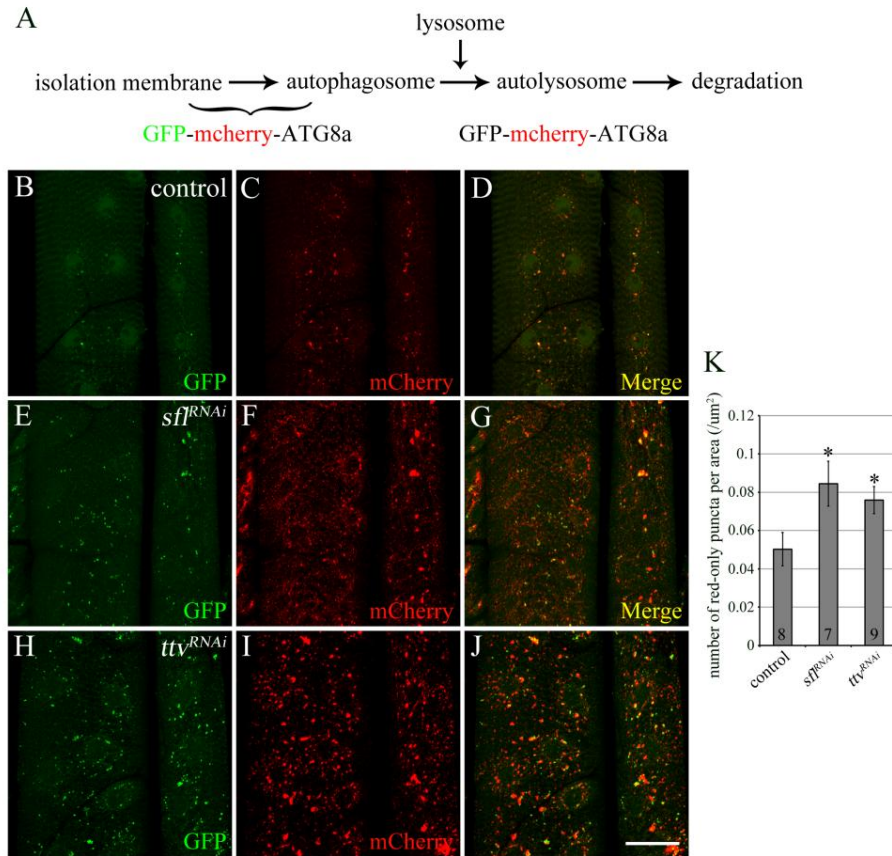


Figure 4.5 Reductions in HS biosynthesis and modification result in a net increase in autophagic flux. **A** To monitor changes in different stages of autophagic flux, a doubly-tagged ATG8a (GFP-mCherry-ATG8a) marker was used to distinguish autophagosomes from autolysosomes. Doubly-tagged ATG8a accumulated in premature autophagosomes, emitting both red and green fluorescence. After autophagosomes fuse with lysosomes, the green fluorescence of GFP is quickly quenched due to the acidic environment in autolysosomes, while the red fluorescence of mCherry is retained. Thus, in merged confocal images, yellow signals

indicate autophagosomes and red signals indicate autolysosomes. **B-J** Confocal images of animals expressing the *GFP-mCherry-ATG8a* transgenic construct in the muscle cells. Compared to control animals bearing no RNAi transgene, larvae expressing muscle-directed RNAi of *sfl* or *ttv* showed a drastic increase in the number of GFP and mCherry labeled patches. Merged images showed that in *sfl*^{RNAi} or *ttv*^{RNAi} expressing muscle cells, a substantial number of mCherry-labeled patches were not co-labeled with GFP, indicating an increase in the number of autolysosomes. **K** Distinct from control cells, muscle cells co-expressing RNAi constructs of *sfl* or *ttv* showed significantly more mCherry-exclusive puncta, indicating a net increase in the level of autophagy in those animals. Scale bar in B-J, 50 μ m. Error bars denote SEM. *, $p < 0.05$. Numbers at the bottom of the bars indicate sample sizes. ANOVA and Tukey's test were used for statistical analysis.

4.3 Increased autophagy alters mitochondrial number and morphology in HS biosynthesis defective animals

As a type of cytosolic organelle, mitochondria are one on the many substrates of autophagy, and can be targeted for recycling to compensate for periods of nutrient deprivation (Youle and Narendra, 2011). Moreover, selective autophagy of mitochondria, termed mitophagy, acts as a quality control mechanism by eliminating aged or damaged mitochondria (Johansen and Lamark, 2011; Youle and Narendra, 2011). Previous analysis of *sfl* mutant larvae demonstrated a significant decrease in the number of mitochondria in the muscle cell (Ren et al., 2009). To replicate and extend this finding, mitochondrial numbers were determined by TEM analysis of the NMJ in larvae expressing either *sfl* or *ttv* RNAi in muscle tissue (Figure 4.6 A-C). At the NMJ, mitochondria are concentrated underneath the postsynaptic membrane. In control flies, mitochondria were the major cellular organelle occupying the subsynaptic cytoplasmic spaces, whereas in animals with reduced *sfl* or *ttv* function, the numbers of mitochondria were dramatically reduced (Figure 4.6 A-C). Statistical analysis showed that these reductions were significant in both *sfl* and *ttv* RNAi bearing animals (Figure 4.6 D).

In *sfl*^{RNAi} expressing muscle, autophagosomes and isolation membranes were found in the immediate vicinity of mitochondria (Figure 4.6 B). The reduction in

mitochondrial density was also accompanied by changes in mitochondrial morphology. Instead of the normally elongated, rod-shape mitochondria seen in control animals, *sfl* RNAi produced curved or ring-shape mitochondria (Figure 4.6, compare F to E, representative mitochondria are indicated with red arrows). Reduction of *ttv* function resulted in less elongated, more rounded mitochondria (Figure 4.6 compare G to E, representative mitochondria are indicated with red arrows). Lysosomes enveloping what appear to be mitochondrial remnants were also seen in the TEM micrographs of animals with compromised HS biosynthesis (Figure 4.6 G, indicated by green arrow heads). We conducted confocal microscopic analysis to evaluate mitochondria morphological changes with mito-GFP, a mitochondrial-targeted recombinant protein (Cox and Spradling, 2003). In contrast to the normal, elongated mitochondria present in control animals, spherical mitochondria were found to be prevalent in animals bearing RNAi lines directed against *sfl*, *ttv* or *botv* (Figure 4.6 H-K, n: nucleus). To determine if mitochondria were associated with autophagosomes, and hence that the reduction of mitochondrial numbers could be the result of enhanced autophagy, mitochondria and autophagosomes were examined simultaneously using a monoclonal mitochondrial antibody, 4C7, and ATG8a-eGFP, an autophagosomal marker. Visualization of mitochondria (red) and autophagosomes (green) by confocal microscopy showed some mitochondria in *sfl*^{RNAi} muscles in close association with autophagosomes (Figure 4.6 L-N, mitochondria enveloped by autophagosomes are indicated with arrows, n: nucleus). Three-dimensional reconstruction of serial confocal sections (a high magnification view of Figure 4.6 N) showed mitochondria were surrounded by autophagosomal membranes, suggesting a role of autophagy in the reduction of mitochondrial number in animals with compromised HS biosynthesis (Figure 4.6 O).

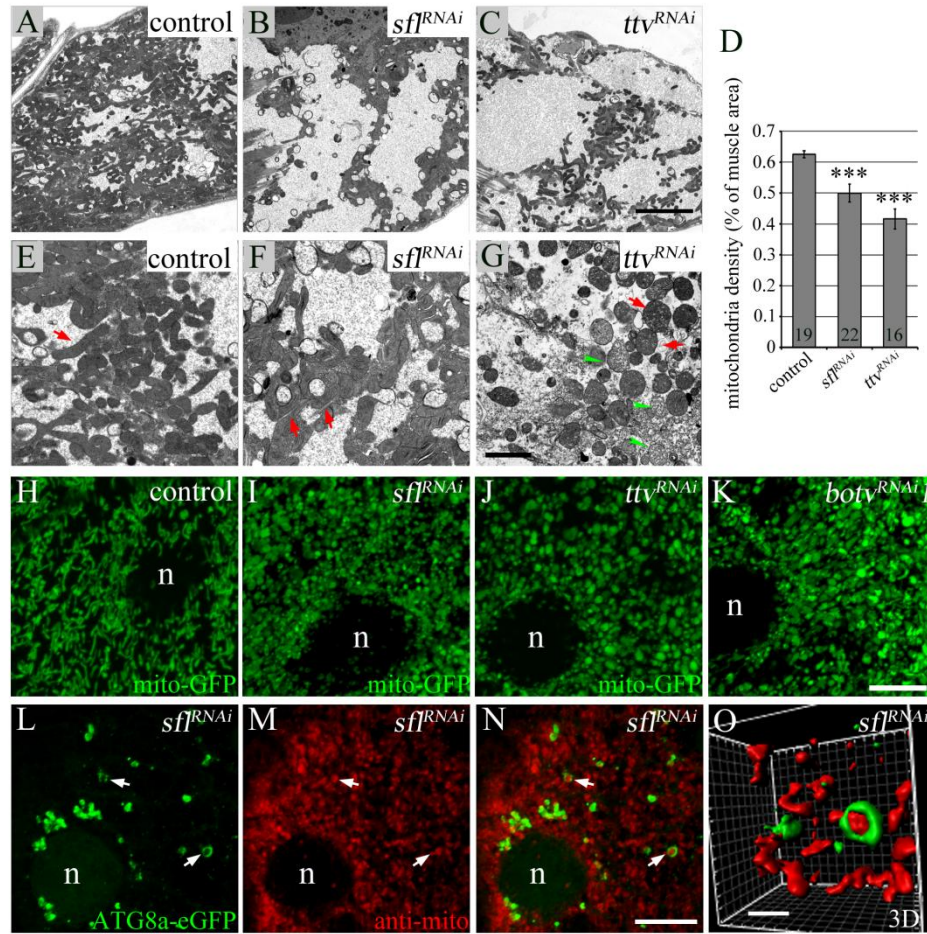


Figure 4.6 Disrupted HS biosynthesis in muscle tissue affects mitochondrial numbers and morphology. **A-C** and **E-G** TEM micrographs of mitochondria in the postsynaptic cytosol. **A-C** Compared with controls (*Mef2-Gal4/+*), the density of mitochondria was decreased in animals with inhibited expression of *sfl* or *ttv* in muscle cells (*Mef2-Gal4>UAS-sfl*^{RNAi} or *Mef2-Gal4>UAS-ttv*^{RNAi}). **D** Quantification of mitochondrial densities (area occupied by mitochondria normalized by cytosolic area) in control and HS biosynthesis compromised larvae. Mitochondrial density decreased significantly in *sfl*^{RNAi} or *ttv*^{RNAi} expressing animals. **E-G** Mitochondrial shape was altered in animals with RNAi-mediated inhibition of *sfl* and *ttv*. **E** In control animals, mitochondria appeared as tubular rods (red arrow). **F** In animals where muscle-directed *sfl*^{RNAi} was expressed, mitochondria were less extended, and bent into ring- or cup-like shapes (red arrows). **G** In *ttv*^{RNAi} expressing muscle, mitochondria were shorter and fatter (red arrows). Lysosomes enveloping membrane remnants were also observed in the proximity with these mitochondria spheroids (green arrow heads). **H** Mitochondria were further visualized using mitochondrially targeted GFP (mito-GFP) and filamentous mitochondria were evident in control animals. **I-K** Spherical mitochondria appeared in HS biosynthesis compromised animals where *sfl*^{RNAi}, *ttv*^{RNAi} or *botv*^{RNAi}

was expressed. **L-O** To determine if decreased mitochondrial density was caused by abnormally elevated autophagy, in *sfl^{RNAi}* expressing muscle, autophagosomes were visualized with ATG8a-eGFP (green) and mitochondria were detected with anti-mitochondrial antibody (red). In the perinuclear region, autophagosomal vesicles containing mitochondria spheroids are indicated by arrows. **O** Three dimensional re-rendering of serial confocal micrographs depicting autophagosome and mitochondrial localization in an animal expressing the *sfl^{RNAi}* construct. A mitochondrion enveloped by an autophagosomal vesicle is shown in a high magnification view. Scale bars in A-C, 5µm; E-G, 2.5 µm; H-N, 10 µm and O, 2 µm. Error bars denote SEM. ***, p-value < 0.001. Numbers at the bottom of the bars indicate sample sizes. ANOVA and Tukey's test were used for statistical analysis.

4.4 Down-regulation of autophagy suppresses phenotypes associated with heparan sulfate biosynthesis deficiency

4.4.1 Compromising *ATG8a* or *ATG8b* function rescues elevated levels of autophagy in animals with reduced *sfl* function

To determine if the increased level of autophagosomes mediated by loss of HS biosynthesis required early components of autophagosome assembly, the effect of reducing *ATG8a* or *ATG8b* gene function on the accumulation of LysoTracker-tagged structures in *sfl* RNAi animals was measured. ATG8a and 8b are the *Drosophila* orthologs of LC3, retaining a high degree of sequence similarity. Both ATG8a and 8b localize to autophagosomes through a ubiquitin-like conjugation system involving ATG4, ATG7 and ATG3 (Ichimura et al., 2000; Ohsumi, 2001; Nakatogawa et al., 2007). These two proteins have some functional redundancy; therefore, RNAi against either one of them only partially impairs autophagosome expansion (Berry and Baehrecke, 2007; Scott et al., 2007). RNAi of *sfl* significantly elevated the level of autophagic vesicles stained with LysoTracker in comparison to controls (Figure 4.7 A, B and G). Reducing the function of *ATG8a* or *8b* with RNA interference, or expressing a dominant-negative form of *ATG8a* (Kuma et al., 2007) all suppressed the effect of *sfl* RNAi on the number of LysoTracker-positive structures in the muscle cell (Figure 4.7 D-G). In contrast, co-expression of *GFP* with *sfl^{RNAi}* did not reduce the level of LysoTracker labeling,

demonstrating that the reduction in LysoTracker staining seen in *ATG8^{RNAi}*, *sfl^{RNAi}* or *ATG8a^{DN}*; *sfl^{RNAi}* co-expressing muscle cells was not due to an additional UAS promoter sequence or titration of Gal4 proteins (Figure 4.7 C and G). The effects of *ATG8a^{RNAi}*, *ATG8b^{RNAi}*, *ATG8a^{DN}* and *GFP* expression in wild-type animals were also measured with LysoTracker staining. Quantitative analysis revealed that reduction of *ATG8a* function by expressing either *ATG8a^{RNAi}* or *ATG8a^{DN}* significantly reduced the number of LysoTracker-positive puncta, while expression of *ATG8b^{RNAi}* or *GFP* did not (Figure 4.7 G). These findings indicate that loss of HS biosynthesis promotes autophagosome formation, a process that was reliant upon two critical components of autophagosome assembly, ATG8a and ATG8b.

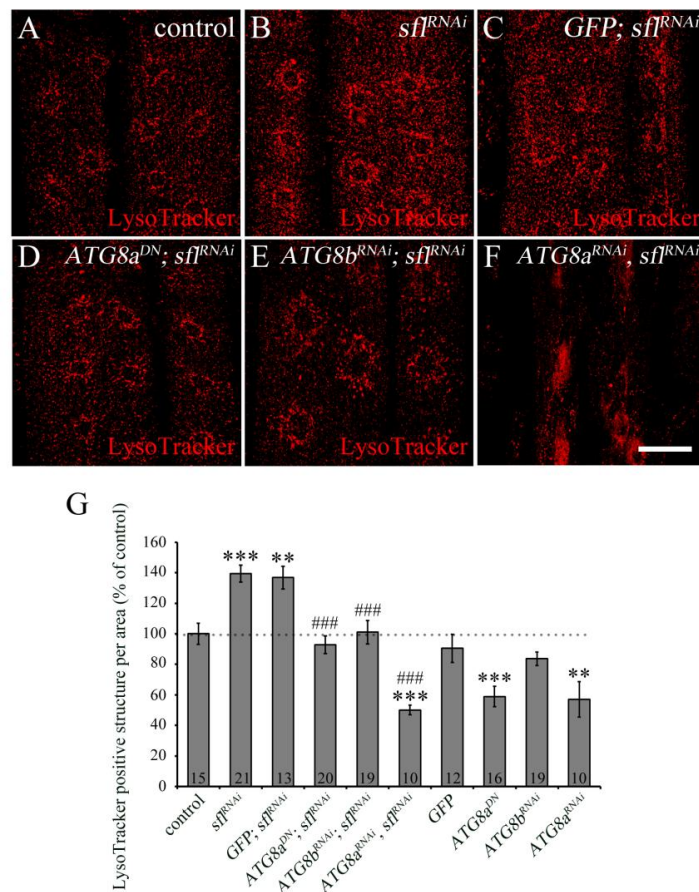


Figure 4.7 ATG8 is essential for increased autophagosome formation in HS biosynthesis compromised animals. A-F Confocal micrographs of LysoTracker staining showed that

reduction of *ATG8* function by RNA interference of *ATG8a/8b* or overexpression of a dominant-negative form of *ATG8a* (*ATG8a^{DN}*), successfully suppressed the elevated level of autophagy in *sfl^{RNAi}* expressed animals. **G** The level of autophagy was quantified by the abundance of LysoTracker-positive structures (per unit of muscle surface area). Average number of LysoTracker-bound structures for each genotype was compared to controls (*Mef2-Gal4/+*) and the normalized values were presented as the relative percent difference. Reduction in *sfl* function by RNAi induced a significant increase in LysoTracker staining, which was rescued to a significant degree by RNAi against *ATG8a/8b* or overexpression of *ATG8a^{DN}*. Expression of *UAS-GFP* (served as *UAS* copy number control) failed to suppress autophagy in *sfl^{RNAi}* expressing animals. Expression of *ATG8a^{RNAi}* or *ATG8a^{DN}* in wild-type animals resulted in significant decreases in the number of LysoTracker-positive structures, whereas expression of *ATG8b^{RNAi}* or *GFP* had no effect on the number of LysoTracker-positive structures. Scale bar in A-F, 50 μ m. Error bars denote SEM. **, $p < 0.01$; ***, $p < 0.001$ for comparisons with *Mef-Gal4/+*. ###, $p < 0.001$ for comparisons with *Mef-Gal4>UAS-sfl^{RNAi}*. Numbers at the bottom of the bars indicate sample sizes. Kruskal-Wallis and Mann-Whitney test were used for statistical analysis. (Transgenic fly lines containing double *UAS* constructs were generated by Jie Xu in this experiment.)

4.4.2 Reducing the levels of autophagy in HS biosynthesis defective animals rescues lethality

HS biosynthesis is required for viability; animals bearing mutations in key enzyme-encoding genes suffer developmental arrest and do not survive to the adult stage (Perrimon et al., 1996; Lin et al., 1999; Lin and Perrimon, 1999; Baeg et al., 2001; Ren et al., 2009). Consistent with published work describing lethality of mutant alleles, animals bearing RNAi constructs targeting *sfl* or *ttv* under the control of a ubiquitously-expressed *Gal4* transcriptional activator, *Da-Gal4*, exhibited lethality at second instar larval and early pupal stages respectively (Table 4.1 up). As an important mechanism for quality control and starvation adaption, autophagy plays dual roles in survival and programmed cell death associated with normal development (Levine and Yuan, 2005). While a basal level of autophagy protects cells through continual clearance of aged or damaged cytoplasmic components, excessive autophagy leads to cell death. Therefore, misregulation of this cellular process mediated by loss of HS biosynthesis could contribute to lethality. To determine if lethality induced by

reduction of *sfl* or *ttv* function is due to elevated levels of autophagy, we examined the developmental stage to which animals with both compromised HS biosynthesis and reduced *ATG8a* or *ATG8b* function survived. Ubiquitous expression of *ATG8a^{DN}* or *ATG8^{RNAi}* constructs partially rescued the lethality caused by *sfl* RNAi, extending survival from the second instar larval stage to pupal and adult stages (Table 4.1 middle). Expression of *GFP* did not affect survival of animals expressing *sfl^{RNAi}*, indicating that the delay in lethality was due to reduced activity of the *ATG8a* or *ATG8b* genes, but not by increased *UAS* copy numbers or reduced availability of Gal4 proteins to bind the *UAS* region of RNAi transgenic construct (Table 4.1 middle). Similarly, reduction of *ATG8a* or *ATG8b* function in *ttv^{RNAi}* expressing animals extended survival from the pre-pupal stage to late pupal stage (Table 4.1 bottom). These findings indicate that the abnormally elevated level of autophagy caused by impaired HS biosynthesis has impacts on developmental progression and lethality.

Table 4.1 Reduction of *ATG8a* or *ATG8b* function extends the survival stage in HS compromised *Drosophila*.

genotype	viability
<i>Da-GAL4/+</i>	adults
<i>Da-GAL4/UAS-sfl^{RNAi}</i>	2 nd instar larvae
<i>Da-GAL4/UAS-GFP; UAS-sfl^{RNAi}</i>	2 nd instar larvae
<i>Da-GAL4/UAS-ATG8a^{DN}; UAS-sfl^{RNAi}</i>	pupae to adults
<i>Da-GAL4/UAS-ATG8a^{RNAi}; UAS-sfl^{RNAi}</i>	pupae
<i>Da-GAL4/UAS-ATG8b^{RNAi}; UAS-sfl^{RNAi}</i>	pupae
<i>Da-GAL4/UAS-ttv^{RNAi}</i>	early pupae (white pupae)
<i>Da-GAL4/UAS-GFP; UAS-ttv^{RNAi}</i>	early pupae (white pupae)
<i>Da-GAL4/UAS-ATG8a^{DN}; UAS-ttv^{RNAi}</i>	pupae to adults
<i>Da-GAL4/UAS-ATG8a^{RNAi}; UAS-ttv^{RNAi}</i>	pupae
<i>Da-GAL4/UAS-ATG8b^{RNAi}; UAS-ttv^{RNAi}</i>	pupae

(This experiment is performed by Jie Xu)

4.4.3 Reducing autophagy in animals with compromised *sfl* function rescues mitochondrial and SSR morphological changes

We have demonstrated that reducing the function of *ATG8a* or *ATG8b* partially suppresses lethality associated with loss of HS biosynthetic function. It remained unknown whether changes in mitochondrial shape and SSR assembly were associated with elevated autophagy and could be rescued by reducing *ATG8a* or *ATG8b* function. To determine if reducing autophagy in animals with compromised *sfl* function would rescue mitochondrial morphological changes, mito-GFP was expressed to visualize mitochondria in muscle cells. Expression of *ATG8a^{RNAi}* largely restored the normal filamentous morphology of mitochondria in animals with reduced *sfl* function (Figure 4.8 A-C). To measure if the decreased number of mitochondria associated with reduction in HS biosynthesis would also be rescued by down-regulation of genes required for autophagy, the density of mitochondria was measured using TEM micrographs. Expression of either *ATG8a^{RNAi}* or *ATG8a^{DN}*, but not *UAS-GFP*, suppressed the reduction in mitochondrial density resulting from loss of *sfl* function (Figure 4.8 D). The influence of the level of autophagy on SSR structure was also examined. TEM sections of the NMJ in animals bearing *sfl^{RNAi}* with or without simultaneous expression of *ATG8a^{RNAi}* or *ATG8a^{DN}* were obtained, and the membrane content of the SSR was measured (Figure 4.8 E-I). In animals expressing both *sfl^{RNAi}* and *ATG8a^{RNAi}*, SSR membrane content (electron dense area divided by total subsynaptic area) was significantly increased compared to animals expressing *sfl^{RNAi}* alone, and was comparable to the SSR in control animals (Figure 4.8 G and I). Co-expression of *ATG8a^{DN}* with *sfl^{RNAi}* was able to partially restore SSR structure, increasing SSR membrane content to a significant level when compared to animals expressing *sfl^{RNAi}* alone (Figure 4.8 H and I). Thus, the reduction in SSR elaboration produced by inhibition of *sfl* function was significantly suppressed by either of the two methods of reducing *ATG8a* function. Together, these results demonstrated that impaired HS biosynthesis brought about both reduced SSR elaboration and the changes in mitochondrial density and morphology were through misregulation of autophagy.

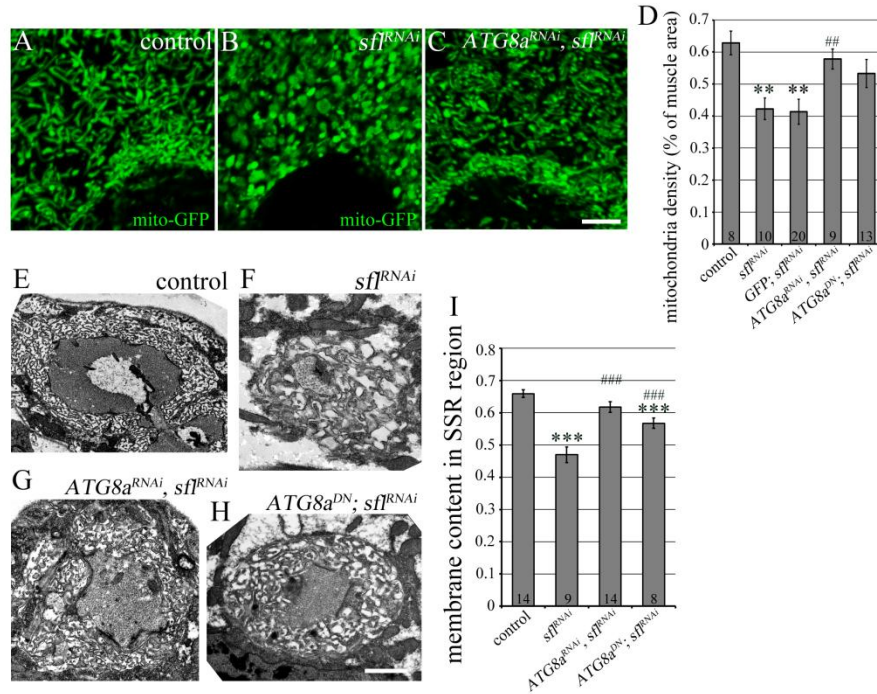


Figure 4.8 Mitochondrial and SSR phenotypes associated with loss of HS modification are suppressed by down-regulation of autophagy. A-C Mitochondria were labeled with mito-GFP and visualized using confocal microscopy. A In control larvae, mitochondria appeared as normally elongated tubules. B In animals with *sfl^{RNAi}* expressed in muscle, mitochondria were spherical in shape. C In animals where *ATG8a^{RNAi}* and *sfl^{RNAi}* constructs were co-expressed in the muscle, mitochondrial morphological abnormality was partially rescued. D Quantitative analysis of TEM micrographs showed that *sfl^{RNAi}* expression significantly reduced mitochondrial density compared to controls. Co-expression of *UAS-GFP* failed to increase the number of mitochondria in *sfl^{RNAi}* expressing animals. Co-expression of *ATG8a^{RNAi}* significantly increased mitochondrial density in *sfl^{RNAi}* expressing animals. Co-expression of *ATG8a^{DN}* and *sfl^{RNAi}* produced a moderate, statistically insignificant increase in mitochondrial density. E-H TEM images of SSR structure at the NMJ of muscles 6 and 7. E Control animals showed compactly assembled SSR. F Abnormally assembled SSR was found in animals with loss of *sfl* function. G and H Expression of either *ATG8a^{RNAi}* or *ATG8a^{DN}* suppressed SSR morphological deficits caused by *sfl^{RNAi}*, enhancing SSR density and membranous elaboration. I Quantification of membrane content in the SSR region. Animals expressing *sfl^{RNAi}* exhibited significant decreases in membrane density compared to control animals. Reduction of *ATG8a* function by expressing either *ATG8a^{RNAi}* or *ATG8a^{DN}* in the muscle restored SSR membrane density in *sfl^{RNAi}* animals to a significant level. Scale bars in A-C, 2 μ m; E-H, 1 μ m. Error bars denote SEM. **, $p < 0.01$; ***, $p < 0.001$ for comparisons with *Mef2-Gal4/+*. ##, $p < 0.01$; ###, $p < 0.001$ for comparisons with *Mef2-*

Gal4>UAS-sff^{RNAi}. Numbers at the bottoms of the bars indicate sample sizes. Kruskal-Wallis and Mann-Whitney test were used for statistical analysis.

4.5 Regulation of autophagy in heparan sulfate biosynthesis compromised animals is mediated by PI3K

4.5.1 Heparan sulfate biosynthetic deficiency does not induce *Xbp1* mediated ER stress

We have demonstrated that compromising HS biosynthesis or modification increases autophagy, however, the mechanism by which HS regulates this process remained to be determined. The influence of HS on autophagy could operate either through a direct functional relationship, or indirectly as a general consequence of reduced HS function. ER stress is known as a cellular response induced mainly by the accumulation of unfolded or misfolded proteins in the ER (Rao and Bredesen, 2004; Zhang and Kaufman, 2004; Schroder and Kaufman, 2005). It can also be induced by defective glycosylation in the Golgi apparatus (Xu et al., 2010). Emerging evidence suggests that ER stress can trigger an autophagic response to protect cells from apoptotic cell death (Ogata et al., 2006; Yorimitsu et al., 2006; Fouillet et al., 2012). It is therefore possible that perturbation of HS biosynthesis or modification, which occurs in the Golgi complex, could induce autophagy indirectly by disrupting the secretory pathway and inducing ER stress. To evaluate this possibility, we examined the expression of an *Xbp1-eGFP* gene fusion reporter construct (Ryoo et al., 2007). *Xbp1* encodes a transcription factor that is activated after Ire-1 mediated mRNA unconventional splicing, which occurs in response to ER stress (Ruegsegger et al., 2001; Shen et al., 2001; Yoshida et al., 2006; Ryoo et al., 2007). The fusion construct integrates an eGFP coding sequence after the *Xbp1* splicing site, in a frame that will only be read through after an alternative splicing event occurs (Ryoo et al., 2007). Therefore, fluorescent eGFP protein will only be translated when ER stress is triggered. This construct has been used successfully as a sensitive indicator of ER stress activation in *Drosophila* (Ryoo et al., 2007; Kang

and Ryoo, 2009; Kang et al., 2012). We used this construct to test for the presence of an Ire-1 mediated ER stress response in animals expressing muscle-directed RNAi against *sfl* or *ttv*, conditions that produce elevated autophagy. In control animals, no eGFP fluorescence was detected in the nucleus of muscles 6 and 7 (Figure 4.9 A). *ninaE* is a *Drosophila rhodopsin-1* gene (Otousa et al., 1985). A misfolded version of the *ninaE* protein, *ninaE*^{G69D}, causes defects in protein maturation and disrupts ER to Golgi transportation, which induces ER stress (Colley et al., 1995; Kurada and Otousa, 1995; Ryoo et al., 2007). Expression of *ninaE*^{G69D} in muscle cells induced a clear eGFP signal in the nucleus, validating the usefulness of this ER stress reporter in our system (Figure 4.9 B). Knockdown of either *sfl* or *ttv* using RNAi did not induce any eGFP expression above the background level seen in control animals (Figure 4.9 C and D). This finding indicates that disruption of HS polymer synthesis or sulfation does not cause an Ire-1 mediated ER stress response. It is therefore unlikely that the elevated levels of autophagy in HS loss-of-function animals occur indirectly as a result of ER stress.

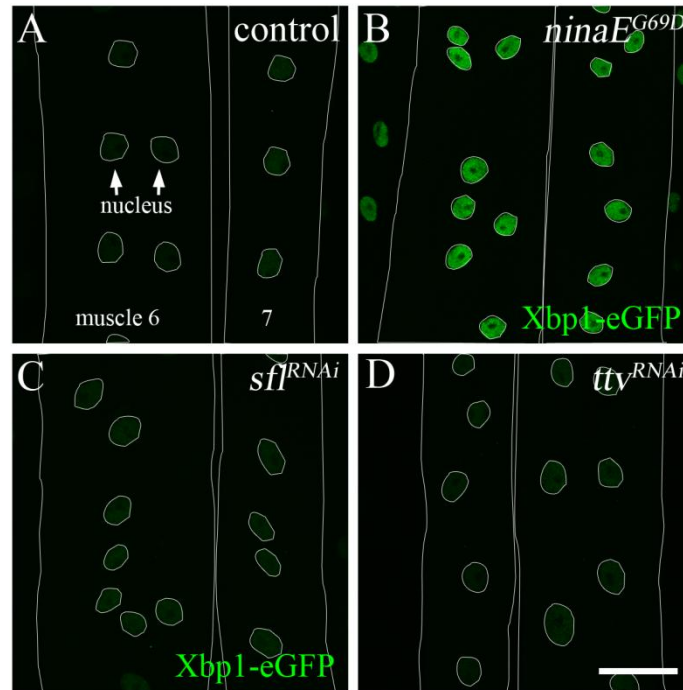


Figure 4.9 ER stress is not induced in animals with inhibited HS biosynthesis. To test if the elevated level of autophagy seen in HS biosynthesis defective animals was due to an induced ER stress response, an ER stress reporter Xbp1-eGFP was employed. **A** In control animals, no eGFP fluorescence was detected in the nucleus of muscle cells (*Mef2-Gal4, UAS-Xbp1-eGFP/+*). **B** GFP fluorescence appeared in the nucleus when ER stress was induced by expressing *ninaE^{G69D}*, validating Xbp1-eGFP as an ER stress reporter in muscle tissue. **C** and **D** GFP fluorescence was not detected in *sfl^{RNAi}* or *ttv^{RNAi}* expressing muscle cells, indicating that Ire-1 mediated ER stress was not induced in those animals. Scale bar in A-D, 50μm.

4.5.2 PI3K plays a role in heparan sulfate modulated autophagy and mitochondrial morphology

One of the signaling molecules known to participate in the regulation of autophagy is class I PI3K, a receptor-linked kinase activated by a number of secreted protein growth factors (Petiot et al., 2000). Down-regulation of PI3K activity is necessary for the induction of autophagy in response to nutrient deprivation and to initiate developmental autophagy during metamorphosis (Rusten et al., 2004; Scott et al., 2004; Berry and Baehrecke, 2007). Many of the signaling systems that activate PI3K are modulated by HS (Abid et al., 2004; Dey

et al., 2010; Sarrazin et al., 2011). We hypothesize that deficits in HS biosynthesis and modification could produce an increase in autophagy through impaired PI3K activation. To determine if PI3K signaling serves a role in the regulation of autophagy at the NMJ, as has been reported for other tissues, the connection between PI3K and autophagy in muscle cells was examined. RNAi induced functional knockdown of *PI3K* in the muscle resulted in increased numbers of both autophagic vesicles marked with LysoTracker and ATG8a-eGFP-positive structures (Figure 4.10 A-F, Q and R). Expression of *PI3K^{RNAi}* also produced shorter and rounder mitochondria in comparison to the normal-sized, rod-shaped mitochondria seen in control animals (Figure 4.10 G and H). These changes are similar to the phenotypes found in animals with compromised HS biosynthesis or modification, suggesting that HS and PI3K may regulate autophagy through a common mechanism.

To further test the hypothesis that HS regulates autophagy by modulating PI3K activity, we determined if the activation of autophagy produced by compromising HS biosynthesis could be rescued by increasing PI3K activity. In the animals with reduced function of either *sfl* or *ttv*, up-regulation of PI3K activity was achieved by overexpressing *Dp110^{WT}*, the wild-type catalytic subunit of PI3K, in the muscle cells (Leevers et al., 1996). In these animals, expression of ATG8a-eGFP was suppressed to background levels, showing that the impact of loss of HS function on autophagy could be completely overcome by modulating PI3K activity (Figure 4.10 I-L and S). To test if mitochondrial morphological deficits observed in HS compromised animals could also be rescued by overexpressing *Dp110^{WT}*, mito-GFP was expressed in the muscle to monitor the changes in mitochondrial morphology. Expression of *Dp110^{WT}* in the muscle of otherwise wild-type animals didn't affect the shape of mitochondria (Figure 4.10 O). However, co-expression of *Dp110^{WT}* in the muscle of animals with reduced *sfl* function restored normal mitochondrial morphology (Figure 4.10 P). These findings indicate a correlation between HS biosynthesis and PI3K activity in the regulation of autophagy and autophagy associated cellular phenotypes.

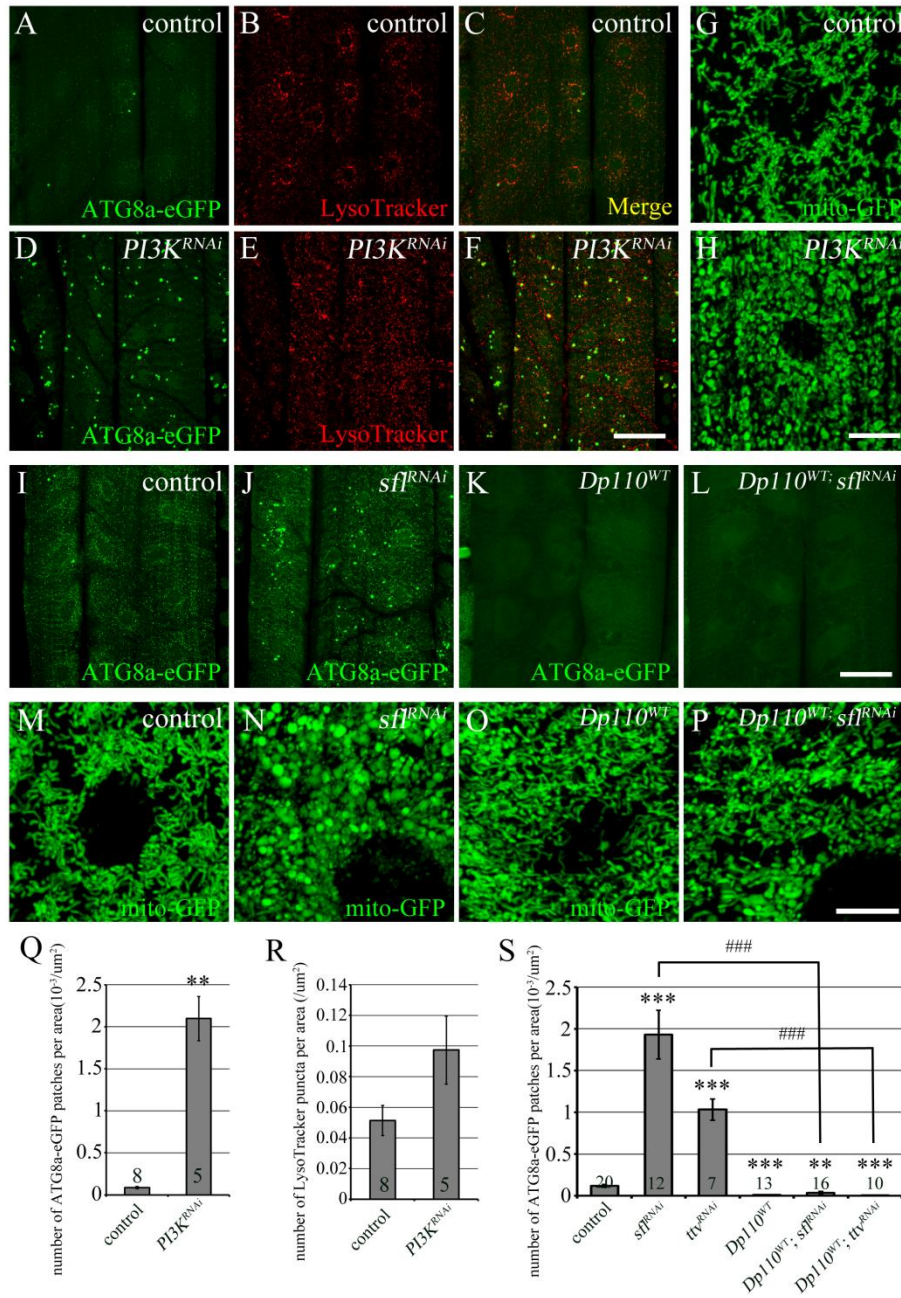


Figure 4.10 PI3K is implicated in the association between HS biosynthesis and autophagy.

A-F Reduction of class I PI3K activity mediated by *PI3K* RNAi induced autophagy in normal fed larvae. Autophagosomes were labeled with ATG8a-eGFP (green) and autolysosomes/lysosomes were labeled with LysoTracker (red). Compared to controls, animals expressing *PI3K^{RNAi}* showed increased numbers of both ATG8a-eGFP labeled and LysoTracker stained structures. **G** and **H** Compared to controls, animals with reduced PI3K activity in the muscle showed less elongated mitochondria, a phenotype that mimics HS biosynthetic deficient animals. **I-L** Increasing PI3K

activity through expression of an active *PI3K* transgene, *Dp110^{WT}*, suppressed autophagosome formation in *sfl^{RNAi}* expressing animals. **I** Control larvae showed basal levels of ATG8a-eGFP expression in the muscle. **J** Autophagosomes labeled with ATG8a-eGFP accumulated in the muscle of *sfl^{RNAi}* expressing animals. **K** Expression of *Dp110^{WT}* in wild-type animals eliminated ATG8a-eGFP-tagged patches. **L** Expression of *Dp110^{WT}* in the muscle completely suppressed the effect of *sfl* RNAi in autophagosome formation. **M-P** Up-regulation of PI3K activity restored normal mitochondrial morphology in *sfl^{RNAi}* animals. **M** Mitochondria in control (*UAS-mito-GFP; Mef2-Gal4/+*) animals appeared as normal-sized rods. **N** Loss of *sfl* function through RNAi induced a more spherical mitochondrial shape. **O** *Dp110^{WT}* expression in wild-type animals didn't affect mitochondrial morphology. **P** Expression of *Dp110^{WT}* suppressed the changes in mitochondrial morphology in *sfl^{RNAi}* expressing muscle. **Q** The number of ATG8a-eGFP-positive patches normalized by muscle surface area in control and *PI3K^{RNAi}* expressing animals. **R** The number of LysoTracker-positive puncta normalized by muscle surface area in control and *PI3K^{RNAi}* expressing animals. **S** Quantification for the average number of ATG8a-eGFP-labeled autophagosomes per muscle surface area in indicated genotypes. Co-expression of *Dp110^{WT}* suppressed autophagosome formation to a significant degree in animals expressing either *sfl^{RNAi}* or *ttv^{RNAi}*. Scale bars in A-F and I-L, 50 μ m; G and H, 10 μ m. Error bars denote SEM. **, $p < 0.01$; ***, $p < 0.001$ for comparisons with *UAS-ATG8a-eGFP; Mef2-Gal4/+*. ###, $p < 0.001$ for comparisons with *UAS-ATG8a-eGFP; Mef2-Gal4>UAS-sfl^{RNAi}* or *UAS-ATG8a-eGFP; Mef2-Gal4>UAS-ttv^{RNAi}*. Numbers at the bottom of the bars indicate sample sizes. Student's t-test was used for panel Q and R. ANOVA and Tukey's test were used for panel S. (Data presented in panels G to L was collected by Jie Xu and analyzed by Na Zhao. Transgenic fly lines expressing both *Dp110^{WT}* and *sfl^{RNAi}/ttv^{RNAi}* were generated by Jie Xu.)

4.5.3 PIP (3,4,5) triphosphate levels are reduced in muscle cells upon inhibition of HS biosynthesis

Previous results showed that PI3K activation suppressed the elevated level of autophagy produced by inhibiting HS biosynthetic genes *sfl* or *ttv*. To further test the hypothesis that HSPGs negatively affect autophagy via activation of PI3K, animals with compromised HS biosynthesis were examined for the level of PIP3, the product of PI3K catalyzed phosphorylation (Auger et al., 1989). The levels of PIP3 were examined in animals with RNA interference of *sfl* or *ttv* using a monoclonal antibody derived against this lipid (Chen et al., 2002). The sensitivity of this antibody was tested by comparing the level of PIP3 immunoreactivity in control and *PI3K^{RNAi}* expressing animals, and a significant decrease was

detected in animals with inhibited *PI3K* expression (Figure 4.11 A, D, E). Reducing HS biosynthesis produced a moderate but significant loss in PIP3 signal at the plasma membrane of muscle cells, suggesting that loss of HS biosynthesis may induce elevated levels of autophagy by decreasing PI3K activity (Figure 4.11 A-C, E). Taken together, we provide evidence to show that HS biosynthesis and sulfation has a strong correlation with PI3K activity in the regulation of autophagy and autophagy-associated mitochondrial phenotypes.

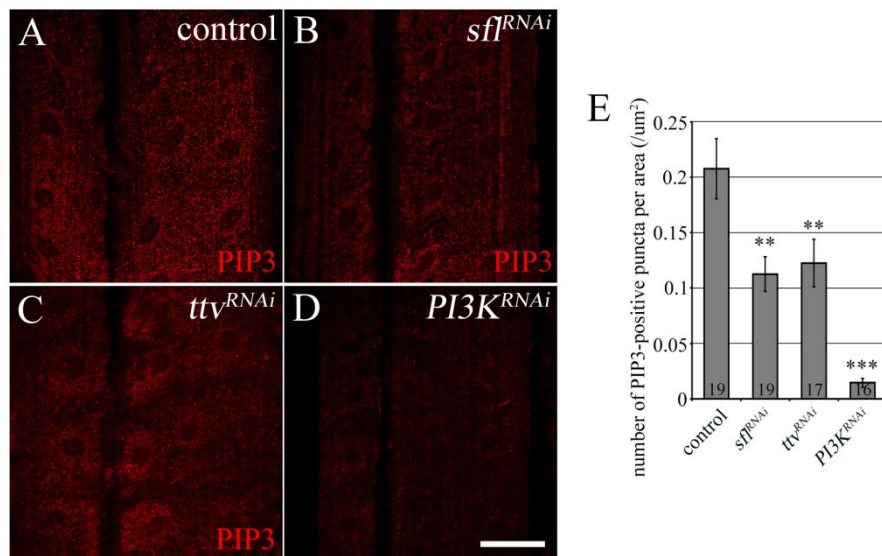


Figure 4.11 Reduction of PI3K activity in HS biosynthesis compromised animals. To evaluate the kinase activity of PI3K in HS biosynthesis compromised animals, PIP3, the product of PI3K activity, was detected using an anti-PIP3 antibody in control, *sfl*^{RNAi}, *ttv*^{RNAi} and *PI3K*^{RNAi} expressing animals. **A** PIP3-positive puncta were evenly distributed throughout the muscle cell of control (*Mef2-Gal4/+*) animals. **B-C** Reduced HS biosynthesis with *sfl* or *ttv* RNAi significantly decreased the levels of PIP3 staining. **D** *PI3K*^{RNAi} was expressed in the muscle, resulting in a dramatic reduction in PIP3 signals, demonstrating the sensitivity of the anti-PIP3 antibody. **E** Average numbers of PIP3-positive puncta per muscle surface area for indicated genotypes. Scale bar in A-D, 50 μm. Error bars denote SEM. **, *p* < 0.01. Numbers at the bottom of the bars indicate sample sizes. Kruskal-Wallis and Mann-Whitney test were used for statistical analysis.

To summarize, this chapter described a novel relationship between HSPG function and a common cellular process, autophagy, capable of influencing the

structural development of postsynaptic specializations. RNA interference of genes essential for HS polymerization and sulfation disrupted subsynaptic membrane organization of muscle cells and resulted in both a decreased number, and altered morphology of mitochondria. These phenotypes were associated with elevated autophagy, and could be rescued by compromising the function of ATG8a or 8b, essential components of the autophagic machinery. A number of findings indicate that HS negatively regulates autophagy via PI3K signaling without inducing an Ire-1 mediated ER stress response. While autophagy is widely accepted as a stress response and quality control mechanism, we demonstrate that HSPG regulated autophagy is critical for synapse assembly during development.

Chapter 5: Gene discovery: a forward genetic screen identifies two novel regulators of synapse assembly at the *Drosophila* NMJ

5.1 An overview of the RNA interference genetic screen to identify genes involved in *Drosophila* NMJ development

Previous work described in chapter 3 demonstrated that *Akt1* controls glutamate receptor composition by specifically governing the distribution of the GluRIIA subunit. However, the molecular mechanism by which this is accomplished and downstream regulatory targets of *Akt1* activity are still unknown. In order to explore potential effectors modulated by *Akt1* that govern GluRIIA localization, as well as to discover novel genes required for synapse assembly, a forward genetic analysis was conducted in our lab. This analysis took advantage of an existing transgenic RNAi library established by Vienna *Drosophila* RNAi Center (VDRC) (Dietzl et al., 2007). The VDRC genome-wide RNAi library currently maintains a total of 31,892 transgenic RNAi lines targeting 13,264 distinct genes, which accounts for about 93.8% of the entire *Drosophila* genome. We selected more than 6,000 independent RNAi transgenic fly lines for our research using the strategy and criteria outlined in Figure 5.1. Unlike the GD lines generated by random P-element insertion, RNAi transgenic flies from KK library were generated by phiC31-mediated single site chromosomal integration (chr2L: 22019296, cytological band 40D3 according to VDRC record). The KK library lines were chosen for this screen to avoid variations in expression pattern caused by positional effects (Bateman et al., 2006; Bischof et al., 2007; Dietzl et al., 2007; Markstein et al., 2008). RNAi transgenic constructs with off-target activity were excluded from our collection because those siRNAs may cause unintentional down-regulation of additional genes through partial sequence complementarity, which would complicate the explanation of any phenotypes observed in these animals (Lin et al., 2005). RNAi lines that caused embryonic lethality or severe global defects in muscle morphology when expressed in the muscle were also removed from the screening library (Schnorrer et al., 2010). The selected transgenic RNAi lines were individually crossed to the muscle-specific *Mef2-Gal4*

driver, and wandering third instar larval progeny were dissected and processed in order to examine GluRIIA localization and SSR membrane elaboration at the NMJ. Thus far, we have examined 513 independent RNAi lines, each targeted to a single protein-coding gene to knock down its expression in the muscle, accounting for about 3% of genes in the entire *Drosophila* genome. A total of 39 RNAi transgenic lines were found to exhibit phenotypic abnormalities in either GluRIIA localization, SSR morphology, or both. 24 of those animals showed decreased GluRIIA concentration at the NMJ, while 8 of them showed an increase in GluRIIA postsynaptic localization. Interestingly, although a number of genes affected GluRIIA expression levels (decrease or increase), knockdown of only one gene (*CG10565*) out of those screened so far produced the robust GluRIIA mislocalization phenotype seen in *Akt1* compromised animals. 22 of the RNAi lines presented with defects in SSR development, including a *Drosophila* *Acinus* gene which has been implicated in autophagic and endocytic trafficking (Haberman et al., 2010). Based on the results of this screen, *Acinus* and *CG10565* were selected for further study and their biological functions will be discussed at greater length in the rest of this chapter.

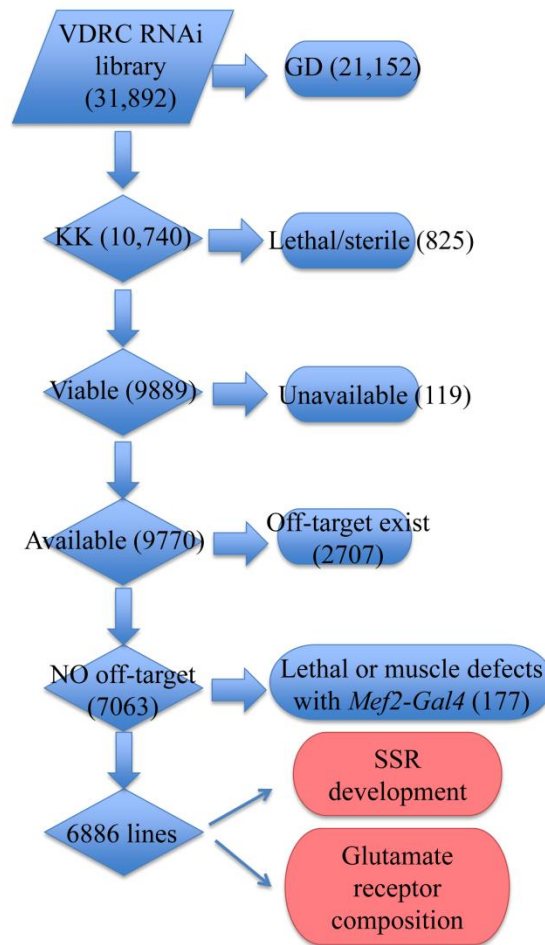


Figure 5.1 Flow chart depicting the collection of RNAi lines selected for use and the experimental outputs of this genetic screen. From the transgenic RNAi library generated in VDRC, “uninteresting” lines were filtered out based on their integration system, lethality, availability and specificity (GD: P-element-based RNAi library; KK: phiC31-based RNAi library; Lethal: die at embryonic or early larval stage; available: in stock; off-target: additional genes besides the intended target affected by RNAi through imperfect complementarity). A final collection consisting of 6,886 independent lines was chosen to perform a large-scale, unbiased, loss-of-function genetic screen. Two specific aims of this screen are: 1. Identify possible downstream effectors of *Akt1* in the regulation of GluRIIA localization. 2. Identify novel proteins essential for SSR development and glutamate receptor composition. (This genetic screen was designed by Scott Selleck and Hyun-Gwan Lee and performed by Joyce Lee, Do Young Kim, Daniel Song, Morgan Brown and Na Zhao.)

5.2 *Drosophila* Acinus governs autophagic degradation of α -spectrin cytoskeleton and affects SSR membrane organization at the NMJ

5.2.1 *Drosophila* Acinus affects SSR membrane organization during NMJ development

In the screen for genes affecting SSR assembly we assayed 513 transgenic *Drosophila* strains, each produced a double-stranded RNA to selectively eliminate a single target gene mRNA expression in muscle cells. *Acinus* (*Acn*), an apoptosis related gene, was identified in this screen for severely disrupted SSR morphology. To elucidate the function of *Acn* during synapse development, a GFP tagged membrane marker mCD8-GFP was expressed in the muscle cell to visualize the SSR, while the neuronal terminal was stained against the presynaptic vesicle marker CSP (Bronk et al., 2005). In control animals, mCD8-GFP was highly concentrated in the postsynaptic region surrounding the presynaptic bouton (marked by immunostaining against CSP), illustrating condensed membrane organization of the SSR (Figure 5.2 A-C). *Mef2-Gal4* directed muscle-specific expression of *Acn*^{RNAi} produced a dramatic change in SSR morphology. The overall fluorescent intensity of mCD8-GFP was markedly reduced, and the GFP fluorescence was less concentrated at the postsynaptic specializations, and was instead more diffusely spread into the extrasynaptic spaces connecting synaptic boutons (Figure 5.2 D-F).

To evaluate the efficacy and specificity of RNAi-mediated knockdown of *Acn* *in vivo*, the levels and distribution of *Acn* were assessed using a polyclonal antibody raised against the C-terminus of *Drosophila* *Acn* (Haberman et al., 2010). *Acn* was prominently concentrated in the nuclei, with only a small amount of proteins detected in the cytoplasm of muscle cells in control animals, consistent with the known distribution pattern of *Acn* in eye disc cells (Figure 5.2 G) (Haberman et al., 2010). *Acn* immunoreactivity was abolished in both nucleus and cytosol upon the expression of *Acn*^{RNAi} in muscle cells (Figure 5.2 H).

The SSR ultrastructural changes induced by loss of *Acn* function were assessed using transmission electron microscopy. Compared to wild-type boutons surrounded by compactly assembled SSR membrane stacks, boutons lacking postsynaptic *Acn* showed severe defects in their SSR structures (Figure 5.2 compare I with J). The SSR membranes were not tightly stacked, and the horizontal alignment between layers was also disrupted in animals lacking *Acn* activity (Figure 5.2 J). These changes were quantified by measuring the SSR thickness and density in TEM micrographs. In the absence of *Acn*, the SSR membrane thicknesses measured in both directions (parallel or orthogonal to muscle surface) were significantly increased (Figure 5.2 K). However, the membrane density measured as the average number of membrane layers within that space was decreased by a significant margin, indicating that the complexity of the SSR was impaired in these animals with inhibited expression of *Acn* (Figure 5.2 L). Taken together, these findings suggest that *Acn* is crucial for maintaining the integrity of subsynaptic membranes.

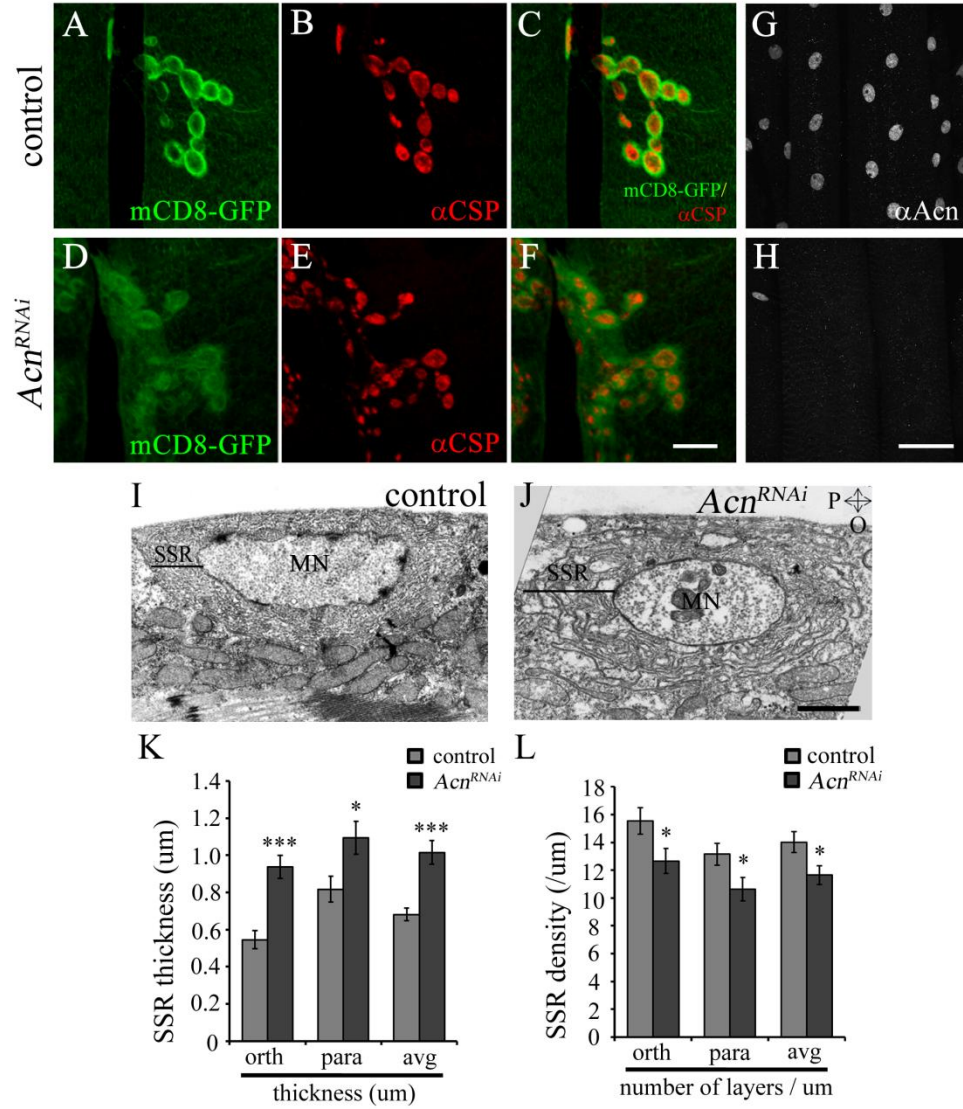


Figure 5.2 Loss of *Acn* in the muscle cells results in morphological defects of the SSR. A-F The SSR was visualized using GFP-conjugated mCD8 transmembrane protein (green), and the presynaptic boutons were marked with anti-CSP antibody staining (red). **A-C** In control animals (*Mef2-Gal4, UAS-mCD8-GFP/+*), presynaptic boutons were enveloped tightly by SSR and the narrow “necks” were clearly formed between neighbor boutons. **D-F** In the animals with muscle-specific RNA interference induced against *Acn* (*Mef2-Gal4, UAS-mCD8-GFP>UAS-Acn*^{RNAi}), SSR structures were severely perturbed and occupied a larger region, including not only the postsynaptic specialization but also “empty” space distant from synaptic boutons. **G** and **H** Acn protein levels were examined with polyclonal anti-Acn antibody (grayscale) in control and *Acn* RNAi animals. **G** in control animals (*Mef2-Gal4, UAS-mCD8-GFP/+*), Acn accumulated predominantly in the nucleus, with only a very small amount of protein detected in the cytosol of

the muscle cells. **H** RNA interference directed by a muscle-specific *Gal4* driver abolished both nuclear and cytoplasmic anti-Acn immunoreactivity. **I-L** Ultrastructural analysis of subsynaptic reticulum. MN: motoneuron; P: parallel; O: orthogonal. SSR thickness is indicated by black bars. **I** Cross-sectional view of a synaptic bouton in a control animal (*Mef2-Gal4/+*). The SSR membrane was normally assembled and tightly associated with presynaptic terminal. **J** In animals where *Acn* expression was suppressed with RNA interference in muscle cells (*Mef2-Gal4>UAS-Acn^{RNAi}*), the SSR was expanded in size, but less compact in membrane organization. **K** Analysis of SSR thickness showed a significant increase in animals lacking postsynaptic *Acn*. **L** Analysis of SSR density (number of membrane layers per μm) showed a significant decrease in animals with compromised *Acn* function in the muscle cells. orth: orthogonal; para: parallel; avg: average of parallel and orthogonal values. Scale bars in A-F, 10 μm ; G and H, 30 μm ; I and J, 1 μm . Error bars denote SEM. *, $p < 0.05$; ***, $p < 0.001$. Mann-Whitney test was used for statistical analysis.

5.2.2 Acinus modulates autophagosome maturation in *Drosophila* muscle cells

The mammalian homolog of *Acn* was initially identified as an apoptotic chromatin condensation factor from bovine thymus lysates (Sahara et al., 1999). Further studies demonstrated that a 17 KD Acn fragment produced by caspase-3 cleavage induced chromatin condensation during apoptosis by enhancing PKC- δ kinase activity and promoting histone H2B phosphorylation (Chan et al., 2007; Hu et al., 2007). Recent studies revealed that Acn participates in transcriptional regulation and RNA processing through the formation of an apoptosis- and splicing- associated protein (ASAP) complex with polypeptides SAP18 and RNPS1 (Schwerk et al., 2003; Murachelli et al., 2012). However, *Drosophila* *Acn* is unnecessary for chromatin condensation but instead, is required for endocytic and autophagic trafficking in photoreceptor cells (Haberman et al., 2010). To determine the role of *Acn* in postsynaptic cells, we employed an autophagosomal marker, ATG8a-eGFP, and a red fluorescent acidotropic probe, LysoTracker, to monitor the formation of autophagosomes and acidified autolysosomes respectively. Confocal microscopic images from control animals showed small ATG8a-eGFP positive puncta evenly distributed throughout the muscle cells with fairly low signal intensity, and LysoTracker-positive structures were distributed primarily in the perinuclear region and modestly spread all over the muscle,

representing a basal level of autophagy under normal circumstances (Figure 5.3 A-C). Remarkably, muscle-specific expression of *Acn*^{RNAi} significantly reduced the number of small ATG8a-eGFP-positive puncta, which were replaced by a number of larger and brighter ATG8a-eGFP patches in the muscle cells (Figure 5.3 D and F, I and J). The number of lysosomes and autolysosomes identified by LysoTracker was also reduced substantially upon *Acn* knockdown in muscle cells (Figure 5.3 E and K).

The nature of the ATG8a-eGFP labeled autophagosomal vesicles was confirmed at the TEM level. Compared to small autophagic vesicles in control animals (Figure 5.3 G), the autophagosomes in animals with *Acn* loss of function, seen to contain cytoplasmic membranes and mitochondria remnants, were of notably larger size (Figure 5.3 H). This observation was consistent with the confocal microscopy experiment showing enlarged autophagosomes labeled with ATG8a-eGFP. Interestingly, the alteration in autophagosome size was accompanied by a significant reduction in the number of autophagic vesicles labeled with LysoTracker, indicating a net decrease in autophagy in these animals. Together, these findings showed that reduced *Acn* activity did not affect the initial formation, extension, or closure of autophagosomes; however, the formation of autolysosomes and the degradation of autophagic cargos were disrupted, suggesting a blockade in autophagosome-lysosome fusion.

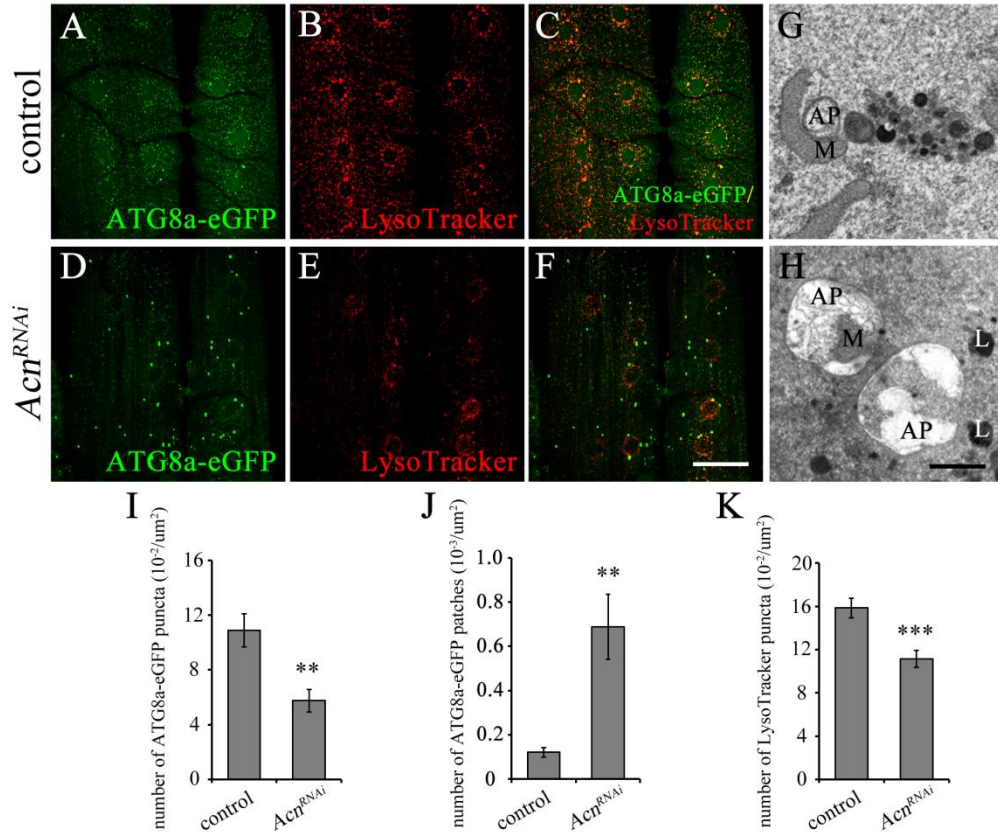


Figure 5.3 Knockdown of *Acn* in muscle cells results in accumulation of autophagosome with enlarged size. **A-F** Live images of muscle cells stained with LysoTracker (red), an acidophilic fluorescent dye that labels lysosomal-autophagic organelles. Autophagosomes were labeled with ATG8a-eGFP (green), an ubiquitin-like conjugating protein. **A** Small puncta labeled with ATG8a-eGFP were prevalent in wild-type muscle cells. **B** LysoTracker-positive autolysosomes and lysosomes appeared as puncta in the muscle cells. **C** Fluorescent signals of ATG8a-eGFP and LysoTracker largely overlapped in the merged image of control animals. **D** In animals expressing *Acn*^{RNAi} in the muscle cells, ATG8a-eGFP labeled small puncta were notably reduced in number, while the amount of larger patches was increased. **E** The number of LysoTracker-positive puncta was dramatically reduced in animals lacking postsynaptic *Acn* expression. **F** Very few vesicles were found doubly-labeled with ATG8a-eGFP and LysoTracker, indicating a blockade in the fusion between autophagosomes and lysosomes. **G** and **H** Transmission electron microscopic analysis of autophagosome morphology in control and *Acn* compromised animals. AP: autophagosome; L: lysosome; M: mitochondria. **G** Autophagosomes adjacent to mitochondria and lysosomal vesicles were observed in control animals. **H** Compared with controls, autophagosomes shown in *Acn* compromised larvae were significantly larger in size. Cytoplasmic membrane remnants and mitochondria debris were enclosed in these autophagosomal vesicles. Lysosomes filled with degradative electron-dense materials were

observed adjacent to autophagosomes. **I** The average number of ATG8a-eGFP labeled small autophagosomes showed statistically significant reduction in animals with inhibited *Acn* expression. **J** Large autophagosomes conjugated with ATG8a-eGFP were significantly increased in animals with reduced *Acn* function. **K** Muscle-directed RNAi knockdown of *Acn* resulted in significant decreases in LysoTracker labeling, indicating a defect in autophagic processing. Scale bars in A-F, 50µm; G-H, 1µm. Error bars denote SEM. **, $p < 0.01$; ***, $p < 0.001$. Student's t-test was used for statistical analysis.

5.2.3 Compromising *ATG8a* function affects SSR membrane organization

Previous results revealed that muscle-specific inhibition of *Acn* disrupted both SSR organization and autophagic trafficking. Although both SSR membrane addition and autophagic-lysosomal degradation involve intracellular membrane trafficking, a correlation between these two processes has not yet been identified. In chapter 4, we reported that in heparan sulfate biosynthesis compromised animals, SSR membrane organization was disrupted (Figure 4.3). Interestingly, the level of autophagy was also affected in these animals by HS mediated signaling pathways (Figure 4.4). Most strikingly, suppression of autophagy by co-expression of *ATG8a^{RNAi}* was able to rescue the SSR abnormalities in HS-compromised animals (Figure 4.8). All of this evidence suggests a connection between SSR organization and levels of autophagy. It was therefore of interesting to ask if a normal level of autophagy is critical for maintaining SSR morphology during NMJ development. *ATG8a* has been implicated in autophagosome formation, serving as a ubiquitin-like conjugation system (Ichimura et al., 2000). RNAi directed against *ATG8a* in muscle cells greatly reduced autophagy levels as evidenced by decreased LysoTracker staining (Figure 4.7). To explore the role of autophagy in SSR assembly, we examined SSR structure in animals with muscle-specific expression of *ATG8a^{RNAi}*. In wild-type animals, mCD8-GFP and anti-DLG immunoreactivity were concentrated at the SSR in a tight association with the presynaptic marker, HRP (Figure 5.4 A-D). Muscle-directed RNAi of *ATG8a* disrupted SSR membrane structure and resulted in the same visible defects seen in *Acn^{RNAi}* animals, supporting the idea that SSR

membrane disorganization was caused by changes in autophagy levels (Figure 5.4 E-H).

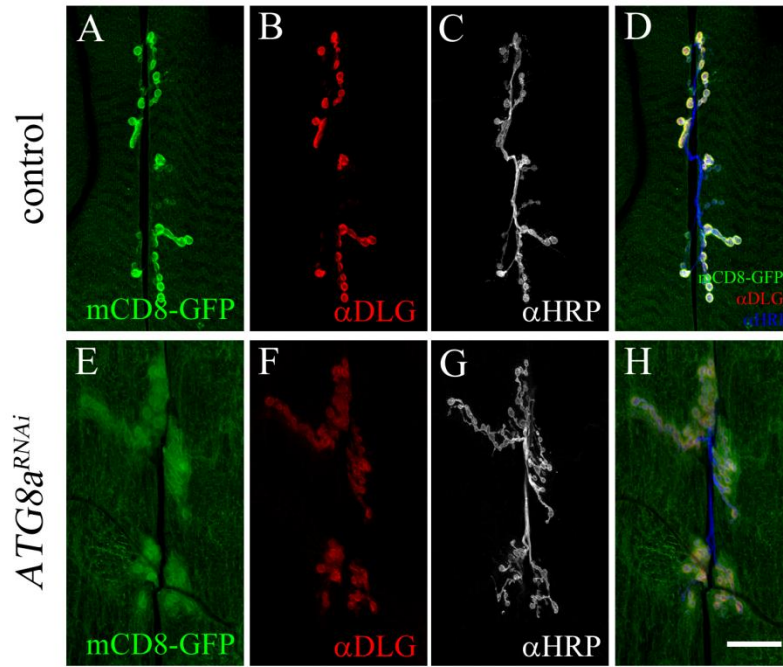


Figure 5.4 *ATG8a* functional reduction results in SSR disorganization and synapse overgrowth. Confocal images of larvae NMJs in the controls and animals expressing *ATG8a*^{RNAi} in muscle cells using the *Mef2-Gal4* driver. The SSR was doubly-labeled with transmembrane protein mCD8-GFP (green) and an antibody recognizing the synaptic scaffold protein DLG (red). Presynaptic membrane was visualized with an anti-HRP antibody (grayscale). **A-D** In control muscle cells, mCD8-GFP and DLG immunoreactivity were highly concentrated at the postsynaptic specializations, surrounding the presynaptic nerve terminals (marked by anti-HRP staining). **E-H** In animals where *ATG8a* was compromised by muscle-exclusive RNAi, mCD8-GFP and DLG immunofluorescence were no longer tightly restricted to postsynaptic regions, and the fluorescent intensity of mCD8-GFP and DLG were dramatically decreased. The NMJs of *ATG8a*^{RNAi} animals were overgrown, indicated by an increase in the number of neuronal branch points and synaptic boutons, marked by anti-HRP. Scale bar in A-H, 30μm.

5.2.4 Suppression of autophagy increases α -spectrin levels in the postsynaptic density

Reduction of *Acn* function affected SSR membrane organization in a manner similar to that observed in *spectrin* compromised animals, wherein the SSR was “delocalized” and loosely assembled (Pielage et al., 2006). Spectrin is a cytoskeletal protein comprised of two α and two β subunits in a heterotetrameric arrangement (De Matteis and Morrow, 2000). Together with short actin filaments and other associated proteins, spectrin forms pentagonal or hexagonal networks, providing mechanical support for the plasma membrane (Bennett and Baines, 2001; Baines, 2010; Xu et al., 2013). In *Drosophila*, spectrin is present both pre- and post-synaptically, and mutations in either α - or β -spectrin affect synapse stability, synaptic protein localization and transmission efficacy (Featherstone et al., 2001; Pielage et al., 2005, 2006). Most interestingly, muscle-specific elimination of α - or β -spectrin using RNAi severely perturbs subsynaptic membrane integrity (Pielage et al., 2006). Given that reductions of both *Acn* and *spectrin* affected SSR architecture, we examined the level of α -spectrin at the synapse, speculating that reduction of *Acn* function may influence the stability of the spectrin network at the *Drosophila* NMJ. In wild-type animals, α -spectrin was highly concentrated at the presynaptic terminal and moderately distributed into the SSR and muscle cells (Figure 5.5 A-C). To our surprise, knockdown of *Acn* in the muscle greatly increased α -Spectrin immunoreactivity at the postsynaptic side without affecting its presynaptic level (Figure 5.5 D-F). Further study of *Acn*^{RNAi} animals showed strong co-localization of α -spectrin and mCD8-GFP, indicating a concordant expansion of SSR and the spectrin network in these animals (data not shown). These results indicated that compromised *Acn* function led to overexpression or accumulation of α -spectrin in the postsynaptic specialization, and that elevated levels of α -spectrin at the NMJ were tightly associated with disorganization of the SSR, suggesting that *Acn* may influence SSR assembly via the control of spectrin.

Muscle-specific expression of *ATG8a*^{RNAi} produced a similar SSR disorganization phenotype as seen for *Acn*^{RNAi} animals, indicating that SSR morphological changes could well be due to decreased levels of autophagy in these animals. Autophagy-mediated lysosomal degradation plays an important role in developmental tissue remodeling, and more specifically, is known to be required for α -spectrin turnover (Woods and Lazarides, 1985; Rusten et al., 2004; Chang and Neufeld, 2010). It is possible that compromised autophagy caused by reductions in *Acn* or *ATG8a* function enhances the spectrin skeleton stability. To explore this possibility, we examined α -spectrin levels and distribution in animals with muscle-specific expression of *ATG8a*^{RNAi}. α -spectrin immunofluorescence detected in muscle-directed *ATG8a*^{RNAi} animals mimicked the prominent phenotype of *Acn*^{RNAi} animals, showing the same extent of increase in postsynaptic localization (Figure 5.5 G-I). These findings demonstrated that decreases in autophagy achieved by *Acn* or *ATG8a* RNAi in the muscle were the cause of α -spectrin accumulation at the NMJ.

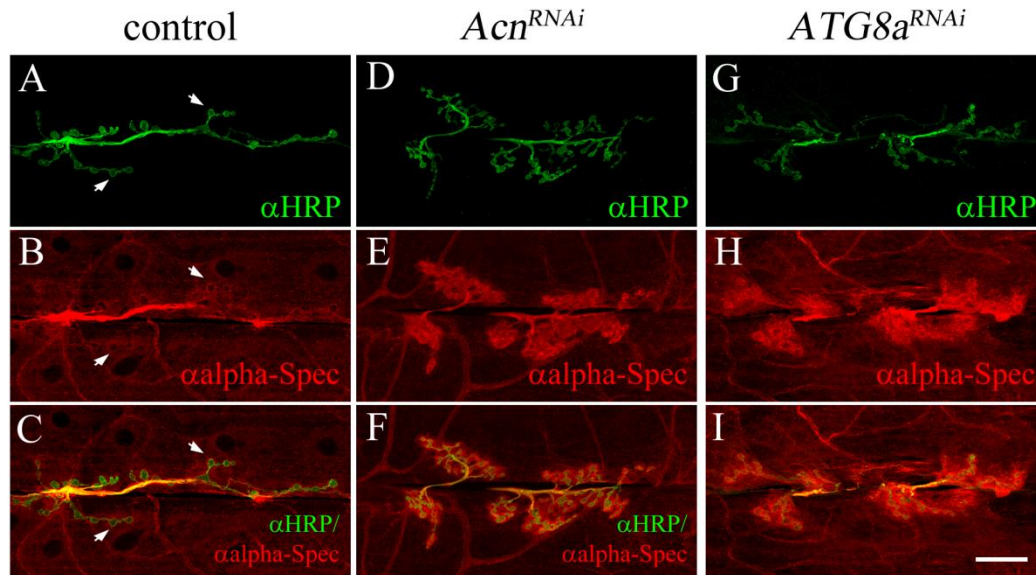


Figure 5.5 Reduced *Acn* or *ATG8a* function leads to over-accumulation of α -spectrin at the NMJ. To investigate the mechanism of autophagy in regulating SSR organization, α -spectrin was detected using mouse monoclonal anti- α -spectrin antibody (red) and presynaptic boutons were

marked with anti-HRP staining (green). **A-C** In genetic controls (*Mef2-Gal4/+*), α -spectrin immunoreactivity was highly concentrated at presynaptic boutons and less prominent in the postsynaptic region. α -spectrin was also modestly distributed throughout the muscle and trachea. Arrows indicate individual boutons labeled with HRP and spectrin immunofluorescence. **D-I** In muscle cells expressing either *Acn*^{RNAi} or *ATG8a*^{RNAi}, α -spectrin immunoreactivity was dramatically increased at the postsynaptic region, leaving the presynaptic α -spectrin level unaffected. Inhibition of *Acn* or *ATG8a* resulted in NMJ overgrowth, as evidenced by anti-HRP immunostaining. Scale bar in A-I, 30 μ m.

5.2.5 Overexpression of α -spectrin in the muscle disrupts SSR membrane organization

While loss-of-function alleles of α - and β -spectrin have been intensively studied, the effect of overexpressing α -spectrin at the *Drosophila* NMJ remains unclear. Previous findings indicate that SSR morphological defects in *Acn*^{RNAi} and *ATG8a*^{RNAi} animals may be caused by accumulation of α -spectrin in the postsynaptic cells. To investigate the effect of elevated α -spectrin in SSR assembly, a UAS-regulated α -spectrin transgene was overexpressed under the control of a muscle-specific driver, *Mef2-Gal4*. Using mCD8-GFP as a marker, α -spectrin overexpression produced an obvious change in SSR structure similar to what was observed with *Acn* or *ATG8a* knockdown (Figure 5.6 E). Antibody staining revealed a marked increase in α -spectrin immunoreactivity throughout the entire muscle including the synaptic region in those animals expressing *spectrin* transgene (Figure 5.6 F). This result indicates that overexpression of α -spectrin has a detrimental effect resulting in SSR disorganization at the *Drosophila* NMJ, supporting the idea that SSR morphological changes in *Acn* and *ATG8a* compromised larvae may be due to the accumulation of α -spectrin in muscle cells.

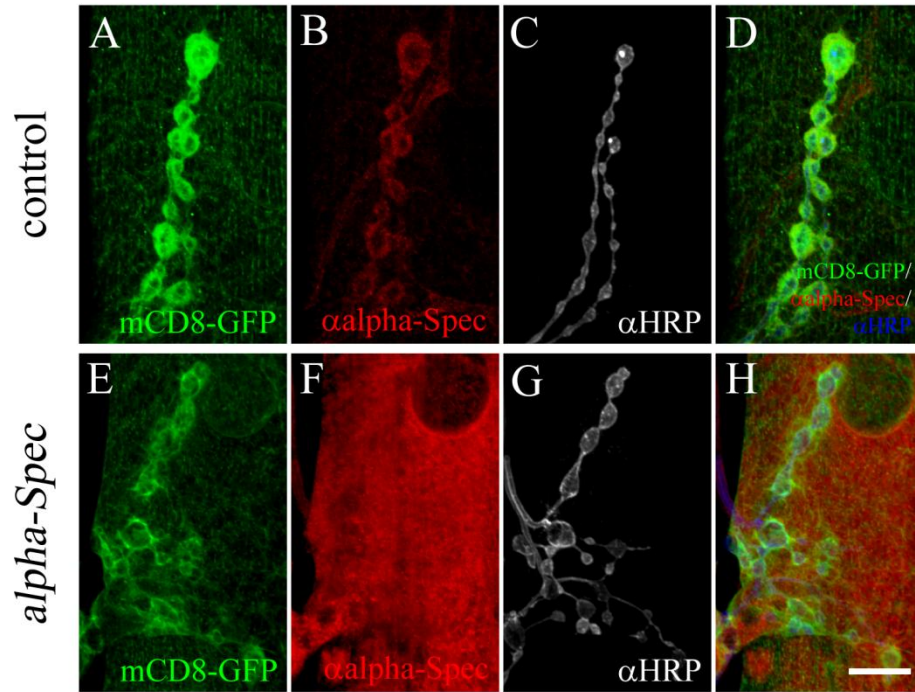


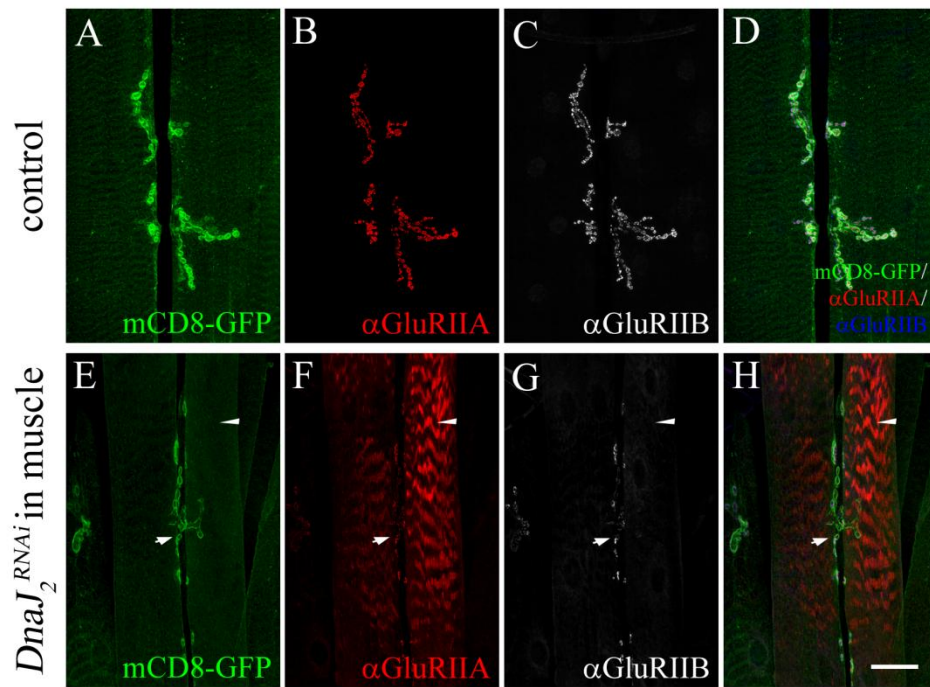
Figure 5.6 Overexpression of α -spectrin in the muscle disrupts SSR organization. A-H Confocal micrographs of the synaptic boutons in control and α -spectrin overexpressing animals. The SSR was visualized with mCD8-GFP (green); α -spectrin was detected by a monoclonal antibody (red), and the presynaptic membrane was labeled with anti-HRP antibody (grayscale). **A-D** In control animals (*Mef2-Gal4, UAS-mCD8-GFP/+*), α -spectrin was present at the postsynaptic specialization, occupying the same subsynaptic area as the mCD8-GFP labeled SSR. **E-H** Animals overexpressing α -spectrin (*Mef2-Gal4, UAS-mCD8-GFP>UAS- α -Spec-myc*) showed disruption in SSR membrane structures. α -spectrin immunoreactivity was greatly increased throughout the muscle cells. Scale bar in A-H, 10 μ m.

5.3 DnaJ2, a chaperone protein that regulates glutamate receptor composition at the *Drosophila* neuromuscular junction

5.3.1 Identification of *DnaJ2* as a functional requirement for the proper localization of GluRIIA at the NMJ

A novel gene, *CG10565*, was identified through an *in vivo* RNAi screen for altered distribution of the glutamate receptor IIA subunit at the synapse. Muscle-directed expression of an RNAi construct derived against *CG10565* produced a dramatic loss of GluRIIA immunoreactivity at the NMJ, with redistribution of GluRIIA to the intracellular membrane compartments. This gene was selected for further study because of this recapitulation of the phenotypes originally observed in animals with reduced *Akt1* function. Having identified *CG10565* as a potential player in this phenotype, we wanted to explore its biological function at the NMJ, and to determine whether or not it was acting as a downstream mediator of *Akt1* in regulating glutamate receptor composition. Genome analysis revealed that *CG10565* belongs to a gene family encoding chaperone proteins DnaJ/Hsp40. Therefore, we named this gene *DnaJ2* to denote its membership in this family and in accordance with the naming of another related gene in *Drosophila*, *DnaJ1* (Kuo et al., 2013). We first determined if *DnaJ2* selectively regulated GluRIIA localization at the NMJ, similar to *Akt1*. An immunocytochemical experiment detecting GluRIIA and IIB levels at the NMJ was performed, and muscle-specific RNA interference of *DnaJ2* resulted in redistribution of GluRIIA into intracellular membrane compartments (arrowheads) without affecting the proper localization of IIB at the postsynaptic specialization (Figure 5.7 A-H, arrows). Several other developmental defects were also observed in animals expressing *DnaJ2^{RNAi}*, including reductions in muscle and synapse size, decreases in the levels of glutamate receptors at the NMJ, as well as decreased fluorescent intensity of the SSR marker mCD8-GFP (Figure 5.7 E-H). These experiments demonstrated that compromising *DnaJ2* function in the muscle altered the localization of one type of glutamate receptor subunit, suggesting a functional connection between *DnaJ2* and *Akt1*.

To further investigate the function of *DnaJ2* in synaptic development, multiple deletion mutants were generated via an imprecise excision of the G4964 P-element insertion in the 5'-UTR of the *DnaJ2* genomic sequence. Transposon-mediated local mutagenesis takes place when a P-element is excised from the genome imprecisely, resulting in deletions of flanking genomic DNA around the insertion site (Ou, 2013). A total of 567 excision mutation stocks were established, and imprecise transposition events were detected by PCR. 15 independent mutants were isolated and recovered from the imprecise excision screen, resulting in an imprecise excision frequency of about 2.6%. The deletions can occur at either the 5'-end or 3'-end of the P-element insertion site. Sequencing results showed that the mutation line #226 deleted the entire genomic region of *DnaJ2* upstream of the original P-element insertion site, as well as a small portion of the 3'-UTR in the neighboring *Ac78c* genomic sequence. Mutation line #275 harbored a 1570 bp deletion towards the 3'-end of *DnaJ2*, removing 2/3 of the genomic sequence which represents half of the protein-coding sequence (Figure 5.7 I). Although the excision-mediated deletions varied in size and location, all of the 15 mutant lines showed strong developmental arrest, and homozygous individuals did not survive beyond the first instar larval stage, indicating an essential role for *DnaJ2* in development and survival.



I WT *DnaJ₂* genome with EP insertion

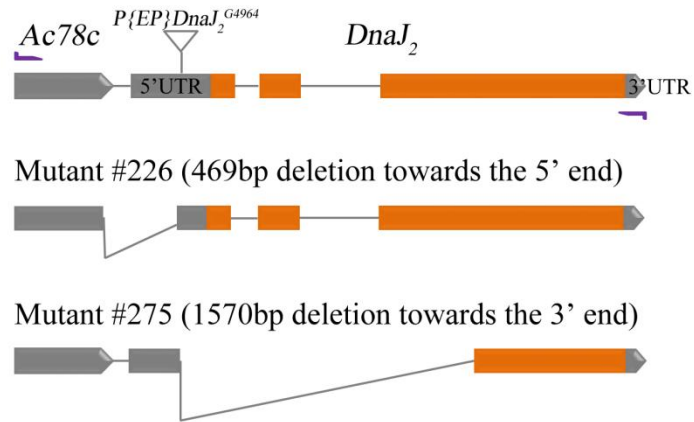


Figure 5.7 Identification of *DnaJ2* for its requirement for synapse assembly and generation of *DnaJ2* mutants. **A-H** Immunodetection of GluRIIA and IIB at the postsynaptic specialization in control and animals with muscle-restricted *DnaJ2* knockdown. GluRIIA was detected with monoclonal anti-GluRIIA antibody (red) and IIB was examined using polyclonal anti-GluRIIB antibody (grayscale). The postsynaptic specialization was visualized with mCD8-GFP, a membrane marker highly concentrated in SSR (Green). **A-D** In control animals (*Mef2-Gal4, UAS-mCD8-GFP/+*), GluRIIA, IIB immunoreactivities and mCD8-GFP colocalized in synaptic boutons. **E-H** In animals with reduced *DnaJ2* function achieved by RNAi in the muscle, GluRIIA was

mislocalized while IIB retained its correct localization at the NMJ. The muscle cells were reduced in size and the synapse was underdeveloped. The SSR, labeled with mCD8-GFP, was also reduced in size and the signal from both GluRIIA and IIB were decreased at the synapse. Arrows indicate synaptic boutons and arrowheads indicate extrasynaptic GluRIIA in stripes. **I** Genome map of *Drosophila* CG10565 (*DnaJ2*) and P-element-mediated mutagenesis. Orange bars represent exons and gray bars represent untranslated regions (UTR). *G4964* is a lethal *EP* insertion into the 5'-UTR of the *DnaJ2* genomic sequence. *Ac78c* is a neighboring gene upstream of *DnaJ2*. To identify deletion mutants by PCR, primers (purple) were designed to amplify a ~3.7kb WT genomic DNA fragment ranging from the 3'-UTR of *Ac78c* to the 3'-end of *DnaJ2*. #226 and #275 are mutations generated by imprecise excisions toward 5'-end and 3'-end respectively. Scale bar in A-H, 30µm.

5.3.2 *In vivo* structure-function analysis of DnaJ2 at the *Drosophila* NMJ

BLAST sequence comparisons showed that DnaJ2 belongs to the DnaJ/Hsp40 co-chaperone family, from which members cooperate with proteins from the partner family DnaK/Hsp70 to facilitate protein folding and translocation (Suzuki et al., 1999; Walsh et al., 2004). The predicted DnaJ2 protein consists of 646 amino acids and shares high sequence identity (41%) with the human and mouse DnaJ orthologs (Figure 5.8 A). DnaJ2 contains two evolutionarily conserved domains: the J domain (red), and the DNA-binding domain (DBD, green, Figure 5.8 A). All of the DnaJ/Hsp40 proteins contain the J domain, which binds to and stimulates the ATPase activities of partner DnaK/Hsp70 proteins (Langer et al., 1992; Young et al., 2004). The three-dimensional structure of the J domain was predicted based on its primary amino acid sequence. The J domain in *Drosophila* DnaJ2 is a 61 amino acid long finger-like structure, consisting of 3 α-helices with a flexible loop region between the second and the third helix (Figure 5.8 B). The finger tip, a highly conserved HPD motif (histidine, proline and aspartic acid) in the loop region, is known to be critical for interacting with DnaK/Hsp70 in other DnaJ family members (Langer et al., 1992; Young et al., 2004).

We have demonstrated a series of defects in NMJ development in animals expressing *DnaJ2^{RNAi}* in the muscle. Whether these defects were independent of

or associated with the co-chaperone function of *DnaJ2* remains to be studied. To determine if the evolutionarily conserved J domain and DBD domain were critical for glutamate receptor targeting to the NMJ, *in vitro* mutagenesis was used to generate mutant *DnaJ2* cDNAs containing deletions of either the J domain or DBD domain (Figure 5.8 C). In addition, a point mutation substituting histidine (107) with glutamine in the conserved HPD motif was generated to specifically address if the predicted interaction with DnaK/Hsp70 was important for DnaJ2's function in regulating GluRIIA localization and synapse growth (Figure 5.8 C). To test the significance of those functional domains in *Drosophila* development, GFP-tagged DnaJ2 proteins containing either one of the deletions or the point mutation were exogenously expressed in a wild-type background using the muscle-specific *Mef2-Gal4* driver, and the subcellular distributions of wild-type and mutated DnaJ2-eGFP proteins were monitored by confocal microscopy (Figure 5.8 D-G). When expressed in the muscle, wild-type DnaJ2 proteins were evenly distributed in both nucleus and cytosol, while the level of Δ J-DnaJ2 was dramatically increased in nucleus and reduced in the cytosol. H107Q-DnaJ2 was concentrated in the nucleus without affecting its level in the cytoplasm. Muscle-restricted expression of the mutant DnaJ2 lacking its DBD domain resulted in increased levels of both cytoplasmic and nuclear DnaJ2. These findings show that the conserved J domain and DBD domain play important roles in DnaJ2 subcellular localization, suggesting a mechanistic link between DnaJ2 structure and glutamate receptor localization.

proteins. The J domain deletion spans residues 76-136 (Δ J-DnaJ2). The H107Q mutation substitutes the histidine107 to glutamine (H107Q-DnaJ2). The DBD domain is close to the C-terminal, therefore a truncated DnaJ2 deleting residues from 589 onward was generated for Δ DBD-DnaJ2. The J domain is indicated in red, and the DBD domain in green. **D-G** Transgenic fly lines expressing wild-type or mutated DnaJ2 fused to an eGFP open reading frame were used to determine the subcellular localization of each mutant DnaJ2 protein in comparison to the wild type protein, in a wild-type background. **D** *Mef2-Gal4* driven muscle-specific expression of wild-type DnaJ2 showed GFP fluorescence in both the nucleus and the cytosol. **E** Compared to WT-DnaJ2, Δ J-DnaJ2 localized primarily in the nucleus. **F** H107Q-DnaJ2 showed higher concentration in the nucleus than in the cytoplasm. **G** Δ DBD-DnaJ2 showed increased concentrations in both cytoplasm and nucleus compared with WT-DnaJ2. Scale bar in D-G, 50 μ m.

5.3.3 Investigation of a functional link between *DnaJ2* and *Akt1* in regulating GluRIIA localization at the *Drosophila* NMJ

Reduction in *DnaJ2* or *Akt1* function in the muscle produced similar phenotypes, namely loss of GluRIIA at the synapse and redistribution of IIA into intracellular compartments. Based on these findings, we suspect that *DnaJ2* and *Akt1* may function via the same mechanistic pathway to influence GluRIIA localization. Three different scenarios were considered that could possibly describe the functional relationship between *DnaJ2* and *Akt1*. First, *DnaJ2* may function upstream of *Akt1*, affecting GluRIIA localization through regulation of *Akt1* activity. Second, *DnaJ2* could act as a direct or indirect downstream effector of *Akt1* in regulating GluRIIA localization. Finally, it is also possible that *DnaJ2* functions in parallel to *Akt1*, using a totally different mechanism to control the distribution of GluRIIA in muscle cells. To determine if *DnaJ2* affects *Akt1* activity, total and phosphorylated Akt1 levels were measured in animals with compromised *DnaJ2* function. As revealed by western blot analysis, the total Akt1 protein level was not affected, and phosphorylated Akt1 showed a modest decrease, upon inhibition of *DnaJ2* in muscle (Figure 5.9 A). To further determine if GluRIIA mislocalization produced by *DnaJ2* RNAi was due to a modest reduction in *Akt1* activity, we overexpressed a constitutively active form of *Akt1* (*Akt1*^{CA}) in the muscle cells to test whether or not increasing *Akt1* activity in *DnaJ2*^{RNAi} animals would rescue the observed defects. Overexpression of *Akt1*^{CA} was unable to

rescue GluRIIA mislocalization caused by *DnaJ2* functional inhibition, therefore it seems less likely that *DnaJ2* functions upstream of *Akt1* with respect to this phenotype (Figure 5.9 B and C).

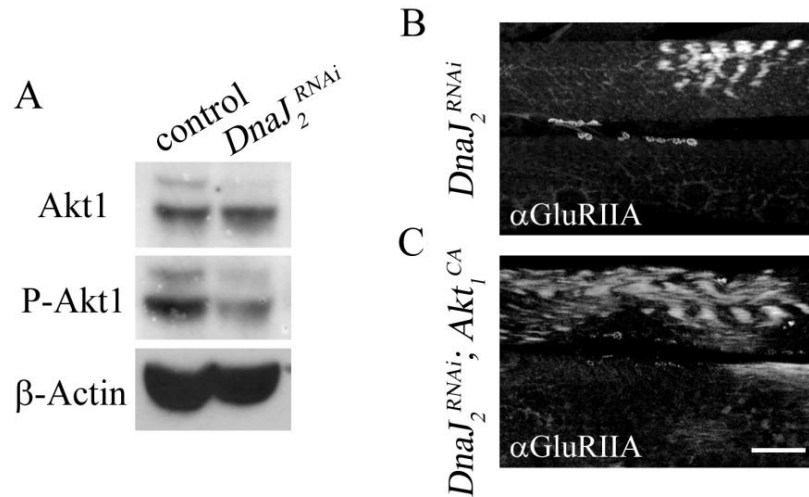


Figure 5.9 In GluRIIA mislocalization, DnaJ2 does not operate upstream of Akt1 in a functionally relevant manner. **A** *DnaJ2* function was compromised by muscle-specific expression of a *DnaJ2^{RNAi}* construct using the *Mef2-Gal4* driver. The level of phosphorylated Akt1 was measured by Western blot. Total muscle proteins were prepared from third instar larval muscles of control animals (*Mef2-Gal4/+*) or animals with muscle-specific knockdown of *DnaJ2* (*Mef2--GAL4>UAS-DnaJ2^{RNAi}*). Total Akt1 was detected with anti-Akt1 antibody and phosphorylated Akt1 was detected with anti-phospho-Ser505 Akt1 antibody. β-Actin was used as the internal control. Phosphorylated Akt1 was modestly reduced in muscles expressing *DnaJ2^{RNAi}* as compared to control, while the level of total Akt1 was not affected by reduced *DnaJ2* function. **B** and **C** GluRIIA localization in the muscle was detected with monoclonal anti-GluRIIA antibody (grayscale). **B** Postsynaptic expression of *DnaJ2^{RNAi}* produced ectopic GluRIIA that distributed into intracellular bands in muscle cells. Some of the GluRIIA immunoreactivity was still correctly localized to the synaptic region. **C** Overexpression of a constitutively active form of *Akt1* (*Akt1^{CA}*) didn't alleviate the defects in GluRIIA localization in animals with reduced *DnaJ2* function. Scale bar in B and C, 30μm.

Chapter 6: Discussion

6.1 *Akt1* controls two facets of synapse development: glutamate receptor composition and subsynaptic membrane elaboration through distinct mechanisms

6.1.1 Overview of primary findings

The work presented in chapter 3 of this thesis demonstrated that *Akt1* controls two essential elements of synapse development, neurotransmitter receptor composition and postsynaptic membrane expansion through separate pathways (Figure 6.1). We have found that *Akt1* was specifically required for the correct assembly of A-type glutamate receptors at the postsynaptic density. Reducing *Akt1* function resulted in a loss of GluRIIA at the synapse accompanied by redistribution of GluRIIA into intracellular membrane structures, without affecting the proper localization of GluRIIB. The analysis of *Akt1* reported here examined morphological and cellular phenotypes caused by both traditional *Akt1* mutant alleles and cell-type specific knockdown achieved by either of two different *UAS-Akt1^{RNAi}* lines. A transheteroallelic combination of *Akt1* mutant alleles (*Akt1¹/Akt1⁰⁴²²⁶*) resulted in loss of GluRIIA from the postsynaptic specialization and redistribution of IIA into intracellular bands. This phenotype was found to be even more pronounced in muscle-directed RNAi of *Akt1* using various muscle-specific *Gal4* drivers (*G14*, *24B*, *Mef2*). The severity of this mislocalization phenotype was strongly correlated with promoter- and temperature-dependent *Gal4* activity, showing its sensitivity to *Akt1* dosage. *Elav-Gal4* directed neuronal expression of *Akt1^{RNAi}* did not affect the localization of GluRIIA, demonstrating that the requirement of *Akt1* in regulating glutamate receptor distribution is restricted to the postsynaptic side. Animals bearing the *Akt1^{RNAi}* construct but no *Gal4* driver served as controls and showed normal GluRIIA localization, proving that this phenotype was not an artifact generated by insertion of the RNAi construct. Two *Akt* transgenic RNAi lines derived from different constructs were employed for knocking down Akt activity in muscles. Both of them showed

GluRIIA mislocalization, further rule out the possibility that those GluRIIA phenotypes were caused by off-target effects using RNA interference. The results obtained using these different genetic tools were consistent and all proved the importance of *Akt1* function in glutamate receptor localization.

We further show that *Akt1* function is critical for normal levels and localization of dorsal and cactus, two molecules shown to affect glutamate receptor expression levels at the synapse, via a post-translational mechanism (Heckscher et al., 2007). Dorsal is the *Drosophila* homolog of NF- κ B, a Rel-family transcription factor well known for its role in immune responses (Ghosh et al., 1998). NF- κ B is constitutively inactive in cytoplasm, sequestered by I κ -B/cactus, an inhibitory molecule that masks the nuclear localization signals (NLS) of NF- κ B proteins. Signaling stimulation through Toll-like receptors and PI3K/Akt/mTOR pathway results in phosphorylation and subsequent degradation of I κ -B, allowing for activation and translocation of NF- κ B into nucleus, where it functions as transcriptional activator to induce target gene expression (Beg and Baldwin, 1993; Ozes et al., 1999; Dan et al., 2008). In *Drosophila*, dorsal and cactus are highly expressed at the NMJ and function outside of the nucleus to influence glutamate receptor localization, playing a regulatory role in trafficking, rather than transcriptional control (Heckscher et al., 2007). We found that the levels of both dorsal and cactus were reduced in animals with knockdown of *Akt1* in the muscle. Notably, in some animals expressing *Akt1*^{RNAi} in the muscle, dorsal showed an altered intracellular distribution that overlapped with the mislocalized GluRIIA. Those results indicate that the function of *Akt1* could be partially mediated via control over the level and localization of dorsal and cactus. However, since the functional specificity of dorsal and cactus in regulating glutamate receptor localization are still poorly understood, whether mislocalized GluRIIA was directly associated with dorsal remains to be clearly defined. Reduction in *Akt1* activity decreases the levels of dorsal and cactus simultaneously, distinct from its role in canonical NF- κ B signaling. Thus, it is possible that *Akt1* regulates dorsal and cactus independent of phosphorylation. Moreover, due to the lack of evidence for

a direct interaction between dorsal and GluRIIA, it is likely that additional downstream targets of *Akt1* influence GluRIIA delivery to the postsynaptic specialization.

It was further revealed that *Akt1* plays an important role in the proportional elaboration of the subsynaptic reticulum in parallel to muscle growth. Reduction in *Akt1* function inhibited normal expansion of the SSR during synapse growth, and abolished membrane addition to the cortical networks in muscle cells. Overexpression of a constitutively active form of *Akt1* was also found to induce formation of ectopic SSR-like membrane structures. The muscle endomembrane system is a complex combination of various membrane compartments, and can be roughly divided into two domains based on their position. The cortical domain includes membrane networks underneath the plasma membrane but above the muscle nuclei, whereas the subcortical domain is located below the nuclei, and is comprised mainly of sarcoplasmic reticulum and t-tubules. Muscle-specific RNAi of *Akt1* produced a notable reduction in the cortical membrane domain and a more compact subcortical membrane domain, resulting in decreased endomembrane complexity and overall muscle cell thickness. These phenotypes were similar to those found in a *Gtaxin* mutant, which suggested the possibility that *Akt1* and *Gtaxin* are involved in the same cellular process (Gorczyca et al., 2007). *Gtaxin* is a *Drosophila* t-SNARE protein with key roles in vesicle fusion and membrane trafficking in a DLG-dependent manner (Gorczyca et al., 2007). Further experiments showed that muscle-directed overexpression of a constitutively active form of *Akt1* (*Akt1*^{CA}) produced ectopic membraneous structures, a phenotype also observed in response to elevated levels of *Gtaxin*. Together, this evidence suggests that *Akt1* activities at the synapse are mediated at least in part via control of *Gtaxin*. *Gtaxin* does contain a consensus site for *Akt1* phosphorylation, and therefore could be a direct target of *Akt1* kinase activity in regulating SSR and endomembrane development of muscle cells. The regulatory roles of *Akt1* in glutamate receptor composition and postsynaptic membrane expansion could be accomplished through separate or identical

downstream effectors. The fact that *Gtaxin* mutants did not disrupt GluRIIA distribution suggests that the control of SSR expansion and glutamate receptor composition mediated by *Akt1* occurs via different molecular mechanisms. Together, we demonstrated *Akt1* can regulate membrane trafficking events to control the formation and function of postsynaptic specializations.

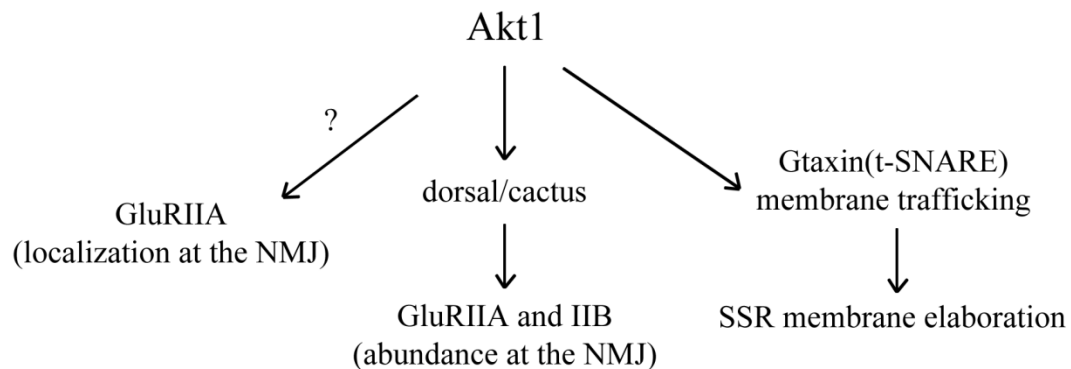


Figure 6.1 Model for Akt1 's regulatory role at the NMJ. Akt1 selectively affects A-type glutamate receptor localization at the NMJ. Compromising Akt1 function reduced the levels of dorsal and cactus at the NMJ, two potential Akt1 targets that regulate GluRIIA and IIB levels. However, loss of Akt1 results in GluRIIA mislocalization to intracellular membrane compartments, without affecting correct targeting of GluRIIB at the NMJ. This result suggests that other Akt1 targets besides of dorsal and cactus are involved as well. Akt1-dependent subsynaptic membrane expansion is mediated through a separate pathway where the *Drosophila* t-SNARE protein Gtaxin acts downstream of Akt1 function.

6.1.2 *Akt1* regulates subunit-selective targeting of glutamate receptors to the postsynaptic specialization

We examined the function of *Akt1* in synapse assembly using both *Akt1* mutants and muscle-specific knockdown of *Akt1* function with RNA interference. Both of these genetic strategies demonstrated that *Akt1* specifically affects glutamate receptor composition by regulating the delivery of one subunit, GluRIIA, to the postsynaptic specialization. In this study, a number of experiments were conducted to evaluate if *Akt1* was required for the localization of specific postsynaptic proteins, or rather served a more generalized role in directing a variety of proteins to this membrane specialization. The correct localization of

GluRIIB, GluRIIC, basigin, DLG, and syndapin in animals with *Akt1* knockdown in the muscle ruled out the possibility that *Akt1* plays a general role in synaptic protein localization.

At the *Drosophila* NMJ, two types of glutamate receptors have been defined by their distinct compositions and physiological properties (Petersen et al., 1997; DiAntonio et al., 1999; Marrus et al., 2004; Featherstone et al., 2005; Qin et al., 2005a; DiAntonio, 2006). GluRIIA subunit-containing receptor (A-type receptor) serves as the primary receptor required for normal postsynaptic function and sensitivity in response to presynaptic glutamate release (Petersen et al., 1997; DiAntonio et al., 1999; Sigrist et al., 2002; Schmid et al., 2008). GluRIIB subunit-containing receptors (B-type receptors) show little response to spontaneous release, probably due to a decreased desensitization time (DiAntonio et al., 1999). By competing with GluRIIA for access to GluRIIC during receptor assembly, GluRIIB plays a regulatory role in adjusting A-type receptor abundance at the synapse (Marrus et al., 2004; Schmid et al., 2008). Differential regulation of GluRIIA and IIB subunit levels at the postsynaptic density could therefore provide a simple mechanism for modulating postsynaptic responses to variable presynaptic inputs during development.

There is evidence to show that type A- and B- receptors are spatially segregated at the NMJ via association with different set of adaptor proteins or cytoskeletal elements. Coracle, a homolog of mammalian protein 4.1 in *Drosophila*, has been shown to specifically influence the anchoring of GluRIIA but not IIB to the postsynaptic specialization (Chen et al., 2005). A physical interaction between coracle and the C-terminus of GluRIIA was essential for actin-dependent trafficking of GluRIIA-containing vesicles to the plasma membrane. Conversely, The *Drosophila* PSD-95 protein, DLG was shown to be necessary for GluRIIB but not IIA localization at the NMJ (Chen and Featherstone, 2005). Our observation that *Akt1* selectively affecting the localization of GluRIIA, but not other glutamate receptor subunits at the NMJ, supporting the idea that A- and B- type receptors

are differentially regulated. It is of interest to know if coracle functionally interacts with *Akt1* and whether coracle-actin cytoskeleton networks are affected by reduction of *Akt1* function.

6.1.3 The origin of postsynaptic glutamate receptors: local synthesis versus trafficking-based models

The coordination of pre- and post-synaptic assembly is critical for developmental and experience-dependent strengthening of *Drosophila* neuromuscular junctions. There is evidence that the incorporation of GluRIIA-containing receptors to growing synapses is essential for active zone formation, bouton addition and synaptic transmission enhancement during larval development (Sigrist et al., 2002; Rasse et al., 2005; Schmid et al., 2008). Although the regulatory mechanisms involved in expression and assembly of glutamate receptors are not perfectly understood, two sources are believed to supply newly synthesized glutamate receptors to postsynaptic densities. GluRIIA could be synthesized distant from the postsynaptic density and delivered to NMJ by exocytosis and lateral diffusion. During the initial stages of embryonic synaptogenesis, glutamate receptors are distributed homogeneously across the cell surface in relatively low densities, however they concentrate rapidly to synaptic sites upon motoneuron innervation (Broadie and Bate, 1993b, a). Electrophysiological evidence suggests that glutamate receptors are not entirely excluded from extrasynaptic regions even in the late larval stages. Glutamate receptor channels away from the junctional area exhibit distinct physiological properties compared with synaptic glutamate receptor channels, as detected with patch-clamp techniques (Nishikawa and Kidokoro, 1995). The existence of a non-synaptic pool of glutamate receptors is further revealed by detection of GluRIIA and IIB immunoreactivities in both the interior and the surface of postsynaptic muscle cells, where they appear as granule-like puncta dispersed throughout the whole muscle with no obvious subcellular enrichment (Karr et al., 2009). This is consistent with the observation that fluorescence photobleaching of the entire

muscle resulted in a greater delay in recovery of GluRIIA at synaptic sites than local bleaching at the junctions, indicating that glutamate receptors are recruited to the postsynaptic specialization from a cell-wide extrasynaptic pool (Rasse et al., 2005). An alternative model involves local translation of GluRIIA at the NMJ. The presence of large aggregates comprising GluRIIA mRNA and translation initiation factor eIF4E, as well as polyA-binding protein (PABP) within or adjacent to SSR indicates “on-site” synthesis and assembly of glutamate receptors (Sigrist et al., 2000). Genetic methods promoting postsynaptic aggregation of translational components resulted in increased postsynaptic GluRIIA levels and enhanced neurotransmission, supporting this alternative hypothesis (Sigrist et al., 2000; Sigrist et al., 2002). Unlike recruiting from extrasynaptic pools, glutamate receptor recovery via subsynaptic translation requires substantially longer times, and therefore is likely to play more of a role in long-term synaptic plasticity (Rasse et al., 2005).

The possible mechanism by which *Akt1* governs GluRIIA localization must therefore involve two different models. For a trafficking-based model, the effects of *Akt1* on GluRIIA localization could be mediated by influencing delivery of GluRIIA-containing vesicles to the plasma membrane, or by affecting the localization to the postsynaptic density following insertion into the plasma membrane. The accumulation of GluRIIA into intracellular membrane compartments argues against the latter hypothesis, because GluRIIA clearly became trapped inside of the cell without reaching the muscle surface. Alternatively, *Akt1* may affect GluRIIA localization by blocking local translocation at the synaptic sites. Given that the dimensions and complexity of SSR membranes decreased significantly with reduced *Akt1* function, it is possible that less subsynaptic structures were available for sustaining translational machinery and GluRIIA mRNAs. However, this local synthesis model fails to explain why GluRIIA would accumulate in intracellular compartments or why a non-specific effect of reduced SSR area would not influence localization of the other receptor subunits, and is therefore unlikely to be the only mechanism used by *Akt1*.

Furthermore, mutations in *Gtaxin* or *DLG* abolished SSR expansion but did not affect GluRIIA localization, showing that alterations in SSR surface area are not inherently accompanied by changes in glutamate receptor composition, although we couldn't exclude the possibility that *Akt1* may block subsynaptic translation of GluRIIA through a SSR-independent mechanism. In addressing the function of *Akt1* in glutamate receptor composition, we favor a model where *Akt1* affects developmental processes required for the selective delivery of GluRIIA from the endomembrane compartment into functional receptor units that arrive at the plasma membrane. It is notable that in mammalian systems, *Akt* is critical for the insulin-stimulated exocytosis of glucose transporter containing vesicles to the plasma membrane (Gonzalez and McGraw, 2006; Grillo et al., 2009). Perhaps *Akt1* governs similar exocytotic processes at synapses. *Akt1* signaling has also shown to be essential for AMPA and GABA_A receptor trafficking in hippocampal neurons, further supporting a role for *Akt1* in trafficking of synaptic proteins (Wang et al., 2003; Qin et al., 2005b; Fujii et al., 2010).

6.1.4 A possible role of *Akt1* in glutamate receptor protein folding

Besides the effects of *Akt1* RNAi on native GluRIIA, we have also examined the influence of *Akt1* on the distribution of an UAS-transgene derived RFP-tagged GluRIIA, monitored both by endogenous RFP fluorescence and anti-RFP antibody detection. It was of note that fluorescent signal from the GluRIIA-RFP was reduced at the synapse, while receptor mislocalization to intracellular compartments was detected only with anti-RFP antibody. Clearly, the RFP epitope of the fusion protein, detected by the anti-RFP antibody, was excluded from the postsynaptic specialization and redirected to an extrasynaptic cellular location as we observed for the endogenous GluRIIA. Muscle-specific *Akt1* knockdown interrupted the proper formation of the RFP domain in the recombinant protein and resulted in an immature/misfolded RFP protein that could not fluoresce (Piatkevich et al., 2010). These results suggest that *Akt1* influences some aspects of protein folding or structural stability required for the fluorescence detection of intact-RFP-tagged GluRIIA proteins. This idea was

further supported by the observation that mislocalized GluRIIA was not assembled into receptor tetramers (GluRIIC was not mislocalized, and showed no overlap with GluRIIA immunoreactivity), probably due to changes in structure that are essential for subunit polymerization. In summary, we propose that *Akt1* function may be required for proper folding of GluRIIA-RFP, thus influencing its post-synaptic targeting.

6.2 Regulation of autophagy in *Drosophila* muscle by HSPG and Acinus is critical for SSR membrane organization at the NMJ

6.2.1 Overview of primary findings

In Chapter 4, we described a novel function identified for HSPGs, a group of extracellular proteins that were well-known for their regulatory roles in cell signaling and morphogenesis. Muscle-specific RNAi of genes encoding enzymes necessary for HS biosynthesis produced a number of cellular deficits including larval lethality, structural abnormalities in subsynaptic membranes, and alterations in the numbers and morphology of mitochondria. Those defects were associated with an elevated level of autophagy in HS-compromised animals and could be rescued by reduction of *ATG8* function, indicating a role of autophagy during synapse development in the absence of a cellular stress response. We also provided evidence that the function of HS in modulating autophagy was mediated via PI3K activity. Together, we demonstrated that cell-surface HSPGs have a broad effect on membrane and organelle organizations. However, the reason that SSR membrane organization was influenced by the level of autophagy in muscle was not clear. Gene discovery of *Acinus* through an unbiased forward genetic screen and analysis for its functions in regulating autophagy provide further evidence that SSR morphology is strongly associated with autophagy level. This work is presented in Chapter 5. In order to identify novel regulators crucial for synapse assembly, a forward genetic screen was performed, looking for genes necessary for GluRIIA localization and SSR development. *Drosophila Acinus*, was found to be required for the organization of

SSR. Further analysis revealed that *Acinus* was required for autophagosome maturation in *Drosophila*, suggesting that NMJ assembly requires appropriate control of this fundamental cellular process. Inhibition of *ATG8a* in muscle cells produced a similar defect in SSR organization, providing additional support for this idea. Importantly, inhibition of *Acn* or *ATG8a* at the postsynaptic NMJ resulted in elevated α -spectrin accumulation, indicating that autophagic degradation of this cytoskeletal component may play an important role in modulating synapse morphology and activity (Figure 6.2).

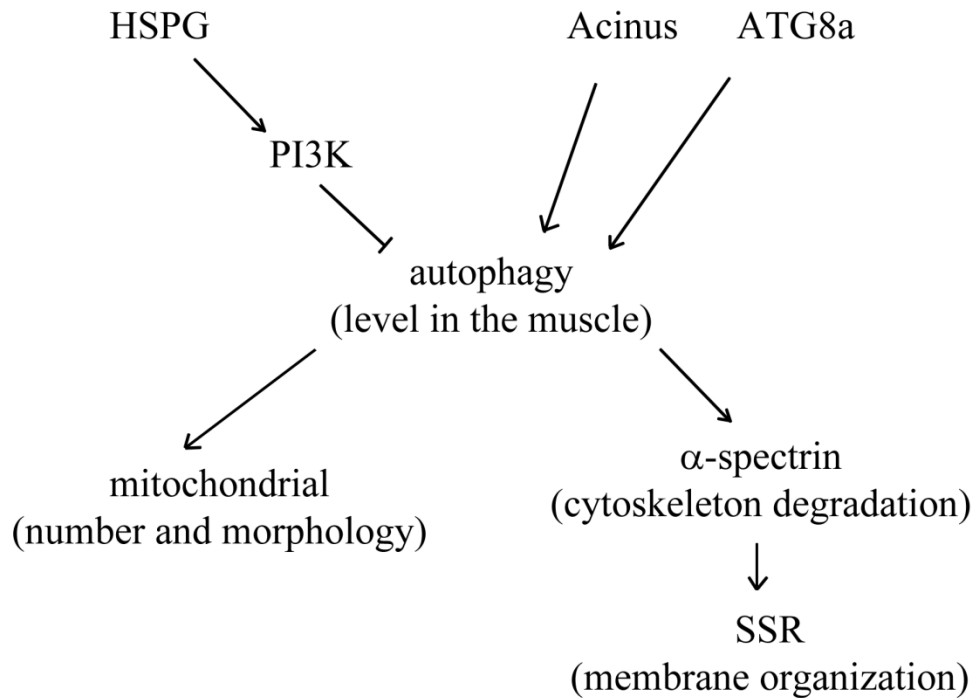


Figure 6.2 Model of HSPG, Acinus and ATG8a's regulation of autophagy during the development of postsynaptic cell specialization. HSPG biosynthesis and modification are critical for maintaining normal level of autophagy in postsynaptic cells. HSPG genetically interact with PI3K, possibly by acting as the co-receptors facilitating growth factor signaling which activates PI3K activity, to negatively regulate autophagy level. Cellular deficits including structural abnormalities in subsynaptic membranes and alterations in the numbers and morphology of mitochondria are associated with changes in autophagy level. Acinus and ATG8a are required for the formation and processing of autophagosomes. Their functions are critical for autophagic degradation of α -spectrin, which then influence SSR membrane organization. Collectively, it is demonstrated from both directions that up- and down-regulation of autophagy have a broad effects on membrane and organelle organizations.

6.2.2 Detection of a net increase in the level of autophagy in HS biosynthesis compromised muscle

To explore the functions of the HS biosynthetic machinery in muscle cells we employed *UAS*-bearing constructs that direct expression of interfering RNAs against different components of the HS synthesis and modification apparatus. TEM analysis of the NMJs in these RNAi expressing animals revealed an abundance of double-membrane bound intracellular organelles, suggesting the formation of autophagosomes. This was confirmed by the discovery of elevated levels of ATG8a-GFP-positive structures in animals with RNAi-mediated knockdown of *ttr*, *botv*, or *sfl*. We note that not all interfering RNAs directed against the three components of the HS biosynthetic pathway had the same effects, for example, *sfl* RNAi produced elevated numbers of LysoTracker-positive structures, whereas RNAi of either *botv* or *ttr* did not. This is likely due to fundamental differences in the processes these enzymes catalyze. *ttr* and *botv* are both involved in polymer extension, and it is possible that the short polymers produced may retain some degree of functionality, or trigger polymerization of a different GAG chain in place of HS. Moreover, *ttr* and *sotv*, the orthologs of vertebrate *EXT1* and *EXT2* respectively, possess some functional redundancy in HS polymerization. This was made evident by the observation that HS biosynthesis was not completely abolished in the *ttr* null mutant, and that wingless signaling was only defective in *ttr/sotv* double mutant (The et al., 1999; Han et al., 2004). It is possible that loss of *ttr* function could be partially compensated by *sotv* in regulating some autophagic processes. To the contrary, loss of *sfl*, a gene that does not affect chain synthesis but rather affects the overall level of sulfation of the *N*-acetyl glucosamine chain, might block function more completely, or indeed have dominant-negative effects, since a very abnormal chain is made. For example, in the absence of *sfl* activity, wingless, FGF and Hedgehog signaling pathways were all severely impaired, while in the *ttr* null mutant, only Hedgehog signaling was affected (The et al., 1999). We have also noted in previous work that null mutants of *sfl* have the most severe

phenotypes, which is consistent with the results presented here (Ren et al., 2009).

The increases in autophagosome levels detected by TEM or ATG8a-eGFP labeling in animals with compromised HS biosynthesis could result from an increase in autophagosome formation or an accumulation of unprocessed autophagosomes. In another words, the same phenotype could be caused by two completely opposite mechanisms: either a net increase in autophagy, or a blockade in autophagosome-lysosome fusion. To determine if there was a net increase in autophagic flux we employed a doubly-tagged *GFP-mCherry-ATG8a* transgene that both labels and distinguishes between autophagosomes and mature, acidic autolysosomes (Nezis et al., 2010). The mCherry protein is acid-resistant, providing fluorescent visualization of acidified compartments, whereas the GFP fluorophore is sensitive to protonation and the fluorescence signal is immediately lost in acidic conditions (Kimura et al., 2007; Zhou et al., 2012). Both autophagosomes and autolysosomes were increased upon compromising HS-biosynthesis, confirming that loss of HS biosynthetic capacity produced a net increase in autophagy.

6.2.3 SSR and mitochondrial phenotypes were associated with HS-dependent autophagic events

The increased level of autophagy in animals with compromised HS synthesis or modification could provide a mechanistic explanation for the diverse set of cellular phenotypes observed in these animals. This idea is supported by a number of observations. First, we were able to directly visualize the engulfment of mitochondria by autophagosomes in muscle cells with compromised HS biosynthesis, explaining their reduced presence in HS biosynthesis compromised animals. Second, reductions in *ATG8* function, achieved by expression of either dominant-negative *ATG8a* or RNAi constructs of *ATG8a/b*, suppressed three cellular phenotypes associated with reductions of HS-synthetic capacity: reductions in mitochondrial density, changes in mitochondrial shape and SSR

morphology. Last but not least, the biological relevance of the interaction between HS-production and autophagy was established on an organismal level by the demonstration that lethality associated with pan-cellular RNAi (using a broadly expressed *Gal4* line, *Da-Gal4*) against genes required for HS synthesis and modification was alleviated by a concurrent reduction in the level of autophagy. These experiments provide strong evidence that cellular deficits found within HS compromised animals result from this singular change in cell physiology, namely enhanced autophagy.

Decreased mitochondrial density in HS biosynthesis compromised animals could also be explained by an interaction between HSPG functions and mitochondrial fission independent of increased levels of autophagy. Compromised HSPG function may influence mitochondrial fission-fusion stasis, resulting in the shortened mitochondria seen in TEM images of animals expressing *sfl*^{RNAi}, *ttv*^{RNAi}, or *botv*^{RNAi}, which would in turn target these irregular structures for autophagic degradation and reduce the total number of mitochondria in the cell. However, this model seems unlikely since *PI3K*^{RNAi} expression in the muscle also altered mitochondrial morphology, and the mitochondria phenotype in HS-loss of function animals can be rescued by reducing *ATG8a* and autophagy function. Autophagosomal clearance of old or damaged mitochondria is an important quality control mechanism for proper cell function (Rambold and Lippincott-Schwartz, 2011; Youle and Narendra, 2011). Mitochondrial size and shape, regulated by fusion-fission dynamics, significantly impacts the selective degradation of mitochondria by autophagy. Elongated mitochondria cannot be efficiently engulfed by autophagosomal vesicles, and thus fission may be an important early step in autophagic degradation of mitochondria (Arnoult et al., 2005; Parone et al., 2008; Twig et al., 2008). We therefore favor the model where mitochondrial morphological change is a consequence of elevated autophagy in HS-compromised muscle.

6.2.4 The mechanism of HS-dependent inhibition of autophagy

The activation of autophagy upon reduction of HS polymer synthesis or sulfation was made evident by a number of markers and cellular phenotypes. We further investigated the cellular and molecular basis of this process. It was formally possible that compromised HS biosynthesis, which takes place in the Golgi, could influence protein folding and stability in the secretory apparatus and produce ER stress. In neurodegenerative disease models constitutively expressing misfolded proteins, ER stress is known to trigger a number of response pathways, including autophagy, to prevent cell death (Fouillet et al., 2012). Therefore we evaluated the possibility that disruption of HS biosynthesis could potentially activate autophagy via an ER stress response. We have several lines of evidence indicating that ER stress is unlikely to be induced in our HS-deficient larvae. In mammalian cells, inhibition of *N*-glycosylation in the Golgi apparatus results in eIF2 α phosphorylation and unconventional splicing of *Xbp1* pre-mRNA, both indicators of ER stress (Xu et al., 2010). However, *N*-linked glycosylation is established as a critical determinant affecting protein folding, whereas glycosaminoglycan modification is not. HS chain addition to proteins provides a negatively charged structure that typically serves to create binding sites for other proteins, promoting the formation of protein complexes, for example FGF receptor dimerization and/or ligand-receptor interactions (Faham et al., 1996; DiGabriele et al., 1998; Lin et al., 1999). In most cases, cell stress induced in the secretory pathway is caused by accumulation of unfolded or mis-modified proteins in the ER or Golgi apparatus (Schroder and Kaufman, 2005). In our experiments, animals lacking HS sulfation (*sfl*^{RNAi} expressed in muscle cell) still traffic comparable levels of glycosaminoglycan-modified proteins to the NMJ, seen with 3G10 antibody staining, so it does not appear that these proteins are accumulating in the secretory apparatus. Previous work from our lab showed that expression of Bip, an ER chaperone protein produced in response to ER stress, was not upregulated in HS biosynthetic mutants (Ren et al., 2009). Finally, the *Xbp1*-eGFP reporter that produces GFP only upon IRE-1-mediated splicing was silent in animals with compromised HS production. We do note that there is more

than one branch of unfolded protein response induced by ER stress. In mammalian cells three sensing systems, mediated by PERK, ATF6 and IRE-1, together constitute the response pathways, and function sequentially to both reduce the biosynthetic burden and increase the capacity for dealing with misfolded proteins (Schroder and Kaufman, 2005; Rasheva and Domingos, 2009). The IRE-1 mediated *Xbp-1* pre-mRNA unconventional splicing will occur only if PERK and ATF6 pathways fail to respond and ameliorate ER stress. Antibodies to assess PERK and ATF6 pathways are not available for *Drosophila*, and we therefore could not measure stress responses mediated by these two sensing systems. However, our result that *Xbp-1* alternative splicing did not take place when HS biosynthesis and modification were blocked established that this branch of ER stress response was not induced.

An alternative model to explain the activation of autophagy upon loss of HS biosynthesis is founded on the well-established role of HSPGs as growth factor co-receptors, facilitating and promoting signaling at the cell surface. Many HSPG-governed secreted protein growth factors signal via PI3K, a known inhibitor of autophagy (Abid et al., 2004; Dey et al., 2010; Kim et al., 2011). Therefore, loss of HS-cooperative signaling that normally aids in PI3K activation could produce a net reduction in PI3K-directed processes and an elevation of autophagy. We describe three results that are consistent with this model: 1) overexpression of *PI3K* in the muscle reduced autophagy on its own and also suppressed the elevated autophagy resulting from loss of HS biogenesis, 2) animals with RNAi-mediated reduction of HS biosynthesis showed reduced PIP3 immunoreactivity, demonstrating there is a measurable effect of HS on PI3K directed signaling, and 3) reduction of PI3K activity produced a prominent mitochondrial morphological deficit that mimicked the phenotypic change of HS-compromised larvae, and this mitochondrial deficit associated with loss of HS function could be rescued by increasing PI3K activity.

6.2.5 Heparan sulfate, autophagy and intracellular membrane trafficking

Previous work established that HS biosynthesis and modification are required for the proper assembly of the neuromuscular junction in *Drosophila* (Ren et al., 2009). Mutations affecting either HS polymer synthesis or sulfation altered the physiology and morphology of both motoneurons and muscle cells. A number of these cellular phenotypes indicated that compromising HS biosynthesis had a negative impact on membrane trafficking events. For example, disrupting heparan sulfate production at the NMJ altered motoneuron bouton number and morphology, resulting in large boutons without satellite buds, a phenotype that corresponds to increased endocytosis (Dickman et al., 2006; Ren et al., 2009). The activity-dependent endocytosis of neurotransmitter vesicles was dramatically elevated in HS biosynthetic mutants, as indicated by increased FM1-43 internalization following motoneuron stimulation. The levels of ER and Golgi markers in the muscle cell as well as the density of mitochondria in the muscle cell immediately beneath the synapse were also altered, suggesting that the organization of these membrane compartments was influenced by loss of HS modification of proteoglycans. However, a molecular mechanism accounting for these diverse phenotypes was not readily apparent.

The influence of HS on autophagy described in our work provided a simple and unified model to account for the phenotypes found upon inhibition of HS biosynthesis at the NMJ. The effect of HS synthesis on mitochondria, numbers and morphology and the elaboration of the postsynaptic specialization, the SSR, suggest that the autophagy pathway influences membrane trafficking processes that ensure the disposition of these two membrane compartments. While autophagy has been established as a mechanism for removing mitochondria that are damaged, or under conditions of cellular nutrient deprivation, our results suggest a more general role of autophagy in the developmental processes that

regulate these membrane compartments, in the absence of cellular stress or damage. Based on these findings, questions are raised concerning the general importance of HS biosynthesis for maintenance of appropriate levels of autophagy in all cell types, especially in neurons. Does HS-regulated autophagy interact with endocytosis in the presynaptic side to influence bouton morphology and synaptic vesicle recycling? It was demonstrated that endocytic kinase proteins Vps34 and Vps15, as well as endosomal sorting complexes (ESCRT-I, -II and -III), are essential for autophagosome initiation and maturation (Rusten et al., 2007; Juhasz et al., 2008; Lindmo et al., 2008). The intersection between components that participate in both autophagy and endocytosis suggests that HS-mediated autophagy may affect synaptic activity through interplay with endocytic trafficking at the presynaptic face of the NMJ.

6.2.6 Mechanisms for activating autophagy have potential therapeutic utility

Autophagy serves as an important mechanism for handling misfolded proteins that can adversely affect cellular physiology and, ultimately, result in cell death (Menzies et al., 2011). The accumulation of misfolded proteins is now understood to play a critical role in many neurodegenerative diseases, including Alzheimer's, Parkinson's, and Prion diseases (Williams et al., 2006; Pan et al., 2008; Metcalf et al., 2012). Indeed, activation of autophagy by the TOR inhibitor rapamycin has been shown to promote clearance of misfolded proteins in mouse models of human neurodegenerative disease (Spilman et al., 2010). Our results suggest an alternative means of activating autophagy, through inhibition of HS biosynthesis or sulfation. It is therefore of great interest to determine if loss or reduction of HS is broadly effective at activating autophagy in varied cell types and in many organisms, including humans.

6.3 An unbiased forward genetic screen to identify regulators of *Drosophila* NMJ development

6.3.1 Overview of primary findings

Previous results described in chapter 3 show that *Akt1* is specifically required for the assembly of A-type glutamate receptors, as well as the elaboration of the postsynaptic specialization. As discussed before, the functions of *Akt1* in synapse development are clearly mediated through distinct pathways, involving but not limited to dorsal/cactus and Gtaxin. Our goal was to use a transgenic RNAi library generated by VDRC (Dietzl et al., 2007) to identify additional *Akt1* downstream effectors and other novel genes required for morphological development of the synapse. In this screen, 513 transgenic *Drosophila* strains, each containing an inducible *UAS-RNAi* construct targeted to a single protein-coding gene, were individually crossed to a muscle-specific *Gal4* driver, and the synapse morphology was examined using immunohistochemistry and confocal microscopy. Compared to a work from the Featherstone lab in which about 30% of the mutants screened were shown to affect glutamate receptor expression or localization (Liebl and Featherstone, 2005), in our screen we only identified one gene (*CG10565*) required for the normal localization of GluRIIA. This apparent low incidence could be explained by several major *differences* in the two screens. First, different genetic approaches were used. For the published work, a collection of P-element transposon insertion mutants generated by Berkeley *Drosophila* Gene Disruption Project (BDGDP) was used. In contrast to the ubiquitous reduction of gene function seen in mutants, the use of interfering RNA-generating transgenes in our analysis provided cell-type specific blockade of function, allowing for restrictive gene-silencing in the postsynaptic side only. We therefore excluded genes with presynaptic functions that influence glutamate receptor localization via an anterograde signaling and instead focused only on the cell-autonomous roles of genes affecting postsynaptic properties. Second, different inclusion criteria were applied for the two screens. To minimize the time-consuming labor required for dissection and confocal microscopy, they decided to include only homozygous lethal mutations in their screen. This choice was based on the experience that severe disruption in glutamate receptor localization typically correlates to larval or pupae lethality. This criterion may have

contributed to the high rate at which their screen identified positive genes. However, the purpose of our analysis was to identify those genes that have specific regulatory functions in synapse assembly without causing general developmental defects. Therefore, *UAS-RNAi* transgenes producing embryonic or early larval lethality or showing severe defects in muscle morphology (missing muscles, split muscles, etc.) were precluded from our screen (Schnorrer et al., 2010). Finally, the two genetic screens were looking for different phenotypes. While their analysis was designed to find mutants that caused any change in GluRIIA expression or localization, including increases, decreases or loss of receptors, our research aimed to identify genes that, when silenced, resulted specifically in mislocalization of GluRIIA, as seen in *Akt1*-compromised animals.

Our screen also identified the apoptosis-related gene *Acn* for its requirement in maintaining SSR integrity. *Acn* has recently been implicated in endocytic and autophagic trafficking in *Drosophila* photoreceptor and fat body cells (Haberman et al., 2010), but has not been previously shown to influence subsynaptic membrane organization. We were particularly interested in characterizing and studying the cellular function of *Acn* in the postsynaptic muscle cells. We showed that the membrane organization of the SSR, monitored with mCD8-GFP or anti-DLG antibody, was disrupted upon *Mef2-Gal4* directed RNA silencing of *Acn*. This morphological change was confirmed by analyzing SSR ultrastructure by TEM, which indicated that the SSR was clearly “decondensed” in both parallel and orthogonal directions. We also showed that the membrane-bound autophagic pathway was blocked in animals with reduced *Acn* function. Our studies further revealed the importance of autophagy in regulating SSR organization. Suppression of autophagy by RNAi of either *Acn* or *ATG8a* resulted in SSR disorganization and synapse overgrowth. These phenotypes could be caused by over-accumulation of α -spectrin at the NMJ, given that overexpression of α -spectrin in the muscle resulted in SSR abnormalities similar to those observed in *Acn* and *ATG8a* RNAi animals.

6.3.2 *Acinus* is required for autophagosome maturation and SSR organization in *Drosophila*

Mammalian Acinus was initially identified for its role in chromatin condensation and DNA fragmentation during apoptosis (Sahara et al., 1999). Despite a high degree of sequence homology, *Drosophila Acn* is functionally distinct from its mammalian ortholog. This was initially revealed by a genetic screen looking for regulators of endosomal trafficking, in which *Acn* was identified for causing pigmentation defects in photoreceptor cells (Kramer, 2010). Our screen identified *Acn* independently as a regulator required for normal subsynaptic organization, which led us to investigate its physiological role in development of the postsynaptic SSR. RNA interference mediated knockdown of *Acn* in the muscle resulted in a loss of immunoreactivity both in the nucleus, where *Acn* is typically located, and in the cytosol of the muscle. Confocal microscopy of *Acn*^{RNAi} animals revealed the appearance of large ATG8a-eGFP-positive patches; however, both small ATG8a-eGFP puncta and LysoTracker-positive vesicles were significantly decreased in number. This was confirmed by TEM analysis of *Acn*^{RNAi} animals showing enlarged autophagosome vesicles of a size that was comparable to the ATG8a-eGFP-labeled vesicles seen in the confocal images. Together, these results indicate that *Acn* is required for autophagosome maturation, which is consistent with the known function of *Acn* in the autophagic response to starvation (Kramer, 2010). However, the relationship between *Acn* related perturbation of autophagy and the observed changes in SSR development remained unclear. To explore the functional link between these two phenotypes, we suppressed autophagy in the muscle by reducing the activity of proteins required for early stages of autophagosome formation. RNAi against *ATG8a*, one of the conjugation systems necessary for vesicle membrane expansion, was induced in the muscle, suppressing the level of autophagy as demonstrated by LysoTracker staining. Abrogation of *ATG8a* function also disrupted normal assembly of the SSR, resulting in a much less compacted membrane structure similar to that observed in *Acn*^{RNAi} animals (Figure 5.4). Thus, both autophagosome formation and maturation are important for

maintaining the normal structure of subsynaptic membranes, indicating a general role of autophagy in organization of the postsynaptic membrane specialization.

6.3.3 Autophagic degradation of α -spectrin and its implication in postsynaptic membrane organization

Spectrin is a cytoskeleton protein consisting of four subunits in an $\alpha_2\beta_2$ heterotetrameric arrangement. By interacting with short F-actin and other cytoskeleton-associated proteins, spectrin forms an extensively cross-linked network underlying the plasma membrane, providing mechanical strength to help maintain cell shape and polarity (Baines et al., 2001; Xu et al., 2013). Appropriate organization of the spectrin-actin network is critical for both pre- and postsynaptic development and stability. Mutations in either α - or β -spectrin subunits disrupted SSR organization as well as presynaptic neurotransmitter release, leading to synapse disassembly and synaptic transmission failure (Featherstone et al., 2001; Pielage et al., 2005, 2006). Degradation of the spectrin network is mediated by proteolytic enzymes calpain and caspase-3 (Wang et al., 1998; Glantz et al., 2007). However, as subunits of a multimeric protein complex, α - and β -spectrin are synthesized in excess of what can be assembled into a stable complex. The unassembled subunits undergo selective and rapid turnover via different degradative pathways (Woods and Lazarides, 1985). While the degradation of β -spectrin happens shortly after synthesis, in about 15 minutes, the half-life of α -spectrin is considerably longer, at approximately 2 hours (Woods and Lazarides, 1985). This difference in the rate of proteolysis occurs because β -spectrin is degraded by soluble cytoplasmic systems in a fast, ATP-dependent manner; while, proteolysis of α -spectrin proceeds by the slower autophagic degradation pathway. Our experiments showed that in animals with reduced *Acn* or *ATG8a* function, autophagic maturation was blocked, accompanied by a marked increase in the level of α -spectrin at the NMJ. This observation is consistent with the mechanism by which unassembled α -spectrin is degraded. While excessive proteolysis of spectrin causes membrane dissolution that ultimately leads to cell death, over-accumulation of spectrin results in reduced

skeleton plasticity and many other morphological defects (Castillo and Babson, 1998; Mazock et al., 2010; Diaconeasa et al., 2013). Therefore, the rapid synthesis and turnover of spectrin may constitute an important mechanism for synaptic plasticity at the *Drosophila* NMJ.

Postsynaptic spectrin-actin scaffolding is essential for subsynaptic membrane arrangement. Synapses lacking either α - or β -spectrin subunits showed severe defects in SSR organization (Pielage et al., 2006). However, the effect of elevated spectrin levels at the NMJ had not yet been determined. Our analysis showed that muscle-directed overexpression of α -spectrin resulted in significantly reduced SSR membrane density, suggesting that morphological alterations of the SSR in *Acn* and *ATG8a* RNAi animals could be the consequence of excess α -spectrin subunits. These findings provide strong evidence to support the idea that autophagic degradation of α -spectrin may contribute to an important regulatory mechanism that governs subsynaptic membrane development, thus affecting synaptic plasticity and function. Nevertheless, we cannot completely rule out the possibility that *Acn* and *ATG8a* may affect SSR development through a mechanism independent of autophagy-involved regulation of spectrin skeleton.

The apparent difference between α - and β -spectrin degradation patterns raised the question whether the level of β -spectrin remained normal at the NMJ in animals lacking *Acn* or *ATG8a* function. Given that the rapid turnover of β -spectrin does not rely on autophagic-lysosomal trafficking, the concentration of β -spectrin should not be affected by reduction of *Acn* or *ATG8a* activity. Because α - and β -spectrin are required in equal quantities, it seemed possible that an imbalance in the levels of these two proteins could cause SSR disorganization in animals with suppressed autophagy. This theory is supported by recent work showing that overexpression of β -spectrin resulted in severe developmental abnormalities and even lethality in multiple tissues, including wing disc, salivary gland, fat body, midgut, and muscle, and that dominant-negative effects of β -spectrin overexpression could be attenuated by co-overexpression of α -spectrin

(Mazock et al., 2010). Thus, the disruptive effects were caused not by simple overexpression, but rather by disproportionality between the levels of the spectrin subunits. It is possible that in *Acn* and *ATG8a* silenced animals, disproportionate accumulation of α -subunit could potentially have adverse effects on SSR development. The possibility that co-expression of β -spectrin can alleviate this dominant-negative effect will be addressed with future experiments.

6.4 Future direction: functional analysis of *DnaJ2* in regulating glutamate receptor composition

6.4.1 Identification and characterization of *DnaJ2*

Previous work demonstrated that *Akt1* controls glutamate receptor composition by specifically governing the distribution of the GluRIIA subunit. However, the molecular mechanism and downstream effectors of *Akt1* activity are unknown. In order to explore potential effectors modulated by *Akt1* in controlling GluRIIA localization, a genetic screen was conducted in our lab and *DnaJ2* (*CG10565*) was identified in this search for genes influencing GluRIIA localization. Follow-up experiments showed that muscle-specific inhibition of *DnaJ2* redistributed GluRIIA into intracellular membrane compartments without affecting the localization of IIB. To further explore the pre- and post-synaptic functions of *DnaJ2*, deletion mutants were generated via P-element mediated imprecise excision. All 15 of the mutants recovered showed early larval lethality in the homozygous state, indicating a crucial role of *DnaJ2* in development and survival. Currently our efforts focus on characterizing those mutants using RT-PCR and Western blotting assays to detect the level of *DnaJ2* mRNA and proteins. Our goal is to obtain at least one functional null allele and one hypomorphic allele that allows examination of moderate effects. A wild-type strain recovered from precise deletion will serve as control for all of these experiments. The loss-of-function effects of *DnaJ2* in regulating glutamate receptor composition and synaptic transmission efficacy will then be determined using both *DnaJ2* RNAi and mutant animals.

6.4.2 *In vivo* structure/function analysis of *DnaJ2*

DnaJ2 belongs to a J domain containing protein family (DnaJ/Hsp40), the members of which serve as co-chaperones for DnaK/Hsp70 proteins. During protein synthesis, Hsp70 binds to unfolded polypeptides, and this interaction is regulated by its ATPase activity; ATP hydrolysis converts Hsp70 from a highly dynamic state to a stable state with low association/dissociation rates (Minami et al., 1996; Bukau and Horwich, 1998). DnaJ/Hsp40 can selectively bind to unfolded substrates and present them to DnaK/Hsp70 proteins. DnaJ/Hsp40 binds to DnaK/Hsp70 through the J domain, which contains an HPD motif that increases the ATPase activity of DnaK/Hsp70, facilitating stability of the chaperone-substrate interaction (Takayama et al., 1999; Landry, 2003; Young et al., 2004). In addition to the J domain, DnaJ2 also contains an evolutionarily conserved DNA-binding domain, the function of which is largely unknown. Our hypothesis is that the physiological role of DnaJ2 in glutamate receptor assembly is based on its classical co-chaperone function that requires the conserved J domain. To test this hypothesis, we generated wild-type and mutated *DnaJ2* cDNAs with deletions of either the J domain or the DBD domain. Given the fundamental role of the HPD motif in mediating DnaJ-Hsp70 interaction, a point mutation at an essential residue within this domain was introduced to *DnaJ2* cDNA, substituting histidine 107 with glutamine. GFP-tagged *DnaJ2* transgenes were expressed in wild-type muscle cells, where deletion or point mutation of the J domain resulted in an obvious translocation of normally cytoplasmic DnaJ2 into nuclei, demonstrating the requirement of the J domain in the maintenance of its cytoplasmic localization. Although undefined, it is possible that DnaJ2 functions in the muscle cytosol to promote GluRIIA folding, therefore we predict that engineered DnaJ2 lacking the J domain will disrupt the localization of GluRIIA at the NMJ by affecting its folding. To evaluate the importance of the conserved J and DBD domains in synapse assembly, we first need to determine if ubiquitous expression of wild-type DnaJ2 in the *DnaJ2* null mutant will fully restore normal glutamate receptor localization. Considering the possible dominant-negative

effect of overexpressing a chaperone protein, promoters with different strength corresponding to different protein expression levels need to be selected carefully. Next, we will test whether the expression of mutant DnaJ2 proteins can rescue the phenotypic defects at the *DnaJ2* null mutant NMJs.

6.4.3 Isolation of DnaJ2 interacting proteins

DnaJ2 belongs to a co-chaperone family which cooperates with binding partners from the Hsp70/Hsc70 family to facilitate protein folding and translocation (Suzuki et al., 1999; Walsh et al., 2004). We hypothesize that the co-chaperone function of DnaJ2 is critical to ensure proper assembly and targeting of GluRIIA to the synapse. Given that the regulatory functions of DnaJ2 are based on its molecular interaction with components of Hsp70/Hsc70 family, the principle idea of this analysis is to isolate DnaJ2's binding partner and determine whether compromising the function of this chaperone also alters the localization of GluRIIA. The yeast-two-hybrid assay provides an easy and sensitive way to identify binding partners of DnaJ2. Vectors containing full-length *DnaJ2* cDNA will be used as bait and a late embryonic stage *Drosophila* cDNA library will serve as prey for this screen. This method enables us to not only identify the chaperone binding partner of DnaJ2 but also test if DnaJ2 physically interacts with GluRIIA. To gain further insights on the precise regions of interaction between the two proteins, deletion constructs of DnaJ2 and its binding partners will be generated and tested by another yeast-two-hybrid assay.

6.4.4 Investigation of the functional link between *DnaJ2* and *Akt1*

DnaJ2 was identified in the genetic screen for regulators of glutamate receptor assembly. The unusual GluRIIA mislocalization phenotype observed in *DnaJ2*^{RNAi} animals was highly similar to the defects caused by reduced *Akt1* function, suggesting that *DnaJ2* and *Akt1* may function via the same pathway to influence IIA localization. The result that overexpression of *Akt1*^{CA} failed to rescue GluRIIA mislocalization defect in *DnaJ2*^{RNAi} animals suggested that *DnaJ2* regulation of GluRIIA localization was unlikely to be mediated by *Akt1*. Therefore our current

focus on whether DnaJ2 could be a potential downstream effector of Akt1 activity in regulating glutamate receptor composition. Given that DnaJ2 does not bear a conserved Akt1 phosphorylation motif (RXRXXS/T), it is unlikely that DnaJ2 is regulated by Akt1 through direct phosphorylation (Datta et al., 1999). The generation of GFP-tagged *DnaJ2* transgenic strains as well as polyclonal anti-DnaJ2 antibody will facilitate further evaluation of the effect of Akt1 on DnaJ2 expression and subcellular distribution. Previous experiments showed that reduction of *Akt1* function resulted in mislocalization of GluRIIA-RFP that could be detected with an anti-RFP antibody but not with RFP fluorescence, suggesting that *Akt1* may affect the folding or stability of the protein structure necessary for recombinant GluRIIA-RFP to fluoresce. Our identification of co-chaperone DnaJ2 through an unbiased genetic screen supports the idea that *Akt1* may be involved in the protein folding machinery required specifically for appropriate assembly of the A-type glutamate receptor. This follow-up experiment aims to determine if glutamate receptor localization defects caused by RNA interference of *Akt1* will be rescued by increasing the chaperone capabilities of DnaJ2 and its corresponding Hsp70/Hsc70 partners.

6.5 Summary

This work has demonstrated the functions of three regulatory components (Akt1, HSPG and Acinus) in the assembly of postsynaptic elements, namely glutamate receptors and SSR. While distinct electrophysiological properties of two types of glutamate receptors have been well described by Goodman and DiAntonio groups, little is known about how they are regulated during the assembly of synapse. At our model synapse, the *Drosophila* NMJ, serine-threonine kinase Akt1 was found to be critical for A-type glutamate receptor localization without affecting B-type receptor targeting. This work unveils a novel mechanism of Akt1 to regulate synapse function by modulating the ratio of two types of glutamate receptors at the postsynaptic specialization.

SSR is the elaborated postsynaptic membrane structure that responsible for local

synthesis of glutamate receptor subunit and attachment of synaptic proteins (Sigrist et al., 2000). Akt1, HSPG and Acinus were all found to be essential for the development or organization of this membrane structure. Akt1 regulates the normal expansion of SSR through a mechanism involving the *Drosophila* t-SNARE protein Gtaxin. HSPG and Acinus are responsible for maintaining proper SSR organization via the control of autophagy, a membrane-bound, lysosome-involved degradation process that long accepted as a stress-responsive mechanism. This work, for the first time, revealed the importance of autophagy in maintaining normal cellular structures (SSR and mitochondria) in the absence of stress or damage. I have also showed the effects of autophagy on the level of α -spectrin, a cytoskeleton protein known to influence SSR organization. This result suggests that HSPG and Acinus could affect SSR organization by regulating autophagic degradation of α -spectrin. In the end, the investigations and findings that I have demonstrated in this thesis work have revealed the mechanisms controlling the development and activity of *Drosophila* NMJ and will be informative to the studies investigating postsynaptic assembly of vertebrate neurons.

References

- Abid R, Guo SD, Minami T, Spokes KC, Ueki K, Skurk C, Walsh K, Aird WC (2004) Vascular endothelial growth factor activates PI3K/Akt/forkhead signaling in endothelial cells. *Arteriosclerosis Thrombosis and Vascular Biology* 24:294-300.
- Altomare DA, Testa JR (2005) Perturbations of the AKT signaling pathway in human cancer. *Oncogene* 24:7455-7464.
- Anderson MS, Halpern ME, Keshishian H (1988) IDENTIFICATION OF THE NEUROPEPTIDE TRANSMITTER PROCTOLIN IN DROSOPHILA LARVAE - CHARACTERIZATION OF MUSCLE FIBER-SPECIFIC NEUROMUSCULAR ENDINGS. *Journal of Neuroscience* 8:242-255.
- Arnoult D, Rismanchi N, Grodet A, Roberts RG, Seeburg DP, Estaquier J, Sheng M, Blackstone C (2005) Bax/Bak-dependent release promotes of DDP/TIMM8a promotes Drp1-mediated mitochondrial fission and mitoptosis during programmed cell death. *Current Biology* 15:2112-2118.
- Atwood HL, Govind CK, Wu CF (1993) DIFFERENTIAL ULTRASTRUCTURE OF SYNAPTIC TERMINALS ON VENTRAL LONGITUDINAL ABDOMINAL MUSCLES IN DROSOPHILA LARVAE. *Journal of Neurobiology* 24:1008-1024.
- Auger KR, Serunian LA, Soltoff SP, Libby P, Cantley LC (1989) PDGF-DEPENDENT TYROSINE PHOSPHORYLATION STIMULATES PRODUCTION OF NOVEL POLYPHOSPHOINOSITIDES IN INTACT-CELLS. *Cell* 57:167-175.
- Augustin H, Grosjean Y, Chen KY, Sheng Q, Featherstone DE (2007) Nonvesicular release of glutamate by glial xCT transporters suppresses glutamate receptor clustering in vivo. *Journal of Neuroscience* 27:111-123.
- Aviezer D, Hecht D, Safran M, Eisinger M, David G, Yayon A (1994) PERLECAN, BASAL LAMINA PROTEOGLYCAN, PROMOTES BASIC FIBROBLAST GROWTH FACTOR-RECEPTOR BINDING, MITOGENESIS, AND ANGIOGENESIS. *Cell* 79:1005-1013.
- Bae SS, Cho H, Mu J, Birnbaum MJ (2003) Isoform-specific regulation of insulin-dependent glucose uptake by Akt/protein kinase B. *J Biol Chem* 278:49530-49536.
- Baeg GH, Lin XH, Khare N, Baumgartner S, Perrimon N (2001) Heparan sulfate proteoglycans are critical for the organization of the extracellular distribution of Wingless. *Development* 128:87-94.
- Baines AJ (2010) The spectrin-ankyrin-4.1-adducin membrane skeleton: adapting eukaryotic cells to the demands of animal life. *Protoplasma* 244:99-131.
- Baines AJ, Keating L, Phillips GW, Scott C (2001) The postsynaptic spectrin/4.1 membrane protein 'accumulation machine'. *Cell Mol Biol Lett* 6:691-702.
- Bate M, Landgraf M, Bate MRG (1999) Development of larval body wall muscles. *Neuromuscular Junctions in Drosophila* 43:25-44.

- Bateman JR, Lee AM, Wu CT (2006) Site-specific transformation of *Drosophila* via phi C31 integrase-mediated cassette exchange. *Genetics* 173:769-777.
- Beg AA, Baldwin AS (1993) THE I-KAPPA-B PROTEINS - MULTIFUNCTIONAL REGULATORS OF REL/NF-KAPPA-B TRANSCRIPTION FACTORS. *Genes & Development* 7:2064-2070.
- Bellacosa A, Kumar CC, Di Cristofano A, Testa JR (2005) Activation of AKT kinases in cancer: Implications for therapeutic targeting. In: *Advances in Cancer Research*, Vol 94 (VandeWoude GF, Klein G, eds), pp 29-+.
- Bellaiche Y, The I, Perrimon N (1998) Tout-velu is a *Drosophila* homologue of the putative tumour suppressor EXT-1 and is needed for Hh diffusion. *Nature* 394:85-88.
- Bennett KL, Bradshaw J, Youngman T, Rodgers J, Greenfield B, Aruffo A, Linsley PS (1997) Deleted in colorectal carcinoma (DCC) binds heparin via its fifth fibronectin type III domain. *J Biol Chem* 272:26940-26946.
- Bennett V (1982) THE MOLECULAR-BASIS FOR MEMBRANE - CYTOSKELETON ASSOCIATION IN HUMAN-ERYTHROCYTES. *Journal of Cellular Biochemistry* 18:49-65.
- Bennett V, Baines AJ (2001) Spectrin and ankyrin-based pathways: Metazoan inventions for integrating cells into tissues. *Physiological Reviews* 81:1353-1392.
- Bernfield M, Gotte M, Park PW, Reizes O, Fitzgerald ML, Lincecum J, Zako M (1999) Functions of cell surface heparan sulfate proteoglycans. *Annual Review of Biochemistry* 68:729-777.
- Berry DL, Baehrecke EH (2007) Growth arrest and autophagy are required for salivary gland cell degradation in *Drosophila*. *Cell* 131:1137-1148.
- Besse F, Mertel S, Kittel R, Wichmann C, Rasse T, Sigrist S, Ephrussi A (2006) *Drosophila* Basigin controls neuromuscular junction growth and synaptic vesicle distribution and release. *Journal of Neurogenetics* 20:86-87.
- Besse F, Mertel S, Kittel RJ, Wichmann C, Rasse TM, Sigrist SJ, Ephrussi A (2007) The Ig cell adhesion molecule Basigin controls compartmentalization and vesicle release at *Drosophila melanogaster* synapses. *Journal of Cell Biology* 177:843-855.
- Bischof J, Maeda RK, Hediger M, Karch F, Basler K (2007) An optimized transgenesis system for *Drosophila* using germ-line-specific phi C31 integrases. *Proc Natl Acad Sci U S A* 104:3312-3317.
- Bishop JR, Schuksz M, Esko JD (2007) Heparan sulphate proteoglycans fine-tune mammalian physiology. *Nature* 446:1030-1037.
- Bosher JM, Labouesse M (2000) RNA interference: genetic wand and genetic watchdog. *Nat Cell Biol* 2:E31-E36.
- Brand AH, Perrimon N (1993) Targeted Gene-Expression as a Means of Altering Cell Fates and Generating Dominant Phenotypes. *Development* 118:401-415.
- Broadie K, Bate M (1993a) Innervation Directs Receptor Synthesis and Localization in *Drosophila* Embryo Synaptogenesis. *Nature* 361:350-353.

- Broadie K, Bate M (1993b) ACTIVITY-DEPENDENT DEVELOPMENT OF THE NEUROMUSCULAR SYNAPSE DURING DROSOPHILA EMBRYOGENESIS. *Neuron* 11:607-619.
- Broadie KS, Bate M (1993c) DEVELOPMENT OF THE EMBRYONIC NEUROMUSCULAR SYNAPSE OF DROSOPHILA-MELANOGASTER. *Journal of Neuroscience* 13:144-166.
- Bronk P, Nie ZP, Klose MK, Dawson-Scully K, Zhang JH, Robertson RM, Atwood HL, Zinsmaier KE (2005) The multiple functions of cysteine-string protein analyzed at Drosophila nerve terminals. *Journal of Neuroscience* 25:2204-2214.
- Brunet A, Datta SR, Greenberg ME (2001) Transcription-dependent and -independent control of neuronal survival by the PI3K-Akt signaling pathway. *Current Opinion in Neurobiology* 11:297-305.
- Budnik V, Koh YH, Guan B, Hartmann B, Hough C, Woods D, Gorczyca M (1996) Regulation of synapse structure and function by the Drosophila tumor suppressor gene *dlg*. *Neuron* 17:627-640.
- Bukau B, Horwich AL (1998) The Hsp70 and Hsp60 chaperone machines. *Cell* 92:351-366.
- Bulow HE, Hobert O (2004) Differential sulfations and epimerization define heparan sulfate specificity in nervous system development. *Neuron* 41:723-736.
- Burridge K, Fath K, Kelly T, Nuckolls G, Turner C (1988) FOCAL ADHESIONS - TRANSMEMBRANE JUNCTIONS BETWEEN THE EXTRACELLULAR-MATRIX AND THE CYTOSKELETON. *Annual Review of Cell Biology* 4:487-525.
- Cash S, Chiba A, Keshishian H (1992) ALTERNATE NEUROMUSCULAR TARGET SELECTION FOLLOWING THE LOSS OF SINGLE MUSCLE-FIBERS IN DROSOPHILA. *Journal of Neuroscience* 12:2051-2064.
- Castillo MR, Babson JR (1998) Ca²⁺-dependent mechanisms of cell injury in cultured cortical neurons. *Neuroscience* 86:1133-1144.
- Chan CB, Liu X, Tang X, Fu H, Ye K (2007) Akt phosphorylation of zyxin mediates its interaction with acinus-S and prevents acinus-triggered chromatin condensation. *Cell Death and Differentiation* 14:1688-1699.
- Chang YY, Neufeld TP (2010) Autophagy takes flight in Drosophila. *Febs Letters* 584:1342-1349.
- Chen K, Merino C, Sigrist SJ, Featherstone DE (2005) The 4.1 protein coracle mediates subunit-selective anchoring of Drosophila glutamate receptors to the postsynaptic actin cytoskeleton. *Journal of Neuroscience* 25:6667-6675.
- Chen KY, Featherstone DE (2005) Discs-large (DLG) is clustered by presynaptic innervation and regulates postsynaptic glutamate receptor subunit composition in Drosophila. *Bmc Biology* 3.
- Chen RY, Kang VH, Chen J, Shope JC, Torabinejad J, DeWald DB, Prestwich GD (2002) A monoclonal antibody to visualize PtdIns(3,4,5)P-3 in cells. *J Histochem Cytochem* 50:697-708.

- Chen WS, Xu PZ, Gottlob K, Chen ML, Sokol K, Shiyanova T, Roninson I, Weng W, Suzuki R, Tobe K, Kadowaki T, Hay N (2001) Growth retardation and increased apoptosis in mice with homozygous disruption of the akt1 gene. *Genes & Development* 15:2203-2208.
- Cho H, Mu J, Kim JK, Thorvaldsen JL, Chu QW, Crenshaw EB, Kaestner KH, Bartolomei MS, Shulman GI, Birnbaum MJ (2001) Insulin resistance and a diabetes mellitus-like syndrome in mice lacking the protein kinase Akt2 (PKB beta). *Science* 292:1728-1731.
- Cingolani LA, Goda Y (2008) Actin in action: the interplay between the actin cytoskeleton and synaptic efficacy. *Nature Reviews Neuroscience* 9:344-356.
- Colley NJ, Cassill JA, Baker EK, Zuker CS (1995) DEFECTIVE INTRACELLULAR-TRANSPORT IS THE MOLECULAR-BASIS OF RHODOPSIN-DEPENDENT DOMINANT RETINAL DEGENERATION. *Proc Natl Acad Sci U S A* 92:3070-3074.
- Collins CA, DiAntonio A (2007) Synaptic development: insights from *Drosophila*. *Current Opinion in Neurobiology* 17:35-42.
- Cox RT, Spradling AC (2003) A Balbiani body and the fusome mediate mitochondrial inheritance during *Drosophila* oogenesis. *Development* 130:1579-1590.
- Currie DA, Truman JW, Burden SJ (1995) DROSOPHILA GLUTAMATE-RECEPTOR RNA EXPRESSION IN EMBRYONIC AND LARVAL MUSCLE-FIBERS. *Developmental Dynamics* 203:311-316.
- Dan HC, Cooper MJ, Cogswell PC, Duncan JA, Ting JPY, Baldwin AS (2008) Akt-dependent regulation of NF-kappa B is controlled by mTOR and Raptor in association with IKK. *Genes & Development* 22:1490-1500.
- Dani N, Nahm M, Lee S, Brodie K (2012) A Targeted Glycan-Related Gene Screen Reveals Heparan Sulfate Proteoglycan Sulfation Regulates WNT and BMP Trans-Synaptic Signaling. *Plos Genetics* 8.
- Datta SR, Brunet A, Greenberg ME (1999) Cellular survival: a play in three Akts. *Genes & Development* 13:2905-2927.
- David G, Bai XM, Vanderschueren B, Cassiman JJ, Vandenberghe H (1992) DEVELOPMENTAL-CHANGES IN HEPARAN-SULFATE EXPRESSION - INSITU DETECTION WITH MABS. *Journal of Cell Biology* 119:961-975.
- De Matteis MA, Morrow JS (2000) Spectrin tethers and mesh in the biosynthetic pathway. *Journal of Cell Science* 113:2331-2343.
- Denzer AJ, Brandenberger R, Gesemann M, Chiquet M, Ruegg MA (1997) Agrin binds to the nerve-muscle basal lamina via laminin. *Journal of Cell Biology* 137:671-683.
- Dey JH, Bianchi F, Voshol J, Bonenfant D, Oakeley EJ, Hynes NE (2010) Targeting Fibroblast Growth Factor Receptors Blocks PI3K/AKT Signaling, Induces Apoptosis, and Impairs Mammary Tumor Outgrowth and Metastasis. *Cancer Research* 70:4151-4162.
- Diaconeasa B, Mazock GH, Mahowald AP, Dubreuil RR (2013) Genetic Studies of Spectrin in the Larval Fat Body of *Drosophila melanogaster*: Evidence for a Novel Lipid Uptake Apparatus. *Genetics* 195:871-+.

- DiAntonio A (2006) Glutamate receptors at the *Drosophila* neuromuscular junction. In: *Fly Neuromuscular Junction: Structure and Function*, Second Edition, pp 165-179. San Diego: Elsevier Academic Press Inc.
- DiAntonio A, Petersen SA, Heckmann M, Goodman CS (1999) Glutamate receptor expression regulates quantal size and quantal content at the *Drosophila* neuromuscular junction. *Journal of Neuroscience* 19:3023-3032.
- Dickman DK, Lu ZY, Meinertzhagen IA, Schwarz TL (2006) Altered synaptic development and active zone spacing in endocytosis mutants. *Current Biology* 16:591-598.
- Dietzl G, Chen D, Schnorrer F, Su KC, Barinova Y, Fellner M, Gasser B, Kinsey K, Oppel S, Scheiblaue S, Couto A, Marra V, Keleman K, Dickson BJ (2007) A genome-wide transgenic RNAi library for conditional gene inactivation in *Drosophila*. *Nature* 448:151-U151.
- DiGabriele AD, Lax I, Chen DI, Svahn CM, Jaye M, Schlessinger J, Hendrickson WA (1998) Structure of a heparin-linked biologically active dimer of fibroblast growth factor. *Nature* 393:812-817.
- Dillon C, Goda Y (2005) The actin cytoskeleton: Integrating form and function at the synapse. In: *Annual Review of Neuroscience*, pp 25-55.
- Dimitroff B, Howe K, Watson A, Campion B, Lee HG, Zhao N, O'Connor MB, Neufeld TP, Selleck SB (2012) Diet and Energy-Sensing Inputs Affect TorC1-Mediated Axon Misrouting but Not TorC2-Directed Synapse Growth in a *Drosophila* Model of Tuberous Sclerosis. *Plos One* 7.
- Dudek H, Datta SR, Franke TF, Birnbaum MJ, Yao RJ, Cooper GM, Segal RA, Kaplan DR, Greenberg ME (1997) Regulation of neuronal survival by the serine-threonine protein kinase Akt. *Science* 275:661-665.
- Duffy JB (2002) GAL4 system in *Drosophila*: A fly geneticist's Swiss army knife. *Genesis* 34:1-15.
- Easton RM, Cho H, Roovers K, Shineman DW, Mizrahi M, Forman MS, Lee VMY, Szabolcs M, de Jong R, Oltersdorf T, Ludwig T, Efstratiadis A, Birnbaum MJ (2005) Role for Akt3/Protein kinase B gamma in attainment of normal brain size. *Molecular and Cellular Biology* 25:1869-1878.
- Ethell IM, Yamaguchi Y (1999) Cell surface heparan sulfate proteoglycan syndecan-2 induces the maturation of dendritic spines in rat hippocampal neurons. *Journal of Cell Biology* 144:575-586.
- Ethell IM, Irie F, Kalo MS, Couchman JR, Pasquale EB, Yamaguchi Y (2001) EphB/syndecan-2 signaling in dendritic spine morphogenesis. *Neuron* 31:1001-1013.
- Evergren E, Benfenati F, Shupliakov O (2007) The synapsin cycle: A view from the synaptic endocytic zone. *J Neurosci Res* 85:2648-2656.
- Faham S, Hileman RE, Fromm JR, Linhardt RJ, Rees DC (1996) Heparin structure and interactions with basic fibroblast growth factor. *Science* 271:1116-1120.
- Featherstone DE, Rushton E, Broadie K (2002) Developmental regulation of glutamate receptor field size by nonvesicular glutamate release. *Nature Neuroscience* 5:141-146.

- Featherstone DE, Davis WS, Dubreuil RR, Broadie K (2001) Drosophila alpha- and beta-spectrin mutations disrupt presynaptic neurotransmitter release. *Journal of Neuroscience* 21:4215-4224.
- Featherstone DE, Rushton E, Rohrbough J, Liebl F, Karr J, Sheng Q, Rodesch CK, Broadie K (2005) An essential Drosophila glutamate receptor subunit that functions in both central neuropil and neuromuscular junction. *Journal of Neuroscience* 25:3199-3208.
- Fouillet A, Levet C, Virgone A, Robin M, Dourlen P, Rieusset J, Belaidi E, Ovize M, Touret M, Nataf S, Mollereau B (2012) ER stress inhibits neuronal death by promoting autophagy. *Autophagy* 8:915-926.
- Fouquet W, Oswald D, Wichmann C, Mertel S, Depner H, Dyba M, Hallermann S, Kittel RJ, Eimer S, Sigrist SJ (2009) Maturation of active zone assembly by Drosophila Bruchpilot. *Journal of Cell Biology* 186:129-145.
- Friedman SH, Dani N, Rushton E, Broadie K (2013) Fragile X mental retardation protein regulates trans-synaptic signaling in Drosophila. *Disease Models & Mechanisms* 6:1400-1413.
- Fujii M, Kanematsu T, Ishibashi H, Fukami K, Takenawa T, Nakayama KI, Moss SJ, Nabekura J, Hirata M (2010) Phospholipase C-related but Catalytically Inactive Protein Is Required for Insulin-induced Cell Surface Expression of gamma-Aminobutyric Acid Type A Receptors. *J Biol Chem* 285:4837-4846.
- Gao XS, Neufeld TP, Pan DJ (2000) Drosophila PTEN regulates cell growth and proliferation through PI3K-dependent and -independent pathways. *Developmental Biology* 221:404-418.
- Geiger B (1983) MEMBRANE-CYTOSKELETON INTERACTION. *Biochimica Et Biophysica Acta* 737:305-341.
- Ghosh S, May MJ, Kopp EB (1998) NF-kappa B and rel proteins: Evolutionarily conserved mediators of immune responses. *Annual Review of Immunology* 16:225-260.
- Glantz SB, Cianci CD, Iyer R, Pradhan D, Wang KKW, Morrow JS (2007) Sequential degradation of alpha II and beta II spectrin by calpain in glutamate or maitotoxin-stimulated cells. *Biochemistry* 46:502-513.
- Gonzalez E, McGraw TE (2006) Insulin signaling diverges into Akt-dependent and -independent signals to regulate the recruitment/docking and the fusion of GLUT4 vesicles to the plasma membrane. *Molecular Biology of the Cell* 17:4484-4493.
- Gorczyca D, Ashley J, Speese S, Gherbesi N, Thomas U, Gundelfinger E, Gramates LS, Budnik V (2007) Postsynaptic membrane addition depends on the discs-large-interacting t-SNARE gtaxin. *Journal of Neuroscience* 27:1033-1044.
- Gorczyca M, Augart C, Budnik V (1993) INSULIN-LIKE RECEPTOR AND INSULIN-LIKE PEPTIDE ARE LOCALIZED AT NEUROMUSCULAR-JUNCTIONS IN DROSOPHILA. *Journal of Neuroscience* 13:3692-3704.
- Gorczyca MG, Phillis RW, Budnik V (1994) THE ROLE OF TINMAN, A MESODERMAL CELL FATE GENE, IN AXON PATHFINDING DURING THE DEVELOPMENT OF THE TRANSVERSE NERVE IN DROSOPHILA. *Development* 120:2143-2152.

- Greengard P, Benfenati F, Valtorta F (1994) SYNAPSIN-I, AN ACTIN-BINDING PROTEIN REGULATING SYNAPTIC VESICLE TRAFFIC IN THE NERVE-TERMINAL. In: Molecular and Cellular Mechanisms of Neurotransmitter Release (Stjarne L, Greengard P, Griller SE, Hokfelt TGM, Ottoson DR, eds), pp 31-45.
- Grider MH, Park D, Spencer DM, Shine HD (2009) Lipid Raft-Targeted Akt Promotes Axonal Branching and Growth Cone Expansion Via mTOR and Rac1, Respectively. *J Neurosci Res* 87:3033-3042.
- Grillo CA, Pirolì GG, Hendry RM, Reagan LP (2009) Insulin-stimulated translocation of GLUT4 to the plasma membrane in rat hippocampus is PI3-kinase dependent. *Brain Res* 1296:35-45.
- Guan B, Hartmann B, Kho YH, Gorczyca M, Budnik V (1996) The *Drosophila* tumor suppressor gene, *dig*, is involved in structural plasticity at a glutamatergic synapse. *Current Biology* 6:695-706.
- Guo HF, Zhong Y (2006) Requirement of Akt to mediate long-term synaptic depression in *Drosophila*. *Journal of Neuroscience* 26:4004-4014.
- Haberman AS, Akbar MA, Ray S, Kramer H (2010) *Drosophila* acinus encodes a novel regulator of endocytic and autophagic trafficking. *Development* 137:2157-2166.
- Hacker U, Nybakken K, Perrimon N (2005) Heparan sulphate proteoglycans: The sweet side of development. *Nature Reviews Molecular Cell Biology* 6:530-541.
- Han C, Belenkaya TY, Khodoun M, Tauchi M, Lin XD, Lin XH (2004) Distinct and collaborative roles of *Drosophila* EXT family proteins in morphogen signalling and gradient formation. *Development* 131:1563-1575.
- Heckscher ES, Fetter RD, Marek KW, Albin SD, Davis GW (2007) NF-kappa B, I kappa B, and IRAK control glutamate receptor density at the *drosophila* NMJ. *Neuron* 55:859-873.
- Hollmann M, Heinemann S (1994) CLONED GLUTAMATE RECEPTORS. *Annu Rev Neurosci* 17:31-108.
- Hu HY (2001) Cell-surface heparan sulfate is involved in the repulsive guidance activities of Slit2 protein. *Nature Neuroscience* 4:695-701.
- Hu Y, Liu Z, Yang SJ, Ye K (2007) Acinus-provoked protein kinase C delta isoform activation is essential for apoptotic chromatin condensation. *Cell Death and Differentiation* 14:2035-2046.
- Huang JX, Manning BD (2009) A complex interplay between Akt, TSC2 and the two mTOR complexes. *Biochem Soc Trans* 37:217-222.
- Ichimura Y, Kirisako T, Takao T, Satomi Y, Shimonishi Y, Ishihara N, Mizushima N, Tanida I, Kominami E, Ohsumi M, Noda T, Ohsumi Y (2000) A ubiquitin-like system mediates protein lipidation. *Nature* 408:488-492.
- Izumikawa T, Egusa N, Taniguchi F, Sugahara K, Kitagawa H (2006) Heparan sulfate polymerization in *Drosophila*. *J Biol Chem* 281:1929-1934.
- Jan LY, Jan YN (1976a) Properties of Larval Neuromuscular-Junction in *Drosophila-Melanogaster*. *J Physiol-London* 262:189-&.

- Jan LY, Jan YN (1976b) L-GLUTAMATE AS AN EXCITATORY TRANSMITTER AT DROSOPHILA LARVAL NEUROMUSCULAR-JUNCTION. *J Physiol-London* 262:215-236.
- Jaworski J, Spangler S, Seeburg DP, Hoogenraad CC, Sheng M (2005) Control of dendritic arborization by the phosphoinositide-3'-kinase-Akt-mammalian target of rapamycin pathway. *Journal of Neuroscience* 25:11300-11312.
- Jia XX, Gorczyca M, Budnik V (1993) Ultrastructure of Neuromuscular-Junctions in *Drosophila* - Comparison of Wild-Type and Mutants with Increased Excitability. *Journal of Neurobiology* 24:1025-1044.
- Johansen J, Halpern ME, Johansen KM, Keshishian H (1989) STEREOTYPIC MORPHOLOGY OF GLUTAMATERGIC SYNAPSES ON IDENTIFIED MUSCLE-CELLS OF DROSOPHILA LARVAE. *Journal of Neuroscience* 9:710-725.
- Johansen T, Lamark T (2011) Selective autophagy mediated by autophagic adapter proteins. *Autophagy* 7:279-296.
- Juhasz G, Hill JH, Yan Y, Sass M, Baehrecke EH, Backer JM, Neufeld TP (2008) The class III PI(3)K Vps34 promotes autophagy and endocytosis but not TOR signaling in *Drosophila*. *Journal of Cell Biology* 181:655-666.
- Kang MJ, Ryoo HD (2009) Suppression of retinal degeneration in *Drosophila* by stimulation of ER-associated degradation. *Proc Natl Acad Sci U S A* 106:17043-17048.
- Kang MJ, Chung J, Ryoo HD (2012) CDK5 and MEKK1 mediate pro-apoptotic signalling following endoplasmic reticulum stress in an autosomal dominant retinitis pigmentosa model. *Nat Cell Biol* 14:409-+.
- Kaplan DD, Zimmermann G, Suyama K, Meyer T, Scott MP (2008) A nucleostemin family GTPase, NS3, acts in serotonergic neurons to regulate insulin signaling and control body size. *Genes & Development* 22:1877-1893.
- Karr J, Vagin V, Chen KY, Ganesan S, Olenkina O, Gvozdev V, Featherstone DE (2009) Regulation of glutamate receptor subunit availability by microRNAs. *Journal of Cell Biology* 185:685-697.
- Keshishian H, Broadie K, Chiba A, Bate M (1996) The *Drosophila* neuromuscular junction: A model system for studying synaptic development and function. *Annu Rev Neurosci* 19:545-575.
- Khare N, Baumgartner S (2000) Dally-like protein, a new *Drosophila* glypican with expression overlapping with wingless. *Mechanisms of Development* 99:199-202.
- Kim E, Niethammer M, Rothschild A, Jan YN, Sheng M (1995) CLUSTERING OF SHAKER-TYPE K⁺ CHANNELS BY INTERACTION WITH A FAMILY OF MEMBRANE-ASSOCIATED GUANYLATE KINASES. *Nature* 378:85-88.
- Kim SH, Turnbull J, Guimond S (2011) Extracellular matrix and cell signalling: the dynamic cooperation of integrin, proteoglycan and growth factor receptor. *Journal of Endocrinology* 209:139-151.
- Kimura S, Noda T, Yoshimori T (2007) Dissection of the autophagosome maturation process by a novel reporter protein, tandem fluorescent-tagged LC3. *Autophagy* 3:452-460.

- Kirkpatrick CA, Selleck SB (2007) Heparan sulfate proteoglycans at a glance. *Journal of Cell Science* 120:1829-1832.
- Klionsky DJ (2007) Autophagy: from phenomenology to molecular understanding in less than a decade. *Nature Reviews Molecular Cell Biology* 8:931-937.
- Klionsky DJ, Emr SD (2000) Cell biology - Autophagy as a regulated pathway of cellular degradation. *Science* 290:1717-1721.
- Kneen M, Farinas J, Li YX, Verkman AS (1998) Green fluorescent protein as a noninvasive intracellular pH indicator. *Biophysical Journal* 74:1591-1599.
- Knox S, Ge H, Dimitroff BD, Ren Y, Howe KA, Arsham AM, Easterday MC, Neufeld TP, O'Connor MB, Selleck SB (2007) Mechanisms of TSC-mediated Control of Synapse Assembly and Axon Guidance. *PLoS One* 2:13.
- Kornau HC, Schenker LT, Kennedy MB, Seeburg PH (1995) DOMAIN INTERACTION BETWEEN NMDA RECEPTOR SUBUNITS AND THE POSTSYNAPTIC DENSITY PROTEIN PSD-95. *Science* 269:1737-1740.
- Kramer H (2010) Acinus A nuclear regulator of autophagy and endocytic trafficking. *Autophagy* 6:974-975.
- Ksiazek I, Burkhardt C, Lin S, Seddik R, Maj M, Bezakova G, Jucker M, Arber S, Caroni P, Sanes JR, Bettler B, Ruegg MA (2007) Synapse loss in cortex of agrin-deficient mice after genetic rescue of perinatal death. *Journal of Neuroscience* 27:7183-7195.
- Kuma A, Matsui M, Mizushima N (2007) LC3, an autophagosome marker, can be incorporated into protein aggregates independent of autophagy. *Autophagy* 3:323-328.
- Kumar V, Zhang MX, Swank MW, Kunz J, Wu GY (2005) Regulation of dendritic morphogenesis by Ras-PI3K-Akt mTOR and Ras-MAPK signaling pathways. *Journal of Neuroscience* 25:11288-11299.
- Kumar V, Fricke R, Bhar D, Reddy-Alla S, Krishnan KS, Bogdan S, Ramaswami M (2009) Syndapin Promotes Formation of a Postsynaptic Membrane System in *Drosophila*. *Molecular Biology of the Cell* 20:2254-2264.
- Kuo Y, Ren S, Lao U, Edgar BA, Wang T (2013) Suppression of polyglutamine protein toxicity by co-expression of a heat-shock protein 40 and a heat-shock protein 110. *Cell Death & Disease* 4.
- Kurada P, Otousa JE (1995) RETINAL DEGENERATION CAUSED BY DOMINANT RHODOPSIN MUTATIONS IN *DROSOPHILA*. *Neuron* 14:571-579.
- Lahey T, Gorczyca M, Jia XX, Budnik V (1994) The *Drosophila* Tumor-Suppressor Gene *Dlg* Is Required for Normal Synaptic Bouton Structure. *Neuron* 13:823-835.
- Lander AD, Selleck SB (2000) The elusive functions of proteoglycans: In vivo veritas. *Journal of Cell Biology* 148:227-232.
- Landgraf M, Bossing T, Technau GM, Bate M (1997) The origin, location, and projections of the embryonic abdominal motoneurons of *Drosophila*. *Journal of Neuroscience* 17:9642-9655.
- Landry SJ (2003) Structure and energetics of an allele-specific genetic interaction between DnaJ and DnaK: Correlation of nuclear magnetic

- resonance chemical shift perturbations in the J-domain of Hsp40/DnaJ with binding affinity for the ATPase domain of Hsp70/DnaK. *Biochemistry* 42:4926-4936.
- Langer T, Lu C, Echols H, Flanagan J, Hayer MK, Hartl FU (1992) SUCCESSIVE ACTION OF DNAK, DNAJ AND GROEL ALONG THE PATHWAY OF CHAPERONE-MEDIATED PROTEIN FOLDING. *Nature* 356:683-689.
- Laski FA, Rio DC, Rubin GM (1986) TISSUE-SPECIFICITY OF DROSOPHILA P-ELEMENT TRANSPOSITION IS REGULATED AT THE LEVEL OF MESSENGER-RNA SPLICING. *Cell* 44:7-19.
- Lauterborn JC, Rex CS, Kramar E, Chen LY, Pandeyarajan V, Lynch G, Gall CM (2007) Brain-derived neurotrophic factor rescues synaptic plasticity in a mouse model of fragile x syndrome. *Journal of Neuroscience* 27:10685-10694.
- Lee C-C, Huang C-C, Hsu K-S (2011) Insulin promotes dendritic spine and synapse formation by the PI3K/Akt/mTOR and Rac1 signaling pathways. *Neuropharmacology* 61:867-879.
- Lee HG, Zhao N, Campion BK, Nguyen MM, Selleck SB (2013) Akt regulates glutamate receptor trafficking and postsynaptic membrane elaboration at the *Drosophila* neuromuscular junction. *Dev Neurobiol* 73:723-743.
- Lee T, Luo LQ (1999) Mosaic analysis with a repressible cell marker for studies of gene function in neuronal morphogenesis. *Neuron* 22:451-461.
- Leevers SJ, Weinkove D, MacDougall LK, Hafen E, Waterfield MD (1996) The *Drosophila* phosphoinositide 3-kinase Dp110 promotes cell growth. *Embo J* 15:6584-6594.
- Levine B, Yuan JY (2005) Autophagy in cell death: an innocent convict? *Journal of Clinical Investigation* 115:2679-2688.
- Liang Y, Annan RS, Carr SK, Popp S, Mevissen M, Margolis RK, Margolis RU (1999) Mammalian homologues of the *Drosophila* slit protein are ligands of the heparan sulfate proteoglycan glypican-1 in brain. *J Biol Chem* 274:17885-17892.
- Liebl FLW, Featherstone DE (2005) Genes involved in *Drosophila* glutamate receptor expression and localization. *Bmc Neuroscience* 6.
- Liebl FLW, Chen K, Karr J, Sheng Q, Featherstone DE (2005) Increased synaptic microtubules and altered synapse development in *Drosophila* sec8 mutants. *BMC Biology* 3:Article No.: 27.
- Lin XH (2004) Functions of heparan sulfate proteoglycans in cell signaling during development. *Development* 131:6009-6021.
- Lin XH, Perrimon N (1999) Dally cooperates with *Drosophila* Frizzled 2 to transduce Wingless signalling. *Nature* 400:281-284.
- Lin XH, Buff EM, Perrimon N, Michelson AM (1999) Heparan sulfate proteoglycans are essential for FGF receptor signaling during *Drosophila* embryonic development. *Development* 126:3715-3723.
- Lin XY, Ruan X, Anderson MG, McDowell JA, Kroeger PE, Fesik SW, Shen Y (2005) siRNA-mediated off-target gene silencing triggered by a 7 nt complementation. *Nucleic Acids Research* 33:4527-4535.

- Lindahl U, Kusche-Gullberg M, Kjellen L (1998) Regulated diversity of heparan sulfate. *J Biol Chem* 273:24979-24982.
- Lindmo K, Brech A, Finley KD, Gaumer S, Contamine D, Rusten TE, Stenmark H (2008) The PI 3-kinase regulator Vps15 is required for autophagic clearance of protein aggregates. *Autophagy* 4:500-506.
- Manning BD, Cantley LC (2007) AKT/PKB signaling: Navigating downstream. *Cell* 129:1261-1274.
- Markstein M, Pitsouli C, Villalta C, Celniker SE, Perrimon N (2008) Exploiting position effects and the gypsy retrovirus insulator to engineer precisely expressed transgenes. *Nature Genetics* 40:476-483.
- Marrus SB, Portman SL, Allen MJ, Moffat KG, DiAntonio A (2004) Differential localization of glutamate receptor subunits at the *Drosophila* neuromuscular junction. *Journal of Neuroscience* 24:1406-1415.
- Mazock GH, Das A, Base C, Dubreuil RR (2010) Transgene Rescue Identifies an Essential Function for *Drosophila* beta Spectrin in the Nervous System and a Selective Requirement for Ankyrin-2-binding Activity. *Molecular Biology of the Cell* 21:2860-2868.
- McCurdy CE, Cartee GD (2005) Akt2 is essential for the full effect of calorie restriction on insulin-stimulated glucose uptake in skeletal muscle. *Diabetes* 54:1349-1356.
- McGuire SE, Roman G, Davis RL (2004) Gene expression systems in *Drosophila*: a synthesis of time and space. *Trends in Genetics* 20:384-391.
- Menzies FM, Moreau K, Rubinsztein DC (2011) Protein misfolding disorders and macroautophagy. *Current Opinion in Cell Biology* 23:190-197.
- Mertens G, Cassiman JJ, Vandenberghe H, Vermeylen J, David G (1992) CELL-SURFACE HEPARAN-SULFATE PROTEOGLYCANS FROM HUMAN VASCULAR ENDOTHELIAL-CELLS - CORE PROTEIN CHARACTERIZATION AND ANTITHROMBIN-III BINDING-PROPERTIES. *J Biol Chem* 267:20435-20443.
- Metcalf DJ, Garcia-Arencibia M, Hochfeld WE, Rubinsztein DC (2012) Autophagy and misfolded proteins in neurodegeneration. *Experimental Neurology* 238:22-28.
- Minami Y, Hohfeld J, Ohtsuka K, Hartl FU (1996) Regulation of the heat-shock protein 70 reaction cycle by the mammalian DnaJ homolog, Hsp40. *J Biol Chem* 271:19617-19624.
- Mizushima N, Levine B, Cuervo AM, Klionsky DJ (2008) Autophagy fights disease through cellular self-digestion. *Nature* 451:1069-1075.
- Monastirioti M, Gorczyca M, Rapus J, Eckert M, White K, Budnik V (1995) OCTOPAMINE IMMUNOREACTIVITY IN THE FRUIT-FLY *DROSOPHILA-MELANOGASTER*. *Journal of Comparative Neurology* 356:275-287.
- Morin X, Daneman R, Zavortink M, Chia W (2001) A protein trap strategy to detect GFP-tagged proteins expressed from their endogenous loci in *Drosophila*. *Proc Natl Acad Sci U S A* 98:15050-15055.

- Murachelli AG, Ebert J, Basquin C, Le Hir H, Conti E (2012) The structure of the ASAP core complex reveals the existence of a Pinin-containing PSAP complex. *Nature Structural & Molecular Biology* 19:378-386.
- Nakatani K, Sakaue H, Thompson DA, Weigel RJ, Roth RA (1999) Identification of a human Akt3 (protein kinase B gamma) which contains the regulatory serine phosphorylation site. *Biochemical and Biophysical Research Communications* 257:906-910.
- Nakato H, Futch TA, Selleck SB (1995) THE DIVISION ABNORMALLY DELAYED (DALLY) GENE - A PUTATIVE INTEGRAL MEMBRANE PROTEOGLYCAN REQUIRED FOR CELL-DIVISION PATTERNING DURING POSTEMBRYONIC DEVELOPMENT OF THE NERVOUS-SYSTEM IN DROSOPHILA. *Development* 121:3687-3702.
- Nakatogawa H, Ichimura Y, Ohsumi Y (2007) Atg8, a ubiquitin-like protein required for autophagosome formation, mediates membrane tethering and hemifusion. *Cell* 130:165-178.
- Nezis IP, Shrivage BV, Sagona AP, Lamark T, Bjorkoy G, Johansen T, Rusten TE, Brech A, Baehrecke EH, Stenmark H (2010) Autophagic degradation of dBruce controls DNA fragmentation in nurse cells during late *Drosophila melanogaster* oogenesis. *Journal of Cell Biology* 190:523-531.
- Nishikawa K, Kidokoro Y (1995) Junctional and extrajunctional glutamate receptor channels in *Drosophila* embryos and larvae. *Journal of Neuroscience* 15:7905-7915.
- Nunes P, Haines N, Kuppuswamy V, Fleet DJ, Stewart BA (2006) Synaptic vesicle mobility and presynaptic F-actin are disrupted in a n-ethylmaleimide-sensitive factor allele of *Drosophila*. *Molecular Biology of the Cell* 17:4709-4719.
- Ogata M, Hino SI, Saito A, Morikawa K, Kondo S, Kanemoto S, Murakami T, Taniguchi M, Tanii I, Yoshinaga K, Shiosaka S, Hammarback JA, Urano F, Imaizumi K (2006) Autophagy is activated for cell survival after endoplasmic reticulum stress. *Molecular and Cellular Biology* 26:9220-9231.
- Ohsumi Y (2001) Molecular dissection of autophagy: Two ubiquitin-like systems. *Nature Reviews Molecular Cell Biology* 2:211-216.
- Otousa JE, Baehr W, Martin RL, Hirsh J, Pak WL, Applebury ML (1985) THE DROSOPHILA NINAE GENE ENCODES AN OPSIN. *Cell* 40:839-850.
- Ou HL (2013) Gene knockout by inducing P-element transposition in *Drosophila*. *Genetics and Molecular Research* 12:2852-2857.
- Owald D, Sigrist SJ (2009) Assembling the presynaptic active zone. *Current Opinion in Neurobiology* 19:311-318.
- Ozes ON, Mayo LD, Gustin JA, Pfeffer SR, Pfeffer LM, Donner DB (1999) NF-kappa B activation by tumour necrosis factor requires the Akt serine-threonine kinase. *Nature* 401:82-85.
- Pan DJ, Dong JX, Zhang Y, Gao XS (2004) Tuberous sclerosis complex: from *Drosophila* to human disease. *Trends Cell Biol* 14:78-85.

- Pan TH, Kondo S, Le WD, Jankovic J (2008) The role of autophagy-lysosome pathway in neurodegeneration associated with Parkinson's disease. *Brain* 131:1969-1978.
- Parone PA, Da Cruz S, Tondera D, Mattenberger Y, James DI, Maechler P, Barja F, Martinou JC (2008) Preventing Mitochondrial Fission Impairs Mitochondrial Function and Leads to Loss of Mitochondrial DNA. *Plos One* 3.
- Parrish JZ, Xu PZ, Kim CC, Jan LY, Jan YN (2009) The microRNA bantam Functions in Epithelial Cells to Regulate Scaling Growth of Dendrite Arbors in *Drosophila* Sensory Neurons. *Neuron* 63:788-802.
- Perrimon N, Bernfield M (2000) Specificities of heparan sulphate proteoglycans in developmental processes. *Nature* 404:725-728.
- Perrimon N, Ni JQ, Perkins L (2010) In vivo RNAi: Today and Tomorrow. *Cold Spring Harbor Perspect Biol* 2.
- Perrimon N, Lanjuin A, Arnold C, Noll E (1996) Zygotic lethal mutations with maternal effect phenotypes in *Drosophila melanogaster* .2. Loci on the second and third chromosomes identified by P-element-induced mutations. *Genetics* 144:1681-1692.
- Petersen SA, Fetter RD, Noordermeer JN, Goodman CS, DiAntonio A (1997) Genetic analysis of glutamate receptors in *Drosophila* reveals a retrograde signal regulating presynaptic transmitter release. *Neuron* 19:1237-1248.
- Petiot A, Ogier-Denis E, Blommaert EFC, Meijer AJ, Codogno P (2000) Distinct classes of phosphatidylinositol 3 '-kinases are involved in signaling pathways that control macroautophagy in HT-29 cells. *J Biol Chem* 275:992-998.
- Pfeiffer BE, Huber KM (2006) Current advances in local protein synthesis and synaptic plasticity. *Journal of Neuroscience* 26:7147-7150.
- Piatkevich KD, Efremenko EN, Verkhusha VV, Varfolomeev DD (2010) Red fluorescent proteins and their properties. *Russian Chemical Reviews* 79:243-258.
- Pielage J, Fetter RD, Davis GW (2005) Presynaptic spectrin is essential for synapse stabilization. *Current Biology* 15:918-928.
- Pielage J, Fetter RD, Davis GW (2006) A postsynaptic spectrin scaffold defines active zone size, spacing, and efficacy at the *Drosophila* neuromuscular junction. *Journal of Cell Biology* 175:491-503.
- Qin G, Schwarz T, Kittel RJ, Schmid A, Rasse TM, Kappei D, Ponimaskin E, Heckmann M, Sigrist SJ (2005a) Four different subunits are essential for expressing the synaptic glutamate receptor at neuromuscular junctions of *Drosophila*. *Journal of Neuroscience* 25:3209-3218.
- Qin Y, Zhu YH, Baumgart JP, Stornetta RL, Seidenman K, Mack V, van Aelst L, Zhu JJ (2005b) State-dependent Ras signaling and AMPA receptor trafficking. *Genes & Development* 19:2000-2015.
- Rafuse VF, Polo-Prada L, Landmesser LT (2000) Structural and functional alterations of neuromuscular junctions in NCAM-Deficient mice. *Journal of Neuroscience* 20:6529-6539.

- Rambold AS, Lippincott-Schwartz J (2011) Mechanisms of mitochondria and autophagy crosstalk. *Cell Cycle* 10:4032-4038.
- Rao RV, Bredesen DE (2004) Misfolded proteins, endoplasmic reticulum stress and neurodegeneration. *Current Opinion in Cell Biology* 16:653-662.
- Rasheva VI, Domingos PM (2009) Cellular responses to endoplasmic reticulum stress and apoptosis. *Apoptosis* 14:996-1007.
- Rasse TM, Fouquet W, Schmid A, Kittel RJ, Mertel S, Sigrist CB, Schmidt M, Guzman A, Merino C, Qin G, Quentin C, Madeo FF, Heckmann M, Sigrist SJ (2005) Glutamate receptor dynamics organizing synapse formation in vivo. *Nature Neuroscience* 8:898-905.
- Raymond CR, Thompson VL, Tate WP, Abraham WC (2000) Metabotropic glutamate receptors trigger homosynaptic protein synthesis to prolong long-term potentiation. *Journal of Neuroscience* 20:969-976.
- Reiff DF, Thiel PR, Schuster CM (2002) Differential regulation of active zone density during long-term strengthening of *Drosophila* neuromuscular junctions. *Journal of Neuroscience* 22:9399-9409.
- Ren Y, Kirkpatrick CA, Rawson JM, Sun M, Selleck SB (2009) Cell Type-Specific Requirements for Heparan Sulfate Biosynthesis at the *Drosophila* Neuromuscular Junction: Effects on Synapse Function, Membrane Trafficking, and Mitochondrial Localization. *Journal of Neuroscience* 29:8539-8550.
- Robertson HM, Preston CR, Phillis RW, Johnsonschlitz DM, Benz WK, Engels WR (1988) A STABLE GENOMIC SOURCE OF P-ELEMENT TRANSPOSASE IN *DROSOPHILA-MELANOGASTER*. *Genetics* 118:461-470.
- Rueggsegger U, Leber JH, Walter P (2001) Block of HAC1 mRNA translation by long-range base pairing is released by cytoplasmic splicing upon induction of the unfolded protein response. *Cell* 107:103-114.
- Rusten TE, Lindmo K, Juhasz G, Sass M, Seglen PO, Brech A, Stenmark H (2004) Programmed autophagy in the *Drosophila* fat body is induced by ecdysone through regulation of the PI3K pathway. *Developmental Cell* 7:179-192.
- Rusten TE, Vaccari T, Lindmo K, Rodahl LMW, Nezis IP, Sem-Jacobsen C, Wendler F, Vincent J-P, Brech A, Bilder D, Stenmark H (2007) ESCRTs and Fab1 Regulate Distinct Steps of Autophagy. *Current Biology* 17:1817-1825.
- Ryoo HD, Domingos PM, Kang MJ, Steller H (2007) Unfolded protein response in a *Drosophila* model for retinal degeneration. *Embo J* 26:242-252.
- Sahara S, Aoto M, Eguchi Y, Imamoto N, Yoneda Y, Tsujimoto Y (1999) Acinus is a caspase-3-activated protein required for apoptotic chromatin condensation. *Nature* 401:168-173.
- Saitoe M, Tanaka S, Takata K, Kidokoro Y (1997) Neural activity affects distribution of glutamate receptors during neuromuscular junction formation in *Drosophila* embryos. *Developmental Biology* 184:48-60.

- Saitoe M, Schwarz TL, Umbach JA, Gundersen CB, Kidokoro Y (2001) Absence of junctional glutamate receptor clusters in *Drosophila* mutants lacking spontaneous transmitter release. *Science* 293:514-517.
- Sarrazin S, Lamanna WC, Esko JD (2011) Heparan Sulfate Proteoglycans. *Cold Spring Harbor Perspect Biol* 3.
- Schmid A, Chiba A, Doe CQ (1999) Clonal analysis of *Drosophila* embryonic neuroblasts: neural cell types, axon projections and muscle targets. *Development* 126:4653-4689.
- Schmid A, Hallermann S, Kittel RJ, Khorramshahi O, Frolich AMJ, Quentin C, Rasse TM, Mertel S, Heckmann M, Sigrist SJ (2008) Activity-dependent site-specific changes of glutamate receptor composition in vivo. *Nature Neuroscience* 11:659-666.
- Schnorrer F, Schonbauer C, Langer CCH, Dietzl G, Novatchkova M, Schernhuber K, Fellner M, Azaryan A, Radolf M, Stark A, Keleman K, Dickson BJ (2010) Systematic genetic analysis of muscle morphogenesis and function in *Drosophila*. *Nature* 464:287-291.
- Schroder M, Kaufman RJ (2005) ER stress and the unfolded protein response. *Mutat Res-Fundam Mol Mech Mutagen* 569:29-63.
- Schwerk C, Prasad J, Degenhardt K, Erdjument-Bromage H, White E, Tempst P, Kidd VJ, Manley JL, Lahti JM, Reinberg D (2003) ASAP, a novel protein complex involved in RNA processing and apoptosis. *Molecular and Cellular Biology* 23:2981-2990.
- Scott RC, Schuldiner O, Neufeld TP (2004) Role and regulation of starvation-induced autophagy in the *Drosophila* fat body. *Developmental Cell* 7:167-178.
- Scott RC, Juhasz G, Neufeld TP (2007) Direct induction of autophagy by Atg1 inhibits cell growth and induces apoptotic cell death. *Current Biology* 17:1-11.
- Serantes R, Arnalich F, Figueroa M, Salinas M, Andres-Mateos E, Codoceo R, Renart J, Matute C, Cavada C, Cuadrado A, Montiel C (2006) Interleukin-1 beta enhances GABA(A) receptor cell-surface expression by a phosphatidylinositol 3-kinase/Akt pathway - Relevance to sepsis-associated encephalopathy. *J Biol Chem* 281:14632-14643.
- Shen XH, Ellis RE, Lee K, Liu CY, Yang K, Solomon A, Yoshida H, Morimoto R, Kurnit DM, Mori K, Kaufman RJ (2001) Complementary signaling pathways regulate the unfolded protein response and are required for *C. elegans* development. *Cell* 107:893-903.
- Shotton DM, Heuser JE, Reese BF, Reese TS (1979) POSTSYNAPTIC MEMBRANE FOLDS OF THE FROG NEUROMUSCULAR-JUNCTION VISUALIZED BY SCANNING ELECTRON-MICROSCOPY. *Neuroscience* 4:427-435.
- Shupliakov O, Bloom O, Gustafsson JS, Kjaerulff O, Low P, Tomilin N, Pieribone VA, Greengard P, Brodin L (2002) Impaired recycling of synaptic vesicles after acute perturbation of the presynaptic actin cytoskeleton. *Proc Natl Acad Sci U S A* 99:14476-14481.

- Siddiqui TJ, Tari PK, Connor SA, Zhang P, Dobie FA, She K, Kawabe H, Wang YT, Brose N, Craig AM (2013) An LRRTM4-HSPG Complex Mediates Excitatory Synapse Development on Dentate Gyrus Granule Cells. *Neuron* 79:680-695.
- Sigrist SJ, Thiel PR, Reiff DF, Schuster CM (2002) The postsynaptic glutamate receptor subunit DGluR-IIA mediates long-term plasticity in *Drosophila*. *Journal of Neuroscience* 22:7362-7372.
- Sigrist SJ, Reiff DF, Thiel PR, Steinert JR, Schuster CM (2003) Experience-dependent strengthening of *Drosophila* neuromuscular junctions. *Journal of Neuroscience* 23:6546-6556.
- Sigrist SJ, Thiel PR, Reiff DF, Lachance PED, Lasko P, Schuster CM (2000) Postsynaptic translation affects the efficacy and morphology of neuromuscular junctions. *Nature* 405:1062-1065.
- Sink H, Whittington PM (1991) LOCATION AND CONNECTIVITY OF ABDOMINAL MOTONEURONS IN THE EMBRYO AND LARVA OF *DROSOPHILA-MELANOGASTER*. *Journal of Neurobiology* 22:298-311.
- Spilman P, Podlutskaya N, Hart MJ, Debnath J, Gorostiza O, Bredesen D, Richardson A, Strong R, Galvan V (2010) Inhibition of mTOR by Rapamycin Abolishes Cognitive Deficits and Reduces Amyloid-beta Levels in a Mouse Model of Alzheimer's Disease. *Plos One* 5.
- Spradling AC, Stern D, Beaton A, Rhem EJ, Laverly T, Mozden N, Misra S, Rubin GM (1999) The Berkeley *Drosophila* Genome Project gene disruption project: Single P-element insertions mutating 25% of vital *drosophila* genes. *Genetics* 153:135-177.
- Spring J, Painesandurs SE, Hynes RO, Bernfield M (1994) *DROSOPHILA* SYNDECAN - CONSERVATION OF A CELL-SURFACE HEPARAN-SULFATE PROTEOGLYCAN. *Proc Natl Acad Sci U S A* 91:3334-3338.
- Staal SP, Hartley JW, Rowe WP (1977) ISOLATION OF TRANSFORMING MURINE LEUKEMIA VIRUSES FROM MICE WITH A HIGH INCIDENCE OF SPONTANEOUS LYMPHOMA. *Proc Natl Acad Sci U S A* 74:3065-3067.
- Staveley BE, Ruel L, Jin J, Stambolic V, Mastronardi FG, Heitzler P, Woodgett JR, Manoukian AS (1998) Genetic analysis of protein kinase B (AKT) in *Drosophila*. *Current Biology* 8:599-602.
- Stocker H, Andjelkovic M, Oldham S, Laffargue M, Wymann MP, Hemmings BA, Hafen E (2002) Living with lethal PIP3 levels: Viability of flies lacking PTEN restored by a PH domain mutation in Akt/PKB. *Science* 295:2088-2091.
- Suzuki DT, Grigliat.T, Williams.R (1971) TEMPERATURE-SENSITIVE MUTATIONS IN *DROSOPHILA-MELANOGASTER* .7. MUTATION (PARATS) CAUSING REVERSIBLE ADULT PARALYSIS. *Proc Natl Acad Sci U S A* 68:890-&.
- Suzuki T, Usuda N, Murata S, Nakazawa A, Ohtsuka K, Takagi H (1999) Presence of molecular chaperones, heat shock cognate (Hsc) 70 and heat shock proteins (Hsp) 40, in the postsynaptic structures of rat brain. *Brain Research* 816:99-110.

- Takayama S, Xie ZH, Reed JC (1999) An evolutionarily conserved family of Hsp70/Hsc70 molecular chaperone regulators. *J Biol Chem* 274:781-786.
- Takei Y, Ozawa Y, Sato M, Watanabe A, Tabata T (2004) Three *Drosophila* EXT genes shape morphogen gradients through synthesis of heparan sulfate proteoglycans. *Development* 131:73-82.
- Tejedor FJ, Bokhari A, Rogero O, Gorczyca M, Zhang JW, Kim E, Sheng M, Budnik V (1997) Essential role for dlg in synaptic clustering of shaker K⁺ channels in vivo. *Journal of Neuroscience* 17:152-159.
- The I, Bellaiche Y, Perrimon N (1999) Hedgehog movement is regulated through tout velu-dependent synthesis of a heparan sulfate proteoglycan. *Molecular Cell* 4:633-639.
- Thisse B, Stoetzel C, Elmessel M, Perrinschmitt F (1987) GENES OF THE DROSOPHILA MATERNAL DORSAL GROUP CONTROL THE SPECIFIC EXPRESSION OF THE ZYGOTIC GENE TWIST IN PRESUMPTIVE MESODERMAL CELLS. *Genes & Development* 1:709-715.
- Thomas U, Kim E, Kuhlendahl S, Koh YH, Gundelfinger ED, Sheng M, Garner CC, Budnik V (1997) Synaptic clustering of the cell adhesion molecule fasciclin II by discs-large and its role in the regulation of presynaptic structure. *Neuron* 19:787-799.
- Thomas U, Ebitsch S, Gorczyca M, Koh YH, Hough CD, Woods D, Gundelfinger ED, Budnik V (2000) Synaptic targeting and localization of Discs-large is a stepwise process controlled by different domains of the protein. *Current Biology* 10:1108-1117.
- Toyoda H, Kinoshita-Toyoda A, Fox B, Selleck SB (2000) Structural analysis of glycosaminoglycans in animals bearing mutations in sugarless, sulfateless, and tout-velu. *J Biol Chem* 275:21856-21861.
- Tschopp O, Yang ZZ, Brodbeck D, Dummler BA, Hemmings-Mieszczak M, Watanabe T, Michaelis T, Frahm J, Hemmings BA (2005) Essential role of protein kinase B gamma (PKB gamma/Akt3) in postnatal brain development but not in glucose homeostasis. *Development* 132:2943-2954.
- Tumova S, Woods A, Couchman JR (2000) Heparan sulfate proteoglycans on the cell surface: versatile coordinators of cellular functions. *International Journal of Biochemistry & Cell Biology* 32:269-288.
- Twig G, Elorza A, Molina AJA, Mohamed H, Wikstrom JD, Walzer G, Stiles L, Haigh SE, Katz S, Las G, Alroy J, Wu M, Py BF, Yuan J, Deeney JT, Corkey BE, Shirihai OS (2008) Fission and selective fusion govern mitochondrial segregation and elimination by autophagy. *Embo J* 27:433-446.
- Via LE, Fratti RA, McFalone M, Pagan-Ramos E, Deretic D (1998) Effects of cytokines on mycobacterial phagosome maturation. *Journal of Cell Science* 111:897-905.
- Walsh P, Bursac D, Law YC, Cyr D, Lithgow T (2004) The J-protein family: modulating protein assembly, disassembly and translocation. *Embo Reports* 5:567-571.

- Wang KKW, Posmantur R, Nath R, McGinnis K, Whitton M, Talanian RV, Glantz SB, Morrow JS (1998) Simultaneous degradation of alpha II- and beta II-spectrin by caspase 3 (CPP32) in apoptotic cells. *J Biol Chem* 273:22490-22497.
- Wang L, Lam G, Thummel CS (2010) Med24 and Mdh2 are Required for Drosophila Larval Salivary Gland Cell Death. *Developmental Dynamics* 239:954-964.
- Wang QH, Liu LD, Pei L, Ju W, Ahmadian G, Lu J, Wang YS, Liu F, Wang YT (2003) Control of synaptic strength, a novel function of Akt. *Neuron* 38:915-928.
- Wang T, Blumhagen R, Lao U, Kuo Y, Edgar BA (2012) LST8 Regulates Cell Growth via Target-of-Rapamycin Complex 2 (TORC2). *Molecular and Cellular Biology* 32:2203-2213.
- Watson RT, Pessin JE (2006) Bridging the GAP between insulin signaling and GLUT4 translocation. *Trends in Biochemical Sciences* 31:215-222.
- Williams A, Jahreiss L, Sarkar S, Saiki S, Menzies FM, Ravikumar B, Rubinsztein DC (2006) Aggregate-prone proteins are cleared from the cytosol by autophagy: Therapeutic implications. *Current Topics in Developmental Biology*, Vol 76 76:89-101.
- Woods CM, Lazarides E (1985) DEGRADATION OF UNASSEMBLED ALPHA-SPECTRIN AND BETA-SPECTRIN BY DISTINCT INTRACELLULAR PATHWAYS - REGULATION OF SPECTRIN TOPOGENESIS BY BETA-SPECTRIN DEGRADATION. *Cell* 40:959-969.
- Xian XJ, Gopal S, Couchman JR (2010) Syndecans as receptors and organizers of the extracellular matrix. *Cell Tissue Res* 339:31-46.
- Xu K, Zhong GS, Zhuang XW (2013) Actin, Spectrin, and Associated Proteins Form a Periodic Cytoskeletal Structure in Axons. *Science* 339:452-456.
- Xu YX, Liu L, Caffaro CE, Hirschberg CB (2010) Inhibition of Golgi Apparatus Glycosylation Causes Endoplasmic Reticulum Stress and Decreased Protein Synthesis. *J Biol Chem* 285:24600-24608.
- Yamaguchi Y (2001) Heparan sulfate proteoglycans in the nervous system: their diverse roles in neurogenesis, axon guidance, and synaptogenesis. *Seminars in Cell & Developmental Biology* 12:99-106.
- Yan D, Lin XH (2009) Shaping Morphogen Gradients by Proteoglycans. *Cold Spring Harbor Perspect Biol* 1.
- Yin ZZ, Xu XL, Frasch M (1997) Regulation of the Twist target gene tinman by modular cis-regulatory elements during early mesoderm development. *Development* 124:4971-4982.
- Yorimitsu T, Nair U, Yang ZF, Klionsky DJ (2006) Endoplasmic reticulum stress triggers autophagy. *J Biol Chem* 281:30299-30304.
- Yoshida H, Oku M, Suzuki M, Mori K (2006) pXBP1(U) encoded in XBP1 pre-mRNA negatively regulates unfolded protein response activator pXBP1(S) in mammalian ER stress response. *Journal of Cell Biology* 172:565-575.
- Youle RJ, Narendra DP (2011) Mechanisms of mitophagy. *Nature Reviews Molecular Cell Biology* 12:9-14.

- Young JC, Agashe VR, Siegers K, Hartl FU (2004) Pathways of chaperone-mediated protein folding in the cytosol. *Nature Reviews Molecular Cell Biology* 5:781-791.
- Zhang H, Zha XM, Tan Y, Hornbeck PV, Mastrangelo AJ, Alessi DR, Polakiewicz RD, Comb MJ (2002) Phosphoprotein analysis using antibodies broadly reactive against phosphorylated motifs. *Journal of Biological Chemistry* 277:39379-39387.
- Zhang KZ, Kaufman RJ (2004) Signaling the unfolded protein response from the endoplasmic reticulum. *J Biol Chem* 279:25935-25938.
- Zheng J, Shen WH, Lu TJ, Zhou Y, Chen Q, Wang Z, Xiang T, Zhu YC, Zhang C, Duan SM, Xiong ZQ (2008) Clathrin-dependent endocytosis is required for TrkB-dependent Akt-mediated neuronal protection and dendritic growth. *J Biol Chem* 283:13280-13288.
- Zhou CH, Zhong W, Zhou J, Sheng FG, Fang ZY, Wei Y, Chen YY, Deng XY, Xia B, Lin J (2012) Monitoring autophagic flux by an improved tandem fluorescent-tagged LC3 (mTagRFP-mWasabi-LC3) reveals that high-dose rapamycin impairs autophagic flux in cancer cells. *Autophagy* 8:1215-1226.
- Zito K, Fetter RD, Goodman CS, Isacoff EY (1997) Synaptic clustering of Fasciclin II and Shaker: Essential targeting sequences and role of Dlg. *Neuron* 19:1007-1016.

Curriculum Vitae

Na Zhao

Education:

2009-present, The Pennsylvania State University. GPA: 3.85/4.00
Ph.D. Candidate in Biochemistry, Microbiology and Molecular Biology Program
Dissertation Advisor: Scott B. Selleck

2005-2009, Xiamen University, China. GPA: 3.82/4.00
B.S. of Life Sciences
Advisor: Chundong Yu

Professional Experience:

2010-2014 Graduate Assistant, The Pennsylvania State University
2009-2010 Teaching Assistant, The Pennsylvania State University
2007-2009 Research Assistant, Xiamen University, China

Publications:

1. **Na Zhao**, Jie Xu, Jielin Xu and Scott B. Selleck. 2014. Heparan sulfate proteoglycans negatively regulate autophagy during development of the *Drosophila* neuromuscular junction. Manuscript submitted to *Journal of Cell Biology*.
2. Hyun-Gwan Lee*, **Na Zhao***, Bridget K. Campion, Michelle N. Nguyen and Scott B. Selleck. 2013. Akt regulates glutamate receptor trafficking and postsynaptic membrane elaboration at the *Drosophila* neuromuscular junction. *Developmental Neurobiology*. 73, 723–743. (* Equal contributions)
3. Brian Dimitroff, Katie Howe, Adrienne Watson, Bridget K. Campion, Hyun-Gwan Lee, **Na Zhao**, Michael B. O'Connor, Thomas P. Neufeld and Scott B. Selleck. 2012. Diet and energy-sensing inputs affect TorC1-mediated axon misrouting but not TorC2-directed synapse growth in a *Drosophila* model of tuberous sclerosis. *PLoS ONE*. 7(2): e30722. DOI:10.1371/journal.pone.0030722
4. Yuji Wang, Pingxin Li, Shu Wang, Jing Hu, Xiangyun Amy Chen, Jianhui Wu, Megan Fisher, Kira Oshaben, **Na Zhao**, Ying Gu, Dong Wang, Gong Chen and Yanming Wang. 2012. Anticancer PAD inhibitors regulate the autophagy flux and the mammalian target of rapamycin complex 1 activity. *The Journal of Biological Chemistry*. DOI:10.1074/jbc.M112.375725
5. Qiang Chen, Yuan Jiang, Yuan An, **Na Zhao**, Yang Zhao and Chundong Yu. 2011. Soluble FGFR4 extracellular domain inhibits FGF19-induced activation of FGFR4 signaling and prevents nonalcoholic fatty liver disease. *Biochemical and Biophysical Research Communications* Vol: 409. DOI: 10.1016/j.bbrc.2011.05.059

Poster Presentation:

December 11-15, 2010, The American Society for Cell Biology 50th Annual Meeting, Philadelphia, USA. Title: “Regulated trafficking of a glutamate receptor subunit by Akt at the *Drosophila* neuromuscular junction.”